The Mathematical Modelling of Caking in Bulk Sucrose

This thesis is presented as partial fulfillment of the requirements for the degree of Master of Engineering in Bio Process Engineering at Massey University

Scott W Billings

B. Tech (Chem)

2002

Abstract

Ever since the need for bulk transportation of sugar, there have been problems with the product caking during storage and transportation. This project was carried out in order to try and understand the mechanisms behind caking, and by mathematically modelling the system, to find the conditions needed to avoid caking, and to compare these to the observations and experiences made by those working in the industry.

A thermal analysis monitor was used to determine if significant quantities of amorphous sucrose existed on the dried sugar, to support the amorphous recrystallisation caking mechanism. The level of amorphous sucrose was found to be less than 0.1%, so it was reasoned that any moisture contribution from such a small fraction, even given its tremendously hygroscopic nature would be negligible in contrast to that from the humidity caking mechanism.

The water activity at which capillary condensation begins to occur significantly was then investigated and found to be 0.8. At this critical water activity, significant capillary condensation between particles occurs, forming liquid bridges between the particles and causing the bed to lump. If the lumped bed is then subjected to an environment with a lower water activity, over time the liquid bridges will begin to crystallise, creating solid bridges between the particles. These solid bridges have several times the mechanical strength of the liquid bridges and it is at this point that the bed is considered to be caked. The data from this experiment was then further used to build a relationship between the water activity of a bed, the radius of the liquid bridges formed by capillary condensation (Kelvin radius), and the resulting lumped strength of the bed.

A model based on the caking of lactose was then adapted for sucrose and validated by testing conditions of heat and moisture migration through a packed bed, and the resulting effect on the strength of caking. Various model parameters were then adjusted between experimentally known values in order to obtain the best-fit possible for the experimental data. The data from the experiment and the model agreed well, however the temperature data did exhibit some scatter, possibly caused by insufficient grounding of the measuring device, making it susceptible to noise.

The model was then used to build up a graph of the effect of initial water activity, cold and hot temperatures on the maximum water activity that a bed would reach at the cold surface. Using the critical water activity, this graph can be used to represent the limits at which sucrose of a certain condition can be stored and transported without the sucrose caking. This also opens paths for future research, as this will allow conditions created by the changing of process conditions such as temperatures and residence times within the driers, to be measured in terms of whether the end product will have a tendency to cake.

Acknowledgements

First of all to the person who invented aluminium tape. This wonderful creation was involved in the success of all of my experimental work (imagine MacGyver with this stuff!).

All at Massey University – Steven, Bogan and especially Kylie for their input and feedback, coupled with their true mastery of postgrad work evasion techniques and expertise with fillet steak. Ann-Marie Jackson, Mike Salheim, Bruce Collins and Gerard Harrigan for your continual help with equipment, I know how hard it is – sort of.

The staff at New Zealand Sugar, especially Viv, Adrian, Bert, Tony, Graham and Warren for pretending to believe that I knew what I was doing. A special thanks to Peter Simpson for having to make me work to prove anything to him, and for allowing me to take a chance at what is now my career.

Peter Tait and all at Tait Controls for their guidance and patients in the "learn software engineering in just 10 weeks" endeavor. The endless harassment about the due date of my thesis was also appreciated (despite popular theory).

My principal supervisor Tony Paterson, mainly for forcing me to think for myself (although your name was mud for the longest time, I cant thank you enough!) and for the time spent helping with all of the aspects of the project. Also for proving that with very little sleep it is possible to design, run and write up an experiment, then present a paper – all in less than a week. Nor can we forget the "sucrose shouldn't be that dissimilar to lactose" statement, which upon reflecting, I could probably get a PhD out of.

My secondary supervisor John Bronlund, for a superb job on the fully working lactose model, which to date, I still don't have (funny, funny man). Also for making sure I always had a tangent to go off on and for all the inspiration in all its forms (especially the "ode for diffusion" – nice one).

A very special thanks to Scott O'Connor for his exceptional performance on his thesis ;-) and to Shaz for all the motivation and support and primo curry.

To all who gave me heaps of grief about finishing my thesis, but still abused my rubber arm. The perpetrators include Aaron and Tracy, Reon, all the Lances, (Palmy, Hawera and Hamilton), Eli, Evil , Nats, Becs^2 , Crow, Mike, Jon, Frankie, Kelly, Lisa - and anyone I have missed – you know who you are. I gave Tony all your details, so be expecting a flaming package on your doorstep anytime soon.

Last but not least my parents for bringing me up right (well not wrong), for always believing in me and for always being there without being there. It means more than you could ever know. It never has or will be easy, but this has made us who we are today.

Table of Contents

CHAPTER 8 Experimental results and model comparison

CHAPTER 9 Model Application – Results and Discussion

CHAPTER 10 Conclusions and Suggestions for Future Work

REFERENCES

APPENDIX A1 Nomenclature

APPENDIX A2 C++ Program

List of Figures

List of Tables

CHAPTER 1

INTRODUCTION

1.1 Problem Description

The caking of sucrose has been a serious problem in the sugar industry since the introduction of bulk handling and transport as early as the 1900's.

Through many years of observation, experience and experimentation, many factors contributing to the caking phenomenon have been described. These include:

- Caking is caused by the migration of moisture caused by temperature gradients across the storage vessel.
- The hygroscopic nature and the physical chemistry of the sugar crystals surface are responsible for moisture absorption.
- Packing at temperatures above ambient can cause sugar to set.
- Products with large crystals and a high coefficient of size variance are more prone to caking.
- Literature suggests rapid drying causes an amorphous layer to form around the crystal, trapping a film of saturated sugar on the crystal surface.
- The amorphous surface allows increased moisture uptake from its surroundings.

From these observations, mechanisms have been conceptualised in order to explain the occurrence of these events. It is the aim of this project to investigate these and attempt to put a solid theoretical base to the caking phenomenon.

1.2 Project aims

There are several specific aims for the project:

- Searching the available literature for existing caking work and determine the parameters to be used in these models.
- To experimentally confirm undocumented parameters to be used by any models.
- Make amorphous sucrose in the lab and use it to find an accurate as possible value for the amorphous content of sucrose at different stages in the production process.
- Determine whether the physical properties of sucrose are similar enough to lactose to be able to be use the model formulated by Bronlund (1997), for modelling the caking of bulk lactose.
- If suitable take the lactose model and adapt, apply and then validate the model for sucrose, using it to generate data suitable for process control within the plant.

CHAPTER 2

Literature Review

Introduction

Today the role of sugar has broadened from its sole use as a sweetener in the early days of production to use for preserving, lower freezing points, bind, help maintain texture and prolong the shelf life of food products. With the recent emphasis on cleaner production and waste minimisation, the sugar industry has been able to capitalise by utilising by-products such as molasses to produce ethanol and other chemicals. More than 100 million tonnes of sugar is produced world wide from sugar cane and sugar beet, with the total consumption figure being similar.

In New Zealand sugar has been produced at the Chelsea sugar refinery since 1894, operating 24 hours a day, 5 days per week, with occasional weekend operations to meet peak demand, producing just over 200,000 tonnes per year.

2.1 Caking Overview

Ever since the need for the bulk transportation of sugar, there have been problems with caking. There are two major mechanisms thought to cause the caking of bulk powders. The first mechanism, humidity caking, can occur because of temperature gradients across bulk quantities of sugar. This causes the movement of moisture toward container extremities, creating areas of high moisture that can become sticky, form inter-particle bridges and then cake (Bronlund, 1997). Temperature gradient is only one mechanism by which humidity caking can occur, but due to the production process is thought to be the one most relevant.

The second proposed mechanism is thought to be caused by the presence of amorphous (non-crystalline) sugar on the surface of the crystal. It is believed that amorphous sugar is formed by quicker drying regimes, and has the ability to absorb large amounts of moisture due to its unordered structure. Once the amorphous sugar begins to absorb moisture it can undergo a glass transition, a change from an immobile glassy state to a "rubbery" state, capable of flow. This allows the sugar crystals to stick at the points of contact between crystals and cake (Mathlouthi and Reiser, 1995).

2.2 Physical Properties of Sucrose

2.2.1 Sucrose Chemistry

The sucrose molecule is composed of twelve carbon, eleven oxygen and twenty two hydrogen atoms, giving it a molecular weight of 342.30 g/mol.

Sucrose is a disaccharide formed from glucose and fructose. The IUPAC (International Union of Pure and Applied Chemistry) nomenclature for sucrose is:

β - D – fructofuranosyl - α - D – glucopyranoside

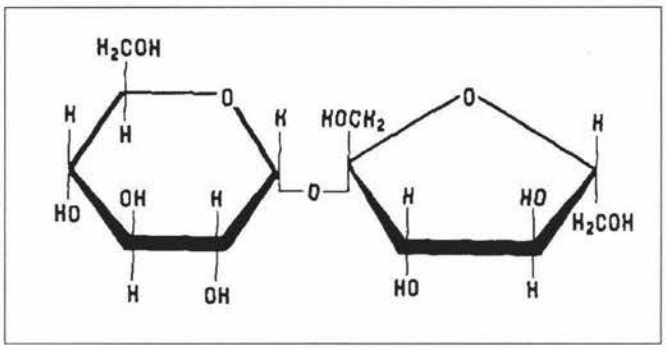

Figure 2.1 Structure of the Sucrose Molecule (Pennington and Baker, 1990)

Pure sugar melts or decomposes at 188°C, has a negative heat of solution of 2 kilo-calories per mol (342.3 grams) and at 20°C has a specific heat of 1.235 J/kg °C, and pH of 7.0 – 7.15.

Sucrose crystals can have three different forms; single crystal, twin crystal and conglomerates. The single crystal is the most common and belongs to the sphenoidic class of monolithic crystal system (Mathlouthi and Reiser, 1995). Twin crystals are common in liquors high in impurities and are formed by rotating one of the single crystals 180° around the horizontal axis to obtain junction with the other single crystal. Conglomerates are also formed in liquors that have a high impurity content and are formed by the random junction of several crystals.

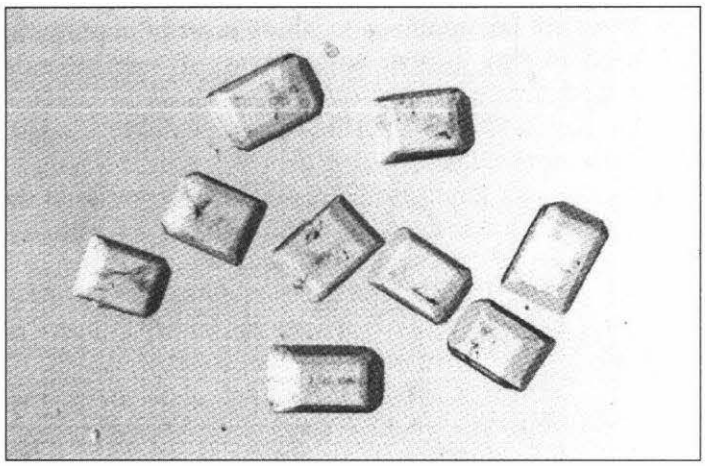

Figure 2.2 Single sucrose crystals (Mathlouthi and Reiser, 1995)

The "typical" crystal is defined as being rectangular with dimensions of 0.2 mm × 0.2 mm × 0.4 mm and having an initial bound moisture content of 0.075 % (Meadows , 1994).

2.2.2 Granulometry

Crystallised sugar is commercially available with various grain sizes required for different food applications. Weight, surface area and volume of sugar crystals passing through different screens was investigated by Pancoast and Junk (1980).

Mesh	Weight of Crystals (mg)	Number of crystals per mg	Surface area of crystal (mm^2)	Volume of crystal (mm^3)	Surface area / mg of crystal (mm^2)
5	69.1	0.014	69.5	43.6	1.004
10	5.0	0.2	12.1	3.16	2.42
20	0.642	1.560	3.08	0.405	4.790
60	0.0165	60.6	0.267	0.0104	16.2
100	0.00352	284.0	0.0957	0.0222	27.2
150	0.00125	800.0	0.0479	0.000788	38.30
200	0.000450	2220.0	0.0242	0.000284	53.7
250	0.000252	3970.0	0.0165	0.000159	65.5
325	0.000088	11400.0	0.00817	0.0000555	93.0

Table 2.1 Granule data for sucrose (Pancoast and Junk, 1980)

2.2.3 Density

2.2.3.1 Particle

The density of sucrose crystals can be derived from crystallographic data. It was first measured at 15°C by Plato, and since official confirmation in 1901 that value found (1587.9 kg/m^3), is still valid for practical purposes (Mathlouthi and Reiser, 1995).
Ciz and Valter (1967) calculated the change in density with temperature, representing it in equation form as:

$$\rho = \frac{\rho_{20}}{1+1.116\times10^{4}\times(T-20)} \qquad \text{equation 2.1}$$

where the value for ρ_{20} , the density at 20°C = 1588.4 kg/m^3 (Helderman, 1927).

2.2.3.2 Bulk

Bulk densities for the different grades of commercial sugar produced was investigated by MacCarthy and Fabre (1989), using masses and volumes of the different grades of sugar.

Sugar Grade	Apperture	Bulk Density
	μm	kg/m^3
Medium	1361	825
Standard Granulated	635	883
Extra fine	375	884
Caster	343	892
Icing	61	607

Table 2.2 Bulk densities for different sugar grades (MacCarthy and Fabre, 1989)

2.3 Properties of Amorphous Sucrose

By definition, amorphous means without shape. Amorphous solids have very long relaxation times and may remain almost indefinitely in a meta-stable state.
Amorphous sugar can result from dry milling, the quenching of the melt, the rapid drying of solutions (spray drying) and freeze drying.

Most of the physical and structural properties of amorphous sugar are moisture dependent. The water content and activity, together with temperature are determining factors of the mobility and re-organisation of sucrose molecules in the amorphous matrix (Mathlouthi and Reiser, 1995).

Amorphous sucrose can be thought of in two ways. The first is a light fluffy icing sugar type of structure and the other is an extremely viscous glass like sucrose solution that is capable of flowing upon the uptake of moisture. It is this form of amorphous sugar that is thought to exist on the surface of the sugar crystals after they leave the centrifugal stage of the refining process.

2.3.1 Glass Transition

A glass transition is when the amorphous material changes from a highly viscous, flow-less "glassy" state to a rubbery "labile" state that is capable of flow. The temperature at which this occurs, the glass transition temperature (T_g) appears to be a good indicator of the transitions that can occur in an amorphous sugar, which include collapse, stickiness and caking during storage (Mathlouthi and Reiser, 1995).

The glass transition temperature for a given material with varying water content can be predicted using the Gordon Taylor equation (equation 2.2), originally formulated for T_g predictions for mixtures of polymers (Roos and Karel, 1991).

$$T_g = \frac{w_1 T_{g1} + k w_2 T_{g2}}{w_1 + k w_2} \qquad \text{equation 2.2}$$

where k is the constant for the material, w_1, T_{g1} w_2, and T_{g2} are the mass fractions and the glass transition temperatures (dry, in Kelvin) of water and sucrose respectfully.

Johari *et al.* (1987) and Mayer (1988) both measured the glass transition temperature for pure water as -135°C and Roos and Karel (1991) reported the value of k for sucrose as 4.7 ± 0.2.

The glass transition temperatures of amorphous sucrose has been investigated by many authors at a range of different temperatures, this data shown in figure 2.3 (page 2 – 6).

As the water content of amorphous sucrose is increased the glass transition temperature decreases, as shown in figure 2.3 below. Depending on the position along the glass transition curve, a 1% increase in moisture content can decrease the glass transition temperature by up to 20°C (Roos and Karel , 1991).

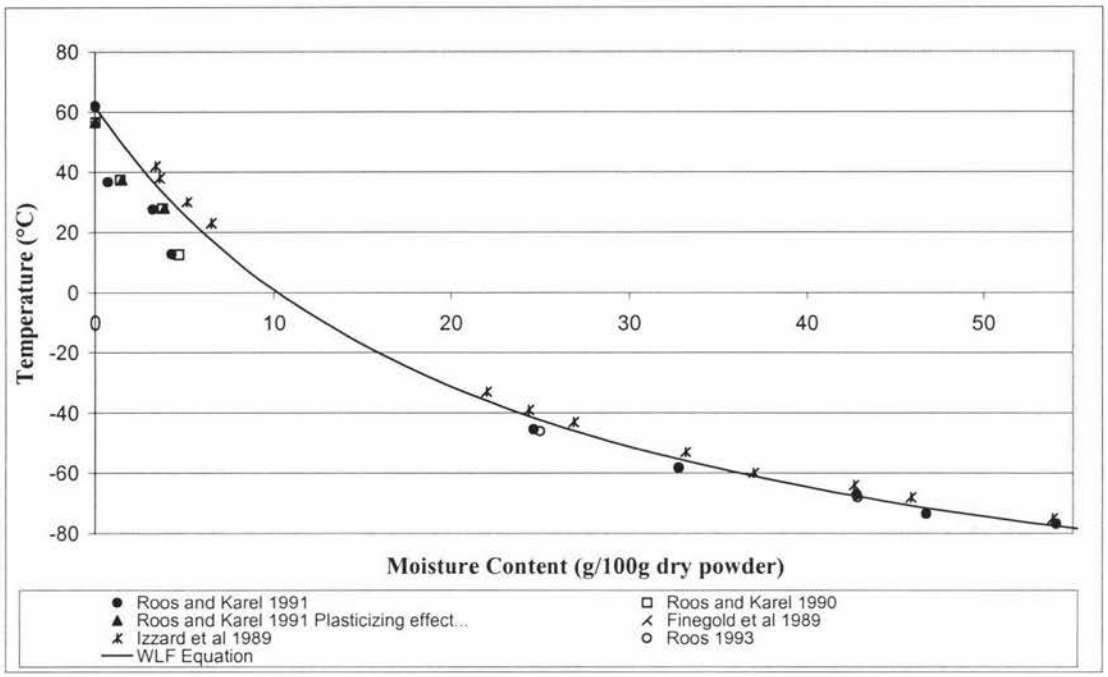

Figure 2.3 Literature data for glass transition temperature (Foster, 2000)

This demonstrates that if amorphous sucrose is exposed to environments that will support moisture absorption (high relative humidity environments), the glass transition temperature will drop to below room temperature, provoking stickiness, collapse, re-crystallisation and eventually caking (Mathlouthi and Reiser, 1995).

Another factor linking amorphous sucrose to caking is that the crystallisation of sugar above the glass transition temperature is time dependent, explaining some of the time delayed occurrences of caking (Roos and Karel, 1991).

2.3.2 Viscosity

The viscosity of amorphous sucrose is important when considering the amorphous caking mechanism, which involves the bridging of crystal surfaces that are in contact with each other, forming sticky agglomerates.

The Williams – Landel – Ferry (WLF) equation (equation 2.3), relates relaxation time of mechanical properties to the temperature above the glass transition temperature (Bronlund, 1997).

Using viscosity values for 70 – 75% sucrose solutions above -30°C, it is possible to use the equation above to calculate the viscosity above T_g. The viscosity at T_g was then calculated

by solving equation 2.3 for all experimental points at respective ($T - T_g$) values to obtain an average value ($\eta_g = 10^{10.666}$ Pa s) (Roos and Karel , 1991).

$$\log\frac{\eta}{\eta_g} = \frac{-17.44(T - T_g)}{51.6 + (T - T_g)} \qquad \text{equation 2.3}$$

where T is the temperature, T_g is the glass transition temperature, η is the viscosity at T and η_g is viscosity at T_g.

2.3.3 Quantification

There are many techniques available for the quantification of amorphous content. Many of these are based on mass changes (gravimetric) but these have the disadvantage of being inaccurate when dealing with small quantities. Other, more accurate techniques, such as calorimetry, are also used but have the disadvantage of being impractical for process control.

2.3.3.1 Calorimetric

Calorimetry is a technique for measuring heat flows associated with physical and chemical processes and is a rate sensitive technique. Micro-calorimetry is a more sensitive form of calorimetry, having a sensitivity in the micro-watts (μW) range.

There are three calorimetric principals – adiabatic, power compensation and heat conduction.

Adiabatic calorimeters measure the temperature change of a reaction vessel as a reaction proceeds. The reaction vessel is insulated so no heat transfer occurs between the vessel and the surrounding environment. The heat quantity evolved from the reaction is the product of the heat capacity of the vessel and the change in temperature.

Raemy *et al.* (1993) uses this technique to detect amorphisim down to the 0.5% level by using a differential scanning calorimeter calibrated with mixtures of crystalline and amorphous sucrose of known proportions. The crystallisation enthalpies of the known mixtures are found by peak integration, and amorphous content is plotted versus enthalpy. Regression was then performed to obtain a fit-line to explain the relationship between the degree of amorphisim (da) and enthalpy.

$$da(\%) = 1.69 \times \text{Enthalpy (J/gDM)} \qquad \text{equation 2.4}$$

This technique has also been done using the heats of solution as opposed to enthalpy of crystallisation, with a linear result also being reported (Gao and Rytting, 1997)

2.3.3.2 X-Ray Diffractometer

There are three ways in which this method can be used to determine the crystalline/amorphous content of a mixture.

1. By making a calibration curve from mixtures containing known fractions of amorphous and crystalline sucrose and measuring the peak height. Peaks of unknown crystalline content can then be compared to these curves and the crystalline/amorphous content found by inspection or interpolation (Palmer *et al.* 1956)

2. By defining a peak that is similar in height to completely crystalline sucrose and then measuring crystallinity as a percentage or fraction of that height. A brass peak of $2\theta = 42.1°$ has been used as the base peak for comparison, due to its identical height to the completely crystalline sucrose peak at $2\theta = 24.8°$ (Palmer *et al.* 1956)

3. By measuring the total area under the sucrose peak and comparing it to the areas under the completely crystalline and completely amorphous peaks. Crystallinity is then defined as the ratio of the area under the sucrose peak to the total peak area for the crystalline and amorphous sucrose peaks (Chinachoti and Steinberg, 1986b).

For the second and third methods, the amorphous content can be found as the difference between the value obtained and 100.

2.3.3.3 Gravimetric

The gravimetric technique for measurement is not as accurate as the other quantification methods but it has the advantage of being able to be used as a rapid technique for determining amorphous content. This gives it the advantage of being more applicable as a technique for process control.

There are two gravimetric techniques that can be used.

2.3.3.3.1 Absorption - desorption

This method is based on the sorption of water by amorphous sucrose and the consecutive desorption of the water induced by the crystallisation of the amorphous part of the sample.

Raemy *et al.* (1993) calculated the degree of amorphisim by placing a sample on a balance, exposing it to an atmosphere with a relative humidity of 40 – 60 percent and then measuring the change in weight with time. From experimentation, it has been found that the amorphous component will absorb up to 4% of its mass in water. Once this maximum humidity is reached, the amorphous layer will crystallise, releasing the total amount of water into the atmosphere. Assuming the maximum water content of amorphous sucrose is 4%, the unknown degree of amorphisim can be calculated using the masses of the different stages of moisture content according to equation 2.5.

$$da(\%) = \frac{10^4}{4} \times \frac{M_{max}(g) - M_{final}(g)}{M_{final}(g)} \qquad \text{equation 2.5}$$

2.3.3.3.2 Mass Balance

The mass balance method for determining the amorphous content was used by Paterson *et. al* (2001) to estimate the degree of amorphisim of lactose samples. This was done by using a mass fraction balance for a sample containing both crystalline and amorphous components and rearranging the formula into the form of equation 2.6.

$$X_{amorphous} = \frac{M_{total} - M_{crystalline}}{M_{amorphous} - M_{crystalline}} \qquad \text{equation 2.6}$$

At a specific water activity the GAB isotherms for crystalline and amorphous sucrose can be used to determine the mass of the sample that is water ($M_{crystalline/amorphous}$) and the total mass ($M_{total}$) is the amount of water lost when the sample is dried.

Due to sugar conditioning and experience with different drying conditions, it is quite unlikely that amorphous sucrose is present in any vast quantity. This will need to be confirmed by an iterative process of starting with the least sensitive method for detecting amorphous sugar. If this technique cannot detect amorphous sugar then use a more sensitive technique and continue this process until either a low level amorphous sugar can be detected or the amount can be deemed insignificant.

2.4 Properties of Sucrose Solutions

One of the most important properties exhibited by sugar is its high solubility in water. The solubility is explained by the chemistry of the molecule, with each having eight hydroxyl groups, three hydrophilic oxygen atoms bound in a circle and twelve hydrogen

atoms. This enables the formation of hydrogen bonds with the water, hydrating the sucrose molecule and allowing easy dissolution in water.

2.4.1 Solubility

Solubility tables have existed for over a century, but the solubility of sucrose in water is best represented graphically as a sucrose – water phase diagram.

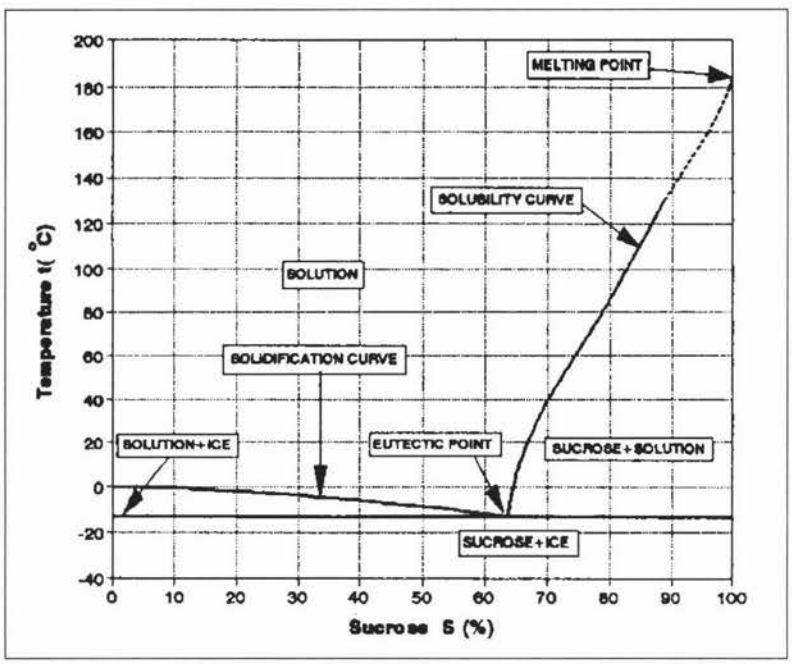

Figure 2.4 Phase temperature diagram for sucrose solutions (Mathlouthi and Reiser, 1995)

As shown, solubility S (%), varies with temperature (T, in °C) and can be related by the equation 2.7 (Mathlouthi and Reiser, 1995).

$$S = 64.397 + 0.7251.T + 000206.T^2 - 9.035 \times 10^{-6}.T^3 \qquad \text{equation 2.7}$$

2.4.2 Surface Tension

Surface tension accounts for the cohesion of water molecules in the liquid state. Because of the sucrose molecule's compatible packing in water, an increase in concentration enhances the air interfacial tension of the water (Mathlouthi and Reiser, 1995)

Concentration (g/100 g of solution)	Surface Tension (N/m)
0	72.68
10	73.51
20	74.70
30	75.89
40	77.08
50	78.27
60	79.46
65	80.06

Table 2.3 Surface tension at 21°C (Mathlouthi and Reiser, 1995)

2.4.3 Density

The density of sucrose solutions can be used as a measure of the purity of the sugar being dissolved, as the presence of impurities effects the density of the solution (Mathlouthi and Reiser, 1995).

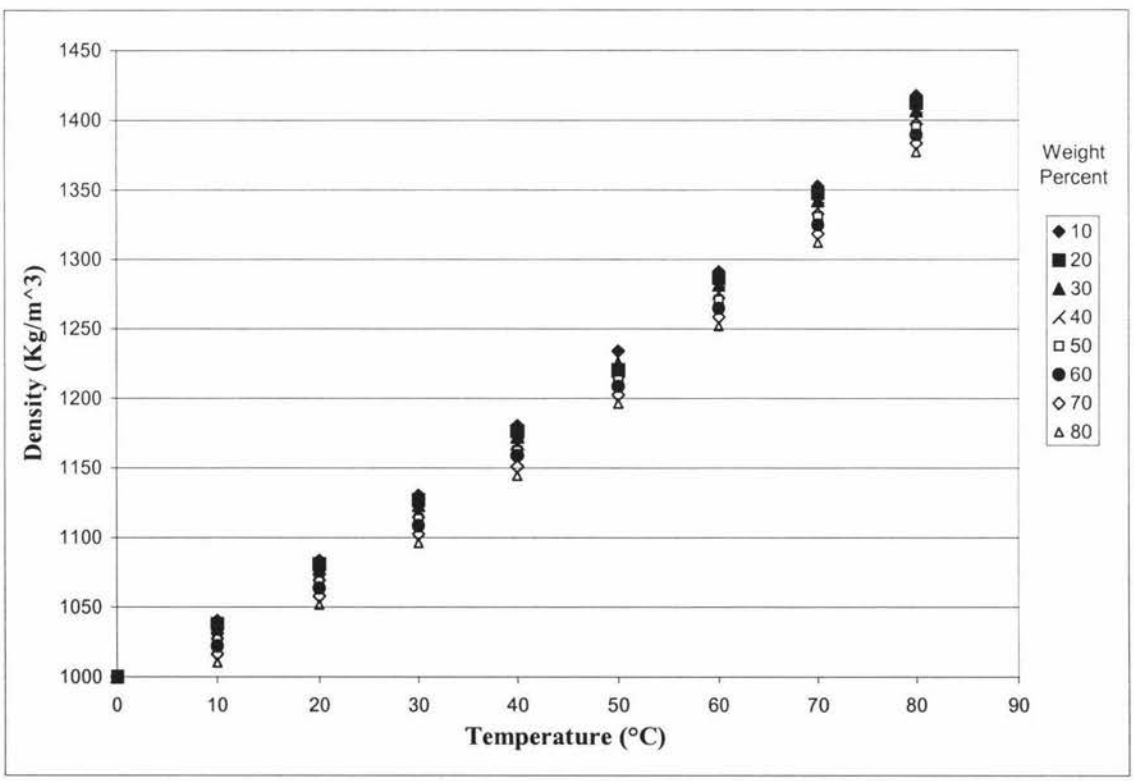

Figure 2.5 Density of sucrose solutions (ICUMSA)

2.5 Thermal Properties

2.5.1 Specific Heat Capacity

Lyle (1997) reported the heat capacity of sucrose and its solutions (in kJ/kg K) between 0 and 100°C.

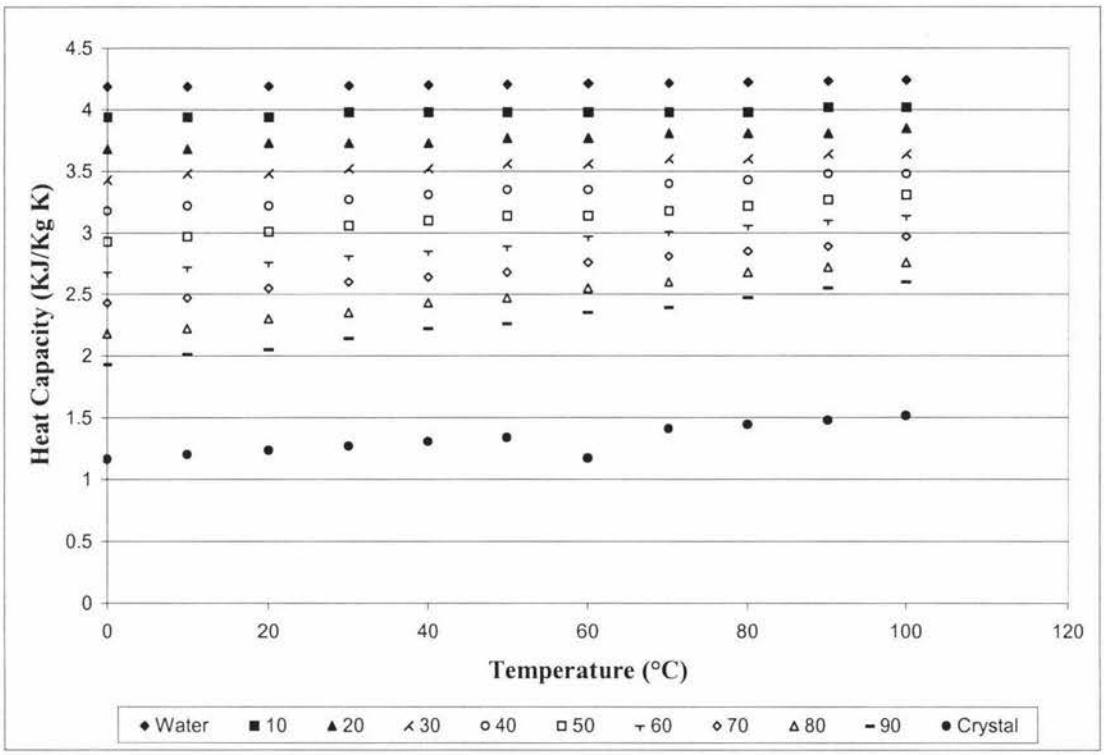

Figure 2.6 Heat capacity of sucrose and its solutions (Lyle, 1957)

Anderson *et al.* (1950) formulated an equation relating the heat capacity of sucrose crystals at different temperatures.

$$C_p = 1.1269 + 4.524 \times 10^{-3} \times T + 6.24 \times 10^{-6} \times T^2 \qquad \text{equation 2.8}$$

where the temperature is in °C. The values obtained by use of equation 2.8 differ slightly from the results found by Lyle, but as an approximation it is good, as it does not require interpolation calculations.

2.5.2 Thermal Conductivity

There are two main methods that can be used to measure the thermal conductivity of a material. These are the guarded hot plate and the infinite cylinder methods.

2.5.2.1 Guarded Hot Plate Technique

Mac Carthy and Fabre (1989), used a steady state guarded hot plate technique to determine the thermal conductivity of crystalline sugar. This involved establishing a unidirectional steady state heat flow through two immobile isotropic samples, located on both sides of a heating plate. The heat flow from the hotplate through the samples is absorbed by heat sinks and the thermal conductivity calculated from Fourier's law of heat conduction.

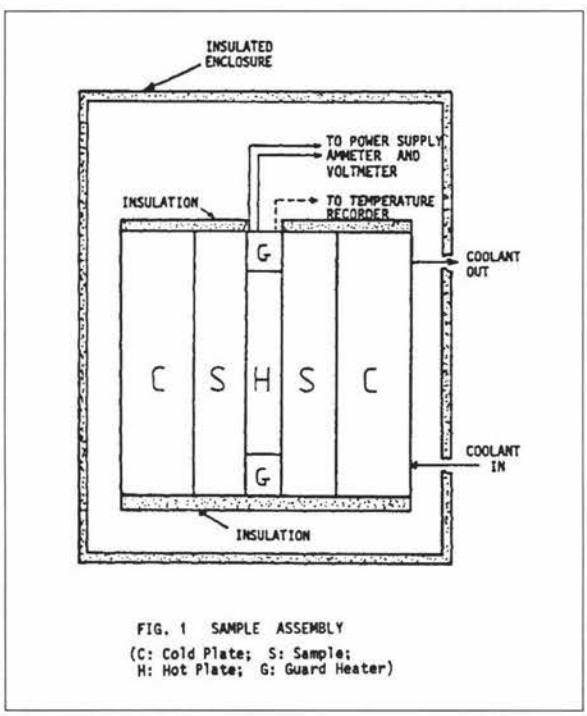

Figure 2.7 Guarded hotplate method for thermal analysis (MacCarthy and Fabre , 1989)

The thermal conductivity was investigated for five different grades of sugar and is shown if figure 2.8 below.

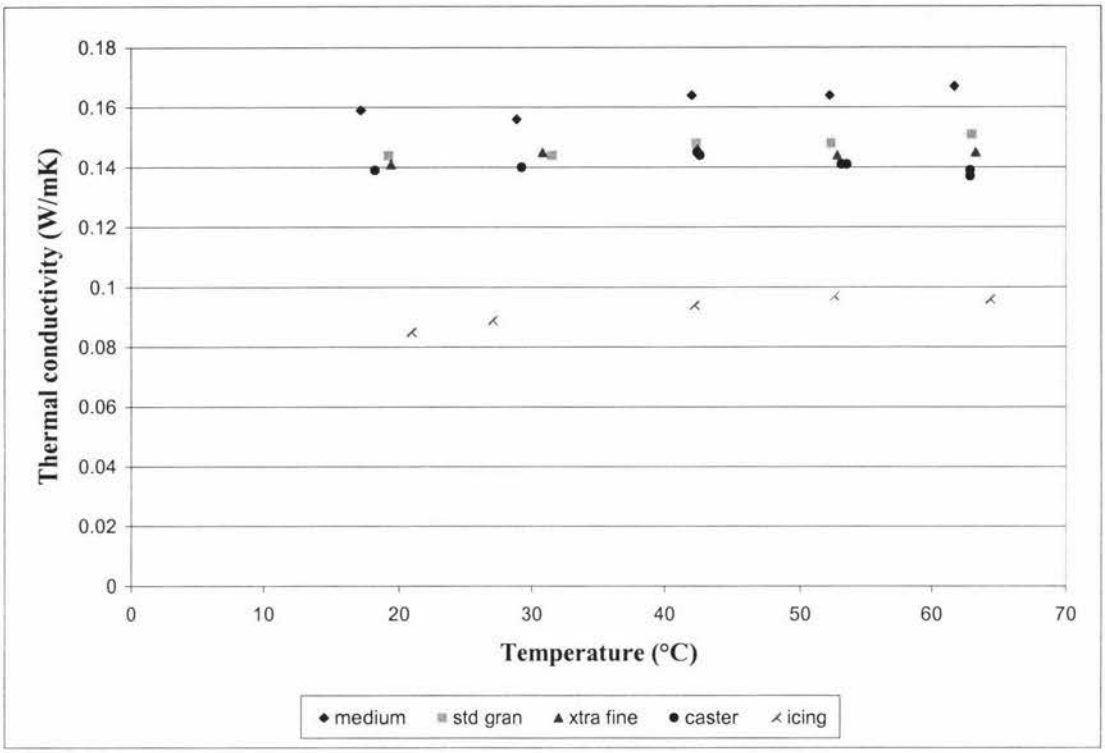

Figure 2.8 Sugar thermal conductivity (MacCarthy and Fabre , 1989)

The problem with this method is that there is no mention of the porosity of the bulk sample. From the parallel model of thermal conductivity (equation 2.9), used by Murakami and Okos (1989), it can be seen that the porosity of the sample will have an impact on the thermal conductivity of the bulk material.

$$\lambda_{\text{effective media}} = (1-\varepsilon)\lambda_{\text{solid phase}} + \varepsilon\,\lambda_{\text{gas phase}} \qquad \text{Equation 2.9}$$

This effect of porosity is incorporated into the infinite cylinder, making it more appropriate for use.

2.5.2.2 Infinite Cylinder Method

The heat conduction through an infinite cylinder can be described by equation 2.10.

$$Y = 1 - 2\sum_{n=1}^{\infty} \frac{\exp(-\beta_n^2 \times \alpha \cdot T / r^2)}{\beta_n J_1(\beta_n)} \qquad \text{equation 2.10}$$

Where T is temperature in °C and Y is the fraction of unaccomplised temperature change in the cylinder. Bronlund (1997) uses this equation in conjunction with experimental data obtained from the temperature time profile of an experimental infinite cylinder to determine the thermal conductivity of lactose. A copper cylinder 300mm long and 80 mm in diameter with thermocouples placed one third and two thirds down the center of the tube and thermocouples taped to the surface were used.

By using equation 2.10 it is possible to quantify any discrepancies in the values obtained from the two methods by accounting for differences in the bulk porosities.

$$\frac{1-\varepsilon_{\text{guarded hot plate}}}{1-\varepsilon_{\text{infinite cylinder}}} = \frac{\lambda_{\text{guarded hot plate}}}{\lambda_{\text{infinite cylinder}}} \qquad \text{equation 2.11}$$

This will allow the calculation of the porosity of the samples used in the guarded hot plate technique reported by M^c Carthy and Fabre (1989) and to adjust it, and recalculate the values for thermal conductivity at the same porosity used in the infinite cylinder experiments. From this an average value from the two methods can be used to represent the thermal conductivity.

2.6 Moisture Relationships

It is the hygroscopic nature of sugar that has lead to problems with the lumping and caking of sugar during storage and transportation. Moisture effects sugar in different ways under different conditions and it is important to understand this in order to be able to restrict or control the caking problem.

2.6.1 Types of Moisture

There are four different types of moisture that have different effects on the physical and storage properties of sugar.

2.6.1.1 Free Moisture

Free moisture is the moisture that is found on the surface of the crystal. Free water is the moisture associated with the sugar as it leaves the centrifuges, existing as a dilute sugar solution that can easily be removed by drying. Free moisture is not associated with the caking of sucrose as it will either evaporate into the ambient surroundings or become bound moisture. To limit the amount of free water leaving the centrifuges the relative humidity in the centrifuges should be kept below 50% (Ludlow and Aukland , 1990).

2.6.2.2 Bound Moisture

Bound moisture is the moisture trapped within the surface film on the crystal.

During the evaporation of free moisture, a syrupy coat of sucrose and water is on the crystal surface. This film is supersaturated and usually has a high level of impurity (ash) (Ludlow and Aukland , 1990). The rate of evaporation from the syrup then exceeds the rate of crystallisation and a film of supersaturated solution is left on the crystal surface. The film surface then solidifies as an amorphous sugar layer of high moisture content (Thompson, 1998), trapping the remaining film on the surface of the crystal. Over a certain time period the crust is dissolved by the moisture being liberated from the crystallisation of the film below. The crust then crystallises with all of the remaining water being free moisture on the surface (Thompson , 1998).

2.6.2.3 Inherent Moisture

Inherent moisture can be thought of as the water actually trapped within the sucrose crystal. This water is possibly part of a sucrose complex including trace amounts of hydrophilic polysaccharides which have hydrated strongly, eliminating water removal by moisture gradient techniques such as drying in an oven or over drying agents such as P_2O_5 (Bagster, 1970). Inherent moisture can only be released by breaking the crystals, which then exposes the crystal inner, which can then be dried by conventional methods. As this moisture is contained in the inner lattice of the crystal and no grinding occurs (such as the grinding of sugar to make icing sugar), so inherent moisture will not contribute to caking (Thompson , 1998).

2.6.2.4 Interstitial Water

Interstitial water is the water vapour found in the air that fills the gaps in the bulk sugar. The amount present is directly related to the temperature of the air and the conditioning conditions of the crystals and it is generally measured as the equilibrium relative humidity. This is because it is considered that the interstitial air is in equilibrium with the bound moisture in the crystal (Ludlow and Aukland , 1990).

2.6.3 Measurement of Moisture Content

There are several techniques available for measuring the moisture content of sugar. Some of these are more accurate than others, while some allow in – line moisture measurement for process control purposes.

2.6.3.1 Dessication

The most widely accepted method for moisture determination in food science research is vacuum desiccation over phosphorus pentoxide for at least one month (Bronlund , 1997). Phosphorous pentoxide maintains an absolute humidity of 0.0193 mg of water per kilogram of dry air, making it an excellent dessicator (Grayson, 1979), but due to the long time requirements this method is not applicable for routine industry based measurements.

2.6.3.2 Oven Drying

The United States Committee on Sugar Analysis procedure for determining the moisture content of sugar is given by Pennington and Baker (1990).

Pre dried aluminium dishes are weighed and a representative sample added and the dish re-weighed. The sample is then placed in an oven for three hours, placed in a dessicator and then re-weighed once the sample has reached ambient temperature.

Three types of ovens can be used, a vacuum oven at 508 – 635 mm Hg and 80 - 85°C, a forced draft or a convection oven at 105°C.

2.6.3.3 Electrical Conductivity

This method uses conductive and capacitive sensors based on the difference between the dielectric constant of water ($\varepsilon = 80$ faraday/m) and dry substances ($\varepsilon < 10$ faraday/m), with the variation in water content invoking a variation in conductance or capacitance of the materials. It has been shown that the dielectric constant is a factor of composition, impurities in the sugar crystals, the temperature, and the presence of the supersaturated film on the surface of the crystal. A variation of 1°C produces a 0.1% change in the reading of water content where conductive sensors are used (Shahhosseini, unknown) .

2.6.3.4 Infra Red Measurement

This technique is based on the principle that infra red (IR) radiation is absorbed by water and when a material absorbs IR, the amount it absorbs is proportional to the moisture content of the material. The moisture of the material can be determined based on the attenuation of the wave, which is transmitted through the material (Shahhosseini, unknown) .

This technique is influenced by the surface conditions of the crystals, the particle size, colour, composition, temperature and humidity. Another limiting factor is that because the

absorption rate is high and the wavelength is small, the penetration depth into the sample cannot be more than several millimeters, limiting it to a surface moisture measuring device (Shahhosseini, unknown) .

2.6.3.5 Microwave Technique

The microwave technique is an experimental technique that deals with the changes induced on a sample by irradiation and not a change in the radiation itself (Shahhosseini, unknown) . The amount of energy stored after a certain period of irradiation is measured and can be related to the attenuation of the wave, and how effectively microwave power has been transmitted to the material.

Unlike other microwave techniques, this method uses high power microwaves, which eliminates the effects of ion levels and hydrogen bonds. This is because regardless of how strong the bonds or high the impurity level, there is still excessive or sufficient amounts of microwave to stimulate and rotate the water molecules. This results in an increase of the water molecule kinetic energy and therefore temperature, so the higher the moisture content the more energy is absorbed and the higher the temperature. If the microwave frequency used is close to the resonant frequency of water, the amount of energy absorbed by the impurities and the crystals themselves is small compared with that of the water, so the energy absorption can be attributed to the water content (Shahhosseini, unknown) .

2.6.3.6 Karl Fischer Titration

This technique involves dissolving the sample in a special solvent, releasing all of the moisture in the crystal. The amount of moisture released is then determined by titration, with the principle of the titration being based on a reaction between specific reagents like formamide (Bruijn and Marijnissen, 1996), or sulfurous acid anhydride and iodine (Roge and Mathlouthi, 2000).

It has recently been shown that it is possible to use this technique to determine the three different types of water in the crystal (Roge and Mathlouthi , 2000).

The equipment is calibrated using sodium tartrate (dihydrate) as a standard. The total water content is then determined by dissolving a sample at high temperature (50°C), using a modified methanol – formamide solvent (2/3 – 1/3 (v/v)).
The surface water is then determined by saturating the previously used solution with sugar and then repeating the titration. The water occluded in the crystals is then found as the difference between the total and surface water contents.

2.6.3.6.1 Karl Fischer moisture content for standard grade sugar

Roge and Mathlouthi (2000) used the Karl Fischer titration method to determine the internal, surface and total water content for 800 μm screened commercial grade sugar.

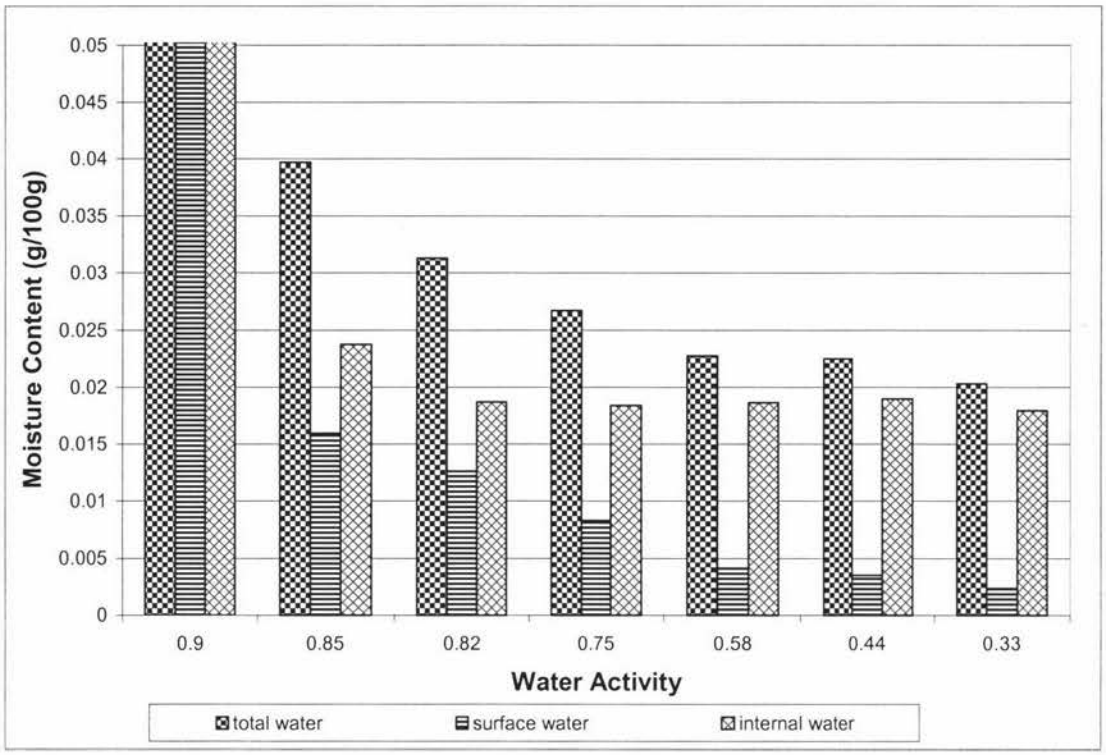

Figure 2.9 Moisture content for standard grade sugar (Roge and Mathlouthi , 2000)

The total water, surface water and internal water at 90% ERH are 5.246%, 5.0579% and 0.1881% respectively.

2.6.4 Water Activity

Water activity describes the condition or relative availability of water for any number of actions and reactions in the material, and may bear little or no relationship to the amount of water present in the system (Troller, 1983).

When at equilibrium with the surrounding environment, the water activity (a_w) is related to the relative humidity by equation 2.12 (below).

$$A_W = \frac{p}{p_0} = \frac{\text{relative humidity}}{100}$$ equation 2.12

where p is the water vapour pressure exerted by material and p_0 is the vapour pressure of pure water at temperature T_0, the equilibrium temperature for the system.

Water activity can also be expressed in terms of solute concentration through its relation to Raoults law:

$$A_W = \frac{n_2}{n_1 + n_2}$$ equation 2.13

where n_1 is the number of moles of solute and n_2 is the number of moles of solvent.

2.6.4.1 Water Activity Measurement

There are many methods for measuring the water activity of a material. These range from vapour pressure manometers (VPM), which measures the vapour pressure of a sample compared to the vapour pressure of water. Other hydrometers, such as dew point hydrometers, work by directing an air stream in equilibration with a sample at a cooled mirror. The point where condensation first starts to form on the face of the mirror, the dew point, is related to the equilibrium relative humidity and can be determined from the use of psychrometric charts (Troller , 1983).

2.7 Sorption Isotherms

For any material, adsorption curves can be found by placing a dry material into an atmosphere of increasing humidity and measuring the increase in weight due to water uptake. Similarly desorption curves can be found by putting a wet material into a low relative humidity environment and measuring the weight loss (Iglesias and Chirife, 1982). The difference between these two curves at different humidities is called hysteresis, which has been proposed by Chinachoti and Steinberg (1986a), to be due to amorphous sucrose.

At equilibrium, a thermodynamically stable situation will evolve and a single equilibrium isotherm will exist, this being the sorption isotherm (Troller , 1983).
These sorption isotherms show the equilibrium relationship between the moisture content of a substance and the water activity at constant temperatures and pressures (Iglesias and Chirife, 1982).

For food materials, moisture sorption isotherms are generally used to predict the microbial and physiochemical stability of foods, determine the end point of food dehydration and to predict sorption isotherms at different temperature by using two or more isotherm graphs (Iglesias and Chirife, 1982).

2.7.1 Determination of Sorption Isotherms

Many methods have been described for measuring the sorption isotherms of foods. Many of these methods have been reviewed by Gal (1975), with most of the methods utilising one of three basic approaches;

- Measurement of moisture content of samples in vacuum dessicators containing saturated salt solutions at atmospheric pressure, which give a certain relative humidity. Water activity can then be measured at different relative humidities.
- Measurement of the vapour pressure of the air in equilibrium with a food at a given moisture content, with a sensitive manometric system.
- Inverse gas chromatography, where a column is packed with the food powder as the stationary phase. This allows the investigation of low water activity levels up to one order of magnitude lower than the other two techniques.

2.7.2 Crystalline Sucrose Sorption Isotherm

Many sorption isotherms have been reported at different temperatures using the different methods discussed above. The results from the different methods vary, especially the chromatography method. For this reason, and the availability of equipment, the first two techniques outlined will be used to measure sucrose sorption isotherms.

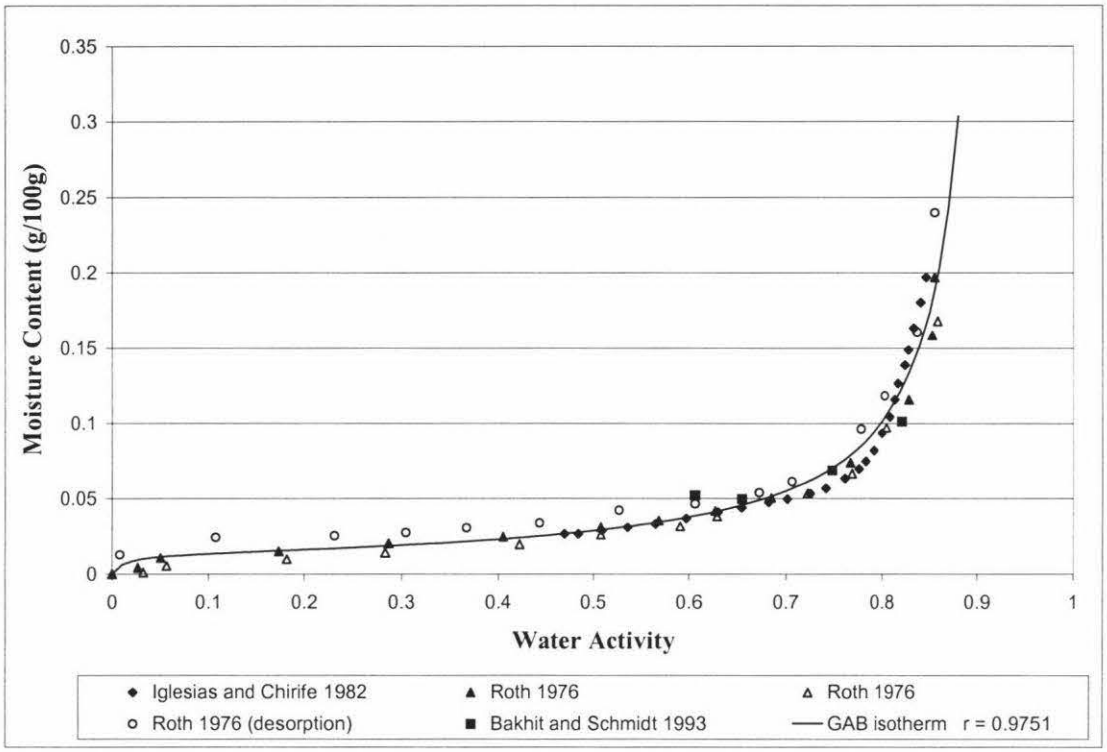

Figure 2.10 Moisture sorption isotherm for crystalline sucrose

Where the a, b and c coefficients for the GAB isotherm data (detailed below), are –0.0125, -29.0078 and 1.037 respectively.

As it can be seen from the graph, the GAB isotherm model fits the literature data for the crystalline sugar isotherm at 20 °C, and will be used to represent this data.

2.7.3 Amorphous Sucrose Sorption Isotherm

Due to the extensive studies being carried out in the food industry into the properties of freeze dried foods such as collapse and glass transitions, amorphous sucrose isotherms are well documented.

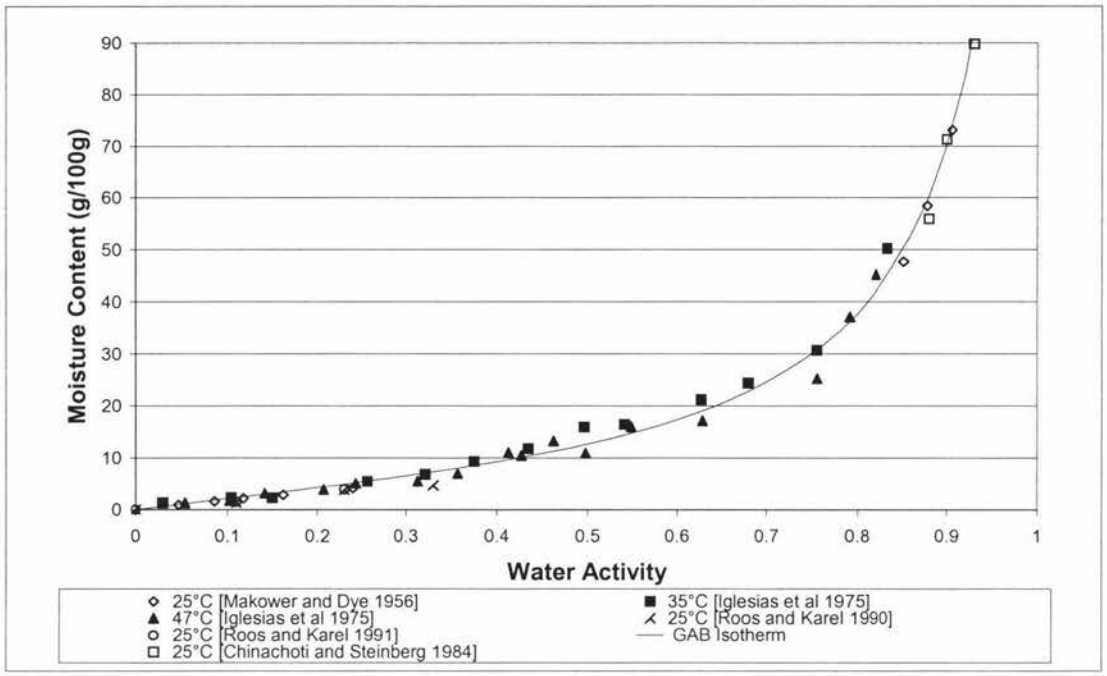

Figure 2.11 Moisture sorption isotherm for amorphous sucrose (Foster , 2000)

The coefficients for the amorphous GAB isotherm (a, b and c), are 9.4905, 0.9696 and 2.3562 respectively.

As with the crystalline sucrose, the GAB isotherm shown represents the data well, and so it also will be used as the amorphous sucrose isotherm. It is important to note the difference in the Y axis scale between the crystalline sucrose isotherm (figure 2.10, page 2 – 21), and the amorphous sucrose isotherm shown in figure 2.11. At a water activity of 0.9, the amorphous isotherm shows a moisture content of close to 200 times that of the crystalline absorption isotherm.

2.7.4 GAB Sorption Isotherm Model

The GAB (Guggenheim – Anderson – De Boer) model is a true kinetic model formulated from first principals. It describes the sorption of a gas to a free solid surface and then a Langmuir type absorption layer onto specific sites on the surface, with condensation on the subsequent layers (Bronlund 1997).

Ideally, the constraint parameters of the model (a, b and c), which represent the physical properties of the material, should be determined independently. This is difficult, so the model is generally fitted against experimental data.

$$Y = \frac{a.b.c.A_W}{(1-b.A_W).(1+(c-1).b.A_W)}$$ equation 2.14

Gekas (1992), described the advantages of the model as;

- having a viable theoretical basis
- describes the sorption behavior of nearly all food for $0 < a_w < 0.9$
- is of simple mathematical form
- it is able to describe some temperature effects by means of an Arrhenius relationship

As it can be seen from the experimental data for the crystalline and amorphous sorption isotherms, the GAB model is a good approximation for the absorption of moisture onto the particles, and the GAB isotherm will be used to describe these isotherms when required in the mathematical modelling.

2.7.5 Sorption Rates

The rate of moisture sorption onto sucrose is important when trying to understand the movement of moisture that occurs in bulk sugar. Knowing the sorption rates will also help the understanding of drying, conditioning, and caking.

These rates will be determined experimentally using a technique described by Bronlund (1997), to determine the sorption rates of α-lactose monohydrate and amorphous lactose.

The apparatus consisted of a plastic chamber with tubing around the bottom that would allow air of a constant relative humidity to be sparged inside. This chamber surrounded the weighing plate of a set of scales, on which a sample covered with a lid was placed. The chamber was allowed to reach steady state at a predetermined relative humidity. The lid was then removed, introducing the sample to a humidity step change, and the change in the samples weight recorded with time.

This experimental technique was used to measure the sorption rate onto packed beds of lactose, in order to show that the sorption process was not limited by the diffusion of moisture onto the particle, but the diffusion of moisture into the packed bed.

2.8 Caking and Caking Mechanisms

2.8.1 Humidity Caking Mechanism

Temperature gradients within the bulk sugar will cause a migration of moisture to occur, creating areas of higher relative humidity. Due to the hygroscopic nature of sugar, moisture is absorbed from the higher relative humidity environment allowing dissolution of the crystal surface (Bronlund , 1997). This creates a syrupy film on the surface of the crystal (Ludlow and Aukland , 1990) and surface tension effects cause capillary condensation to occur, which forms liquid bridges of saturated sugar at the points of contact between the crystals, "lumping" the sugar.

If the lumped sugar is then exposed to air of lower relative humidity, desorption will occur, the saturated liquid bridge will become supersaturated and crystallise, forming solid bridges between the crystals (Bronlund , 1997). The strength of the subsequent solid bridge far exceeds that of the liquid bridge, with the solid bridge formation process being accelerated by a drop in temperature, as the rate of crystallisation will increase, reducing the time required for solid bridges formation. This is especially a problem in environments that have a high daily temporal shift (Ludlow and Aukland , 1990).

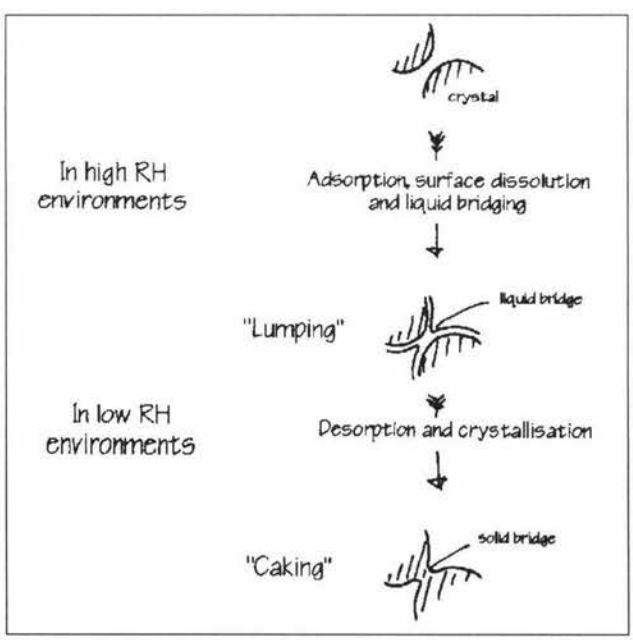

Figure 2.12 Humidity caking mechanism (Bronlund , 1997)

The strength of the solid bridge can be strong enough so that sometimes the forces encountered during transportation are not enough to break them (Ludlow and Aukland, 1990).

The high relative humidity environments are created by temperature gradients, which can be easily set up under bulk storage conditions (Bagster, 1970).

Temperature gradients can arise from two main situations:

1) placing hot sugar from the drying stage on top of sugar that has been left in the ambient environment, or conditioned at a lower temperature and allowed to cool (Bagster, 1970)

2) in places with a low ambient temperature placing sugar directly into storage silo, creating a temperature gradient between the sugar and the silo walls (Ludlow and Aukland, 1990).

2.8.2 Amorphous Caking Mechanism

Amorphous caking is thought to be possible when a significant level of amorphous material exists on the surface of the sugar crystal. If moisture is absorbed and/or the temperature of the environment increases, the amorphous sugar can undergo a glass transition. The now more labile amorphous sugar can flow toward the points of contact between the crystals because of surface tension forces, forming a rubber bridge (Bronlund , 1997). Sugar in this state is described as "sticky" rather than "lumped" because of the higher viscosity of the amorphous solution compared with the saturated solution.
If the amorphous sugar remains above its glass transition temperature for extended periods of time, or if a critical moisture content is allowed to be reached, then crystallisation will occur. As with the humidity caking mechanism described above, this forms solid inter-particle bridges with a far superior strength to the liquid/rubber bridges.

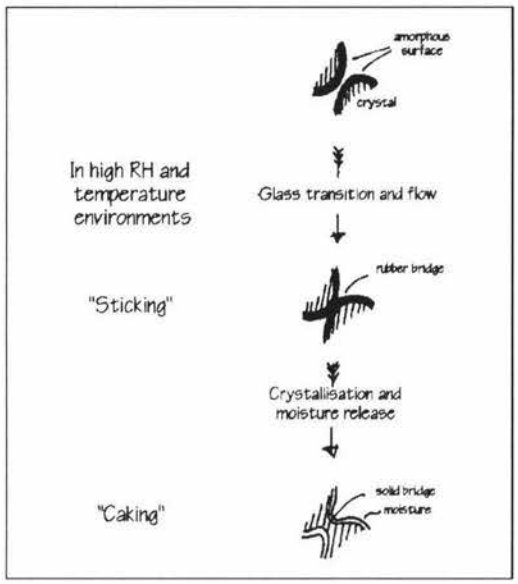

Figure 2.13 Amorphous caking mechanism (Bronlund , 1997)

2.8.3 Caking Strength Quantification

The ability to be able to quantify the degree to which a sugar has caked is important when testing the conditions under which caking occurs. Tests should be quick, easy to perform and be able to be carried out nearly anywhere in the process.

Most of the caking tests measure the ease of flow either by tilting the container until the material flows out (from a test tube or an agar dish (friability)) or by measuring the angle of the sides of a sample that has been poured out (angle of repose).

2.8.3.1 Penetrometer

A modified version of the penetrometric test used by Baker and Mai (1982), was used by Bronlund (1997), to quantify the degree of caking in lactose powders.
The modification made was to use thirty-two 1mm diameter pins pressed into a plastic disk, in a regular circular pattern to a constant depth. This provided enough strength so that the pins did not bend or dis-align, effectively creating a multi point penetrometry technique.

The pins were mounted onto a probe that was connected to a counter weight system, which allowed the probe to be set up weightlessly above the sample. Weights were then added to the top of the probe, and a force – distance penetrated table recorded until a breakthrough was observed.

2.8.3.2 Blow Test

This test was developed by Paterson and Bronlund (2000), to measure the caking strength of milk powders.

The blow test involves blowing air over the powder through a tube of fixed diameter, at a set distance above the powder until the surface breaks up. The airflow for this to occur is taken as an empirical strength measurement.

A similar test was described by Bagster (1970), to measure the caking of stored coal, using airflow to dislodge the coal particles.

2.9 Modelling of Moisture Migration

By being able to predict how moisture will move under specific conditions it is possible to predict the onset of caking and therefore be able to monitor process conditions and prevent this from occurring.

This allows for the optimisation of the process, saving money in both plant efficiency and reduction of wasted product.

2.9.1 Modelling of Caking in Bulk Lactose

The model formulated by Bronlund (1997), to predict and minimise the effect of caking in the production of bulk lactose was based on the principle of moisture migration due to temperature gradients within a bulk in storage.

The model was formulated by describing how one dimensional moisture transport could occur due to a temperature gradient, and using that to predict how moisture would move in a cooling bag. The model could then be used to predict when critical moisture values would occur under a described set of conditions, and cause caking.

The conceptual model used is shown in figure 2.14

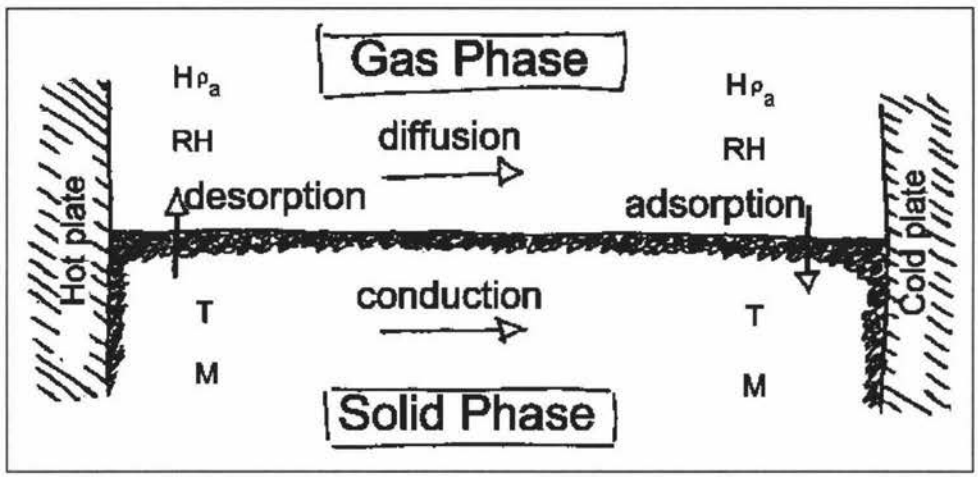

Figure 2.14 Concept for moisture transport model (Bronlund , 1997)

The physical basis of the model was summarised as;

- one dimensional heat and moisture transport through a packed bed
- initially lactose has a constant moisture content throughout the bed
- a temperature gradient is applied across the bed
- the solid and gaseous phases are considered as continua with interaction over adjacent surfaces
- moisture diffusivity and thermal conductivity are treated as effective properties of the porus matrix.

One of the assumptions that were made in the formulation of the model was that the diffusion process was instantaneous, as proved by the sorption rate experimental work described above.

It is unclear as to whether this assumption can be made when modelling moisture transportation in bulk sucrose. In a model for the conditioning of refined sugar presented by Meadows (1994), a comparison of the rates of four processes considered to be occurring during conditioning were calculated in order to find the rate limiting process.

The four mechanisms are:

1) the crystallisation of the sucrose molecules in the supersaturated film, liberating water molecules and diluting the film
2) the evaporation of the water molecules at the interface between the surface of the film and the proposed solid amorphous outer layer
3) Water molecules diffusing through the porous amorphous layer in the vapour phase
4) The stripping of the water molecules from the outer surface of the amorphous layer by a combination of diffusion and convection into the bulk interstitial air

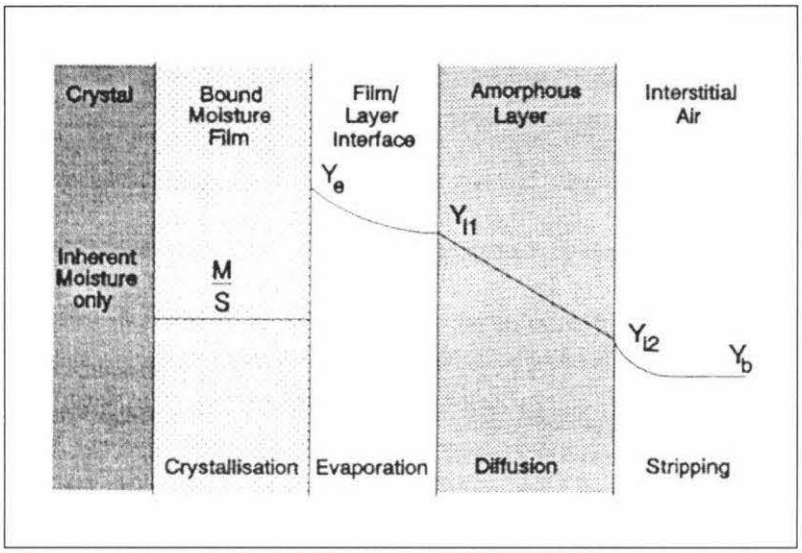

Figure 2.15 Theoretical conditioning model (Meadows , 1994)

The calculation of the rates for these four processes was based on a "typical" crystal being conditioned in air at 40 °C with 20% relative humidity.

The reported rates were 4.4 seconds for the crystallisation process, 0.12 seconds for the evaporation and stripping processes (approximated by an equation for the rate of drying) and 12101 seconds for the diffusion process.

With the time for the diffusion process being so large and therefore rate determining, the other processes were considered to be infinitely fast in comparison and therefore ignored.

The concept of crystallisation occurring and the molecules migrating and assimilating onto the amorphous layer on the surface of the film (effectively meaning the crystal grows from the outside in), is a theory that sways from the ideas of most authors. The popular theory is that the film dissolves the amorphous surface layer, with molecules migrating through the film to the main lattice. Is it realistic for water in the vapour phase to take 12101 seconds (3.361 hours), to diffuse through a layer of porus amorphous 1×10^{-5} m thick?

If this model cannot be ignored then it will not be possible to make the assumption that the diffusion process is instantaneous, meaning that the model presented by Bronlund (1997), may need to be modified to allow time for the diffusion process to occur.

A way to test this could be to modify the model to include a time delay for the diffusion process, compare this to a model with no time delay and see how they compare to actual conditions encountered when conditioning.

Closure

From the data presented in the literature it appears that some conformation work for certain parameters will be necessary. The sorption isotherm for sugar at 20°C is fitted well to the GAB isotherm, but there are indications that there may be some temperature dependence on the isotherms, which will need to be investigated. It will also be beneficial to construct an isotherm that focuses on the absorption at higher water activities at temperatures of 45°C and 35°C, the temperatures of the sugar leaving the dryers and the conditioning silo.

The first step will be to validate the amorphous layer theory presented by Meadows (1994). This can be done by using several of the methods described above, starting with the least sensitive (gravimetric) and moving up to the most sensitive (micro-calorimetry).

From here the model used by Bronlund (1997) can be modified where necessary and applied to the sugar refining conditions experienced at New Zealand Sugar. The model will provide insight as to what storage and transport conditions will need to be maintained in order to reduce or prevent the occurrence of caking of bulk sugars.

CHAPTER 3

Crystalline and Amorphous Sorption Rates

Introduction

Irrespective of caking mechanism, two important processes are the diffusion of water vapour through the packed bed and the sorption of water into the sugar. Bronlund's model assumes that absorption is rapid compared with diffusion. Meadows indicated that the diffusion process of moisture leaving a trapped layer of supersaturated (or amorphous) sucrose was not instantaneous and may be rate limiting. In this chapter, the rates of absorption and diffusion were investigated for sucrose to confirm whether this assumption was valid.

3.1 Sorption rate model

Paterson *et al* (2001), formulated a model to predict the adsorption rates of moisture onto packed beds of lactose with differing degrees of amorphous content. The model had the form of an equation solved by Crank (1964). This was modified to include a factor to account for the characteristics of a bed with an amorphous content.

$$\frac{M_t}{M_\infty} = 1 - \sum_{m=0}^{\infty} \frac{8}{(2m+1)^2 \pi^2} \exp\left[-\frac{D}{1+k} (2m+1)^2 \pi^2 \frac{t}{4l^2} \right] \qquad \text{equation 3.1}$$

The k′ value is the reaction rate constant for the model, and the validity of this model is dependent on being able to make an assumption that a linear fit for k′ can be applied to the sorption isotherm over the RH range that is being used.

The diffusion model calculates the fraction of unaccomplished change in the mass average moisture content (M_t / M_∞) in a bed of material at time t. In this work the model has been used to predict the moisture adsorption profile for samples of sucrose in packed beds with, and without, amorphous sucrose present.

3.2 Free diffusion model k′ value

The k′ value in the model represents the reaction rate constant for the free diffusion model, and is a function of porosity (ε) and the slope of the sorption isotherm for the material ($n^{/}$).

$$k^{/} = \frac{1-\varepsilon}{\varepsilon.\rho_a}.\rho_s.n^{/} \qquad \text{equation 3.2}$$

Work done by O'Donnell (1998) showed that k′ was a function of the absolute humidity (H), of the system and would therefore change, so for the free diffusion model to be valid the value of k′ needs to stay relatively constant. O'Donnell (1998), proved that if the moisture sorption isotherm for the material was linear over the relative humidity range being investigated, then the k′ value would remain constant enough for the model to be valid.

The initial sorption rate experiments for the crystalline sucrose was carried out over a 0 – 40% relative humidity range. From the sorption isotherm over this range the predicted moisture uptake was calculated at 0.023 g of moisture per 100 g of sugar. Because of the limited capacity of the equipment and not wanting the sample in the dish to become too deep (> 10mm), the sample size was limited to 10 grams. This would correspond to a moisture uptake of 0.0023g, which is not reproducibly measurable from a four decimal place scale. To avoid this problem it was decided to carry out the experimental in the range of the absorption isotherm where the rate of moisture uptake was large, so that a small sample would absorb a measurable amount of moisture.

The 0.8 – 0.9 water activity range was chosen, as the predicted moisture increase for the 10g sample would be 0.05g, which is measurable on four decimal place scale. The linearity of this region for the k′ assumption was not as good as the 0 – 0.4 Aw region, but it was seen to be acceptable under the circumstances.

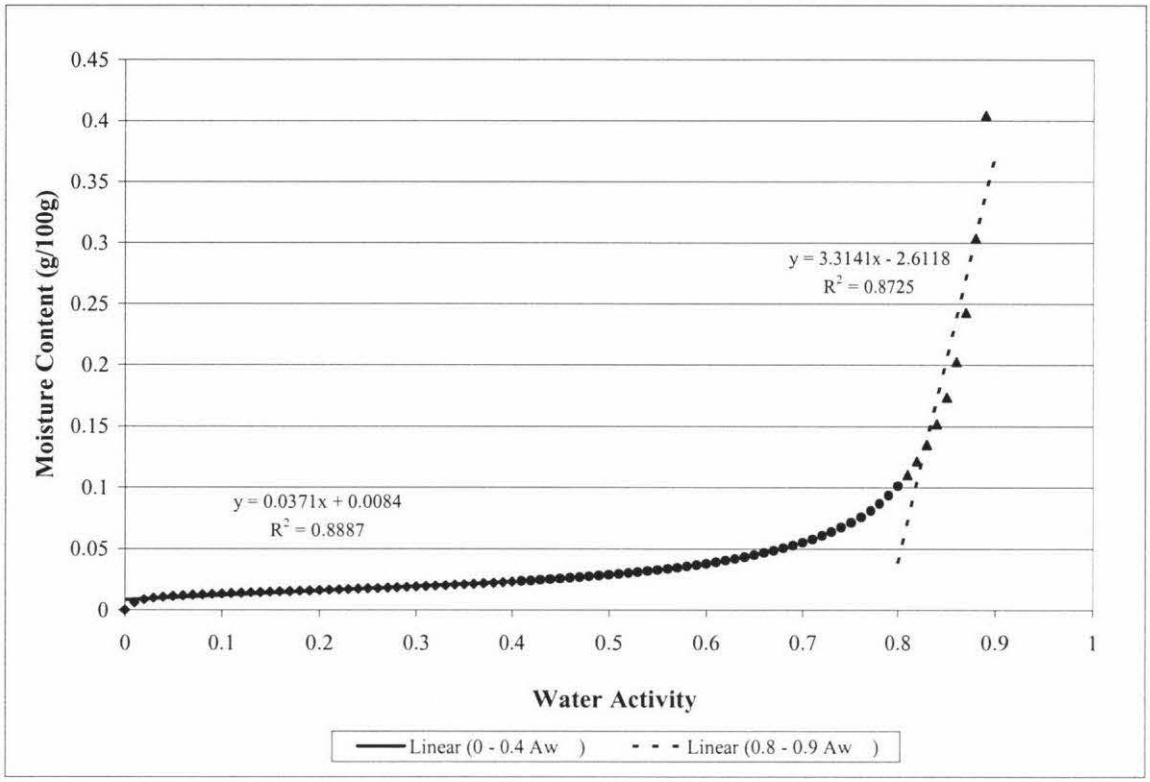

Figure 3.1 Crystalline isotherm linear assumption for k parameter

Due to the extremely hygroscopic nature of the amorphous sucrose the 0 – 0.4 water activity range presented no measurability problem, with the predicted moisture increase calculated at 0.928g for a 10g sample.

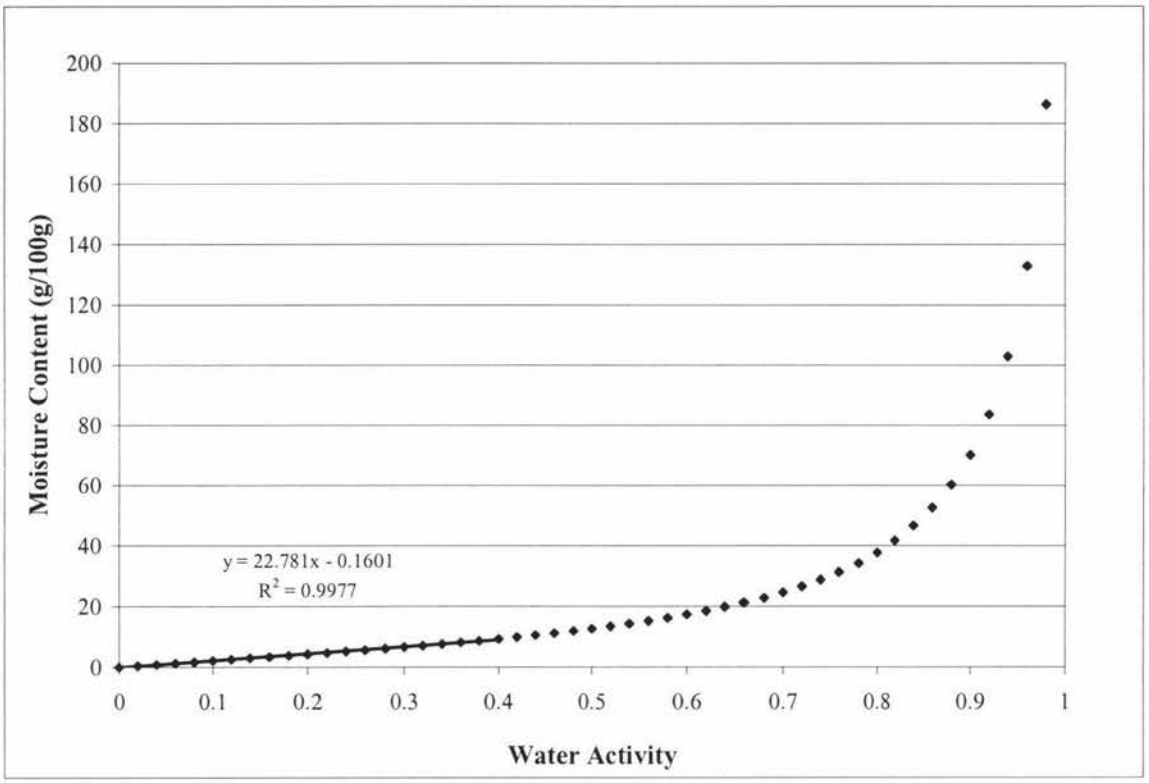

Figure 3.2 Amorphous isotherm linear assumption for k′ value.

The linear fit for the amorphous GAB isotherm is very good, with a R^2 value of 0.9977 compared to the crystalline linear line, which has a value of 0.8725. This would suggest that the sorption model for the amorphous sucrose should predict the experimental data better than the crystalline experimental data.

3.3 Crystalline sorption rate experimental

In order to ensure that the sugar had no moisture it was placed in a vacuum oven at 80°C for three hours and then stored over P_2O_5 for several days, to allow it to return to room temperature, therefore ensuring complete dryness. 10g of the dried sugar was then placed in a moisture dish and spread out as evenly as possible and smoothed to the top of the container with the back of a knife to form the packed bed. By keeping reasonable bed depths (~10mm) we can get a good idea of the relative rates of the adsorption and diffusion process while not having exceptionally large experimental times.

A Mettler Toledo dew point generator was used to provide the humidified air to the chamber enclosing the scale weigh table. A PC based program, CATT 2 (computer aided thermodynamic tables 2), was used to predict the dew point at which the desirable relative humidity would be in the chamber based on the ambient temperature of the laboratory. In order to minimise the effects of ambient temperature on the experiment via

effecting the dew point, the majority of the experimental was carried out at night where temperature change would not be as extreme as during the day.

At the start of the experiment, the sample was covered with a lid and placed in the scales with the humidifying chamber over top. The dew point generator was switch on, and the chamber allowed time to fill with the humidified air. Once the relative humidity of the air became stable, the lid was removed and the sample introduced to a step change in relative humidity. The change in the weight of the sample over time was measured until no more moisture uptake was observed.

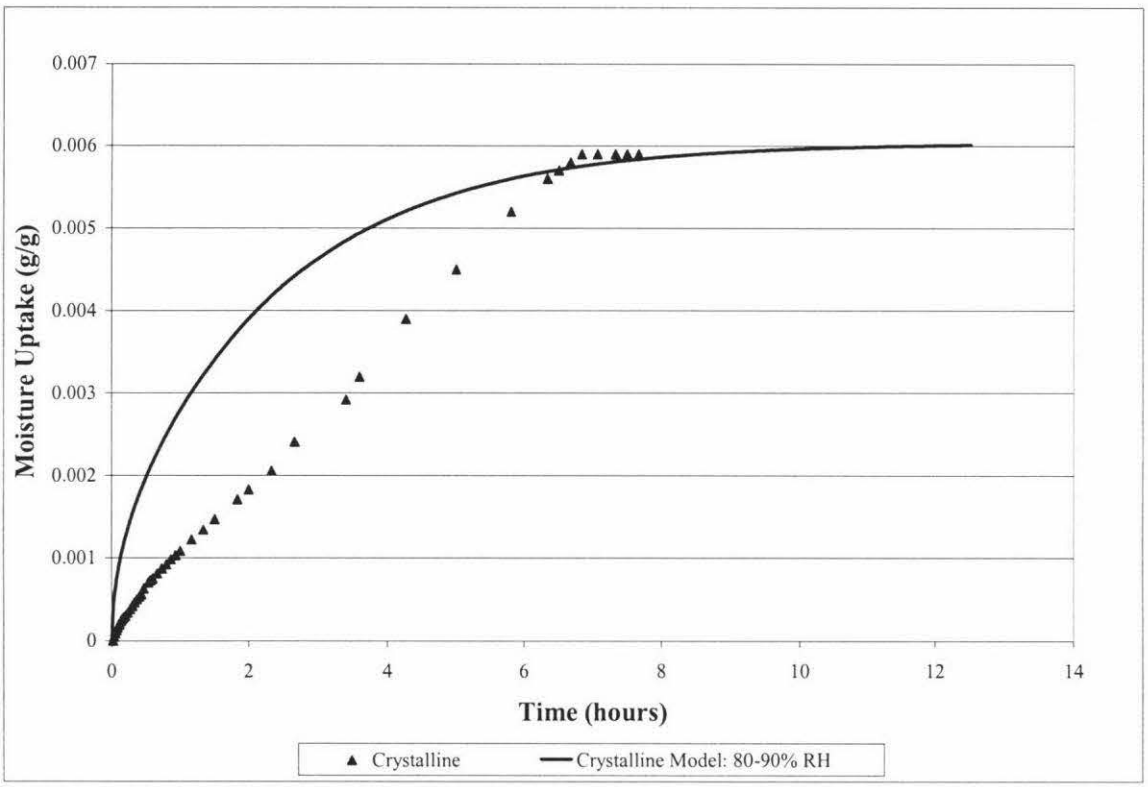

Figure 3.3 Experimental and model crystalline absorption profiles

The graph, representing equation 3.1 with the value for diffusion as 2.58×10^{-5} (Cussler and Crank, 1976), and the experimental data do not agree with each other. The model assumes that the adsorption of moisture onto the surface of the particles occurs much faster than the process of the moisture diffusing into the packed bed, and hence the diffusion process being the rate limiting process. The results here show that this is not the case for sucrose, and in fact the absorption of the moisture onto the surface of the particles is the rate limiting step, which at a relative humidity of between 80 and 90% is no surprise.

This means that for crystalline sucrose, the sorption process will be governed by the time taken for the surface to take up moisture, not any diffusion processes within or through the bed.

3.4 Amorphous sorption rate experimental

Amorphous sugar was prepared by spray drying a seeded 50% sugar solution at 160°C in an Anhydro LAB S1 spray drier fitted with a rotary disc atomiser. The product was initially checked under a polarising microscope for signs of light that would be let through spaces in a crystalline lattice, and therefore indicate that the sample had a degree of crystallinity. Once passing the initial inspection, the degree of amorphisim was then determined by mass balance gravimetric methods and later confirmed by thermal analysis. The sugar was calculated to be 70% amorphous, and it was decided that this would be sufficient to demonstrate the extremely hygroscopic nature of amorphous sucrose. This meant that it was possible to use the 0 – 40% RH range initially desired for the crystalline samples. From the isotherms it was predicted that a 10g sample would absorb 0.93g of moisture.

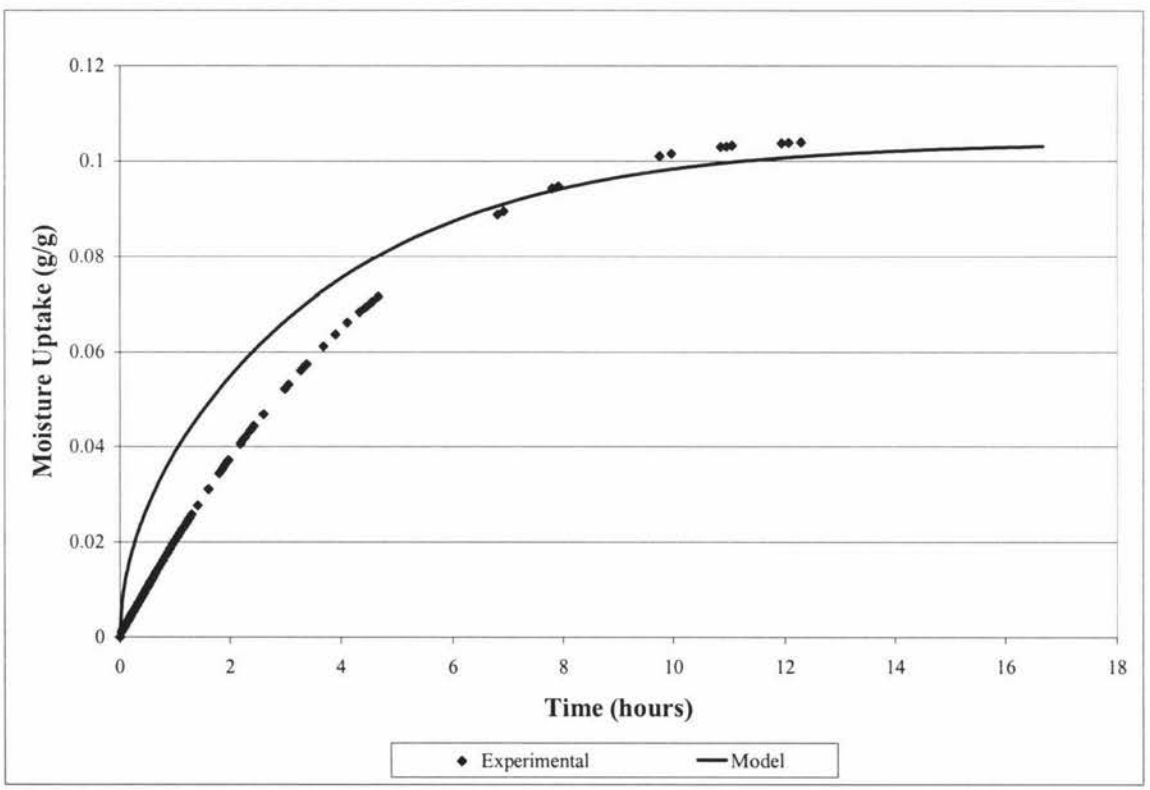

Figure 3.4 Experimental and model amorphous absorption profiles

It can be seen in figure 3.4 that the amorphous experimental data is better fitted by the model than the crystalline. However it is still slower at the start than the model predicts it should be. This indicates that the adsorption of moisture onto the individual particles is a significant factor in the time of adsorption.

This indicates that the model for moisture movement through a packed bed may need to be modified to accurately fit the experimental data.

3.5 Amorphous Recrystallisation

When the absorption of moisture onto the amorphous sucrose was allowed to continue until an equilibrium weight was reached, the final weight of the sample was lower than when it started due to the loss of moisture from the recrystallisation of the amorphous component of the sample.

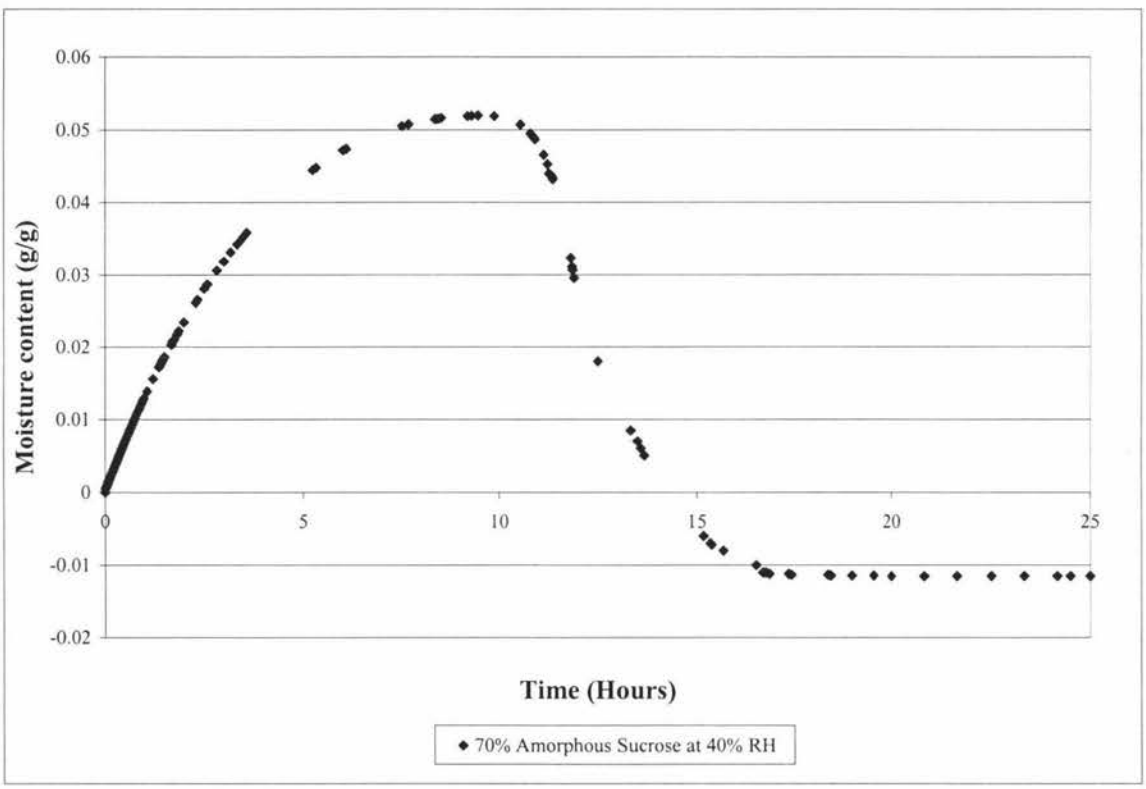

Figure 3.5 Complete moisture absorption profile for partially amorphous sample

The graph shows the rapid absorption of moisture followed by the release of moisture upon re-crystallisation. The re-crystallisation occurs because the moisture uptake lowers the glass transition temperature to below the temperature of the sample, which means that the molecules will have enough mobility to move past each other. Thus they will be able to align themselves and crystallise.

The re-crystallisation process was complete after a total of 16 hours and liberated close to 0.012g of moisture. This moisture would be free moisture in a packed bag, which can then liquefy the surface of the crystal, allowing the formation of liquid bridges between

the surfaces of the adjacent crystals. The extra moisture released into the air would then move to other parts of the bed allowing the process to continue and spread throughout the bed, lumping it.

Due to the time required for the sample to take up enough moisture for a glass transition to occur, the lumping process could occur during transportation. If the sugar was then left in storage there would be no movement and therefore no way for the liquid bridges being formed, to be broken up. Any further time spent without transportation would allow the liquid bridges to crystallise and form solid bridges, caking the sugar.

Closure

The free absorption model used assumes that the absorption of moisture onto the particles occurs instantaneously. The fit between the experimental results for the crystalline and amorphous samples indicates that there is a delay in the absorption of moisture onto the particles. This may effect the accuracy of the lactose model, and it may need modifying.

The moisture absorption profile for amorphous sucrose has shown that if moisture is available, sugar with an amorphous content will absorb it and undergo a glass transition, which could then lead to the caking of sugar in storage.

This stresses the importance of finding if any amorphous sucrose content is present after the conditioning process, as this will allow recommendations as to the effectiveness of the drying and conditioning processes currently in use, in order to prevent the caking of sugar in storage.

CHAPTER 4

Determination of Amorphous Content

Introduction

The amorphous caking mechanism requires amorphous sugar to be present. This chapter describes experiments to measure the amorphous content of the sugar and therefore determine whether the amorphous caking mechanism is likely to be significant. Gravimetric methods of measuring amorphous content will be used as a primary measure of the amorphous content of sugar sampled from different points in the sugar production process. A thermal activity monitor (TAM), will then be used to detect amorphous content to a limit of 0.1%, which is more accurate than any of the other methods described in the literature.

4.1 Gravimetric analysis

Mass balance and absorption – desorption methods were used to get an initial indication as to the degree of amorphisim of sugar at different points in the production process. The areas where sugar was sampled and tested were at the end of the centrifuging process, the bottom of each of the two driers, the bottom of the storage silo, and after the bagging process. These are the points in the sugar production process where moisture is removed, so measurements were made around these points to get an idea of the change in moisture content at these different stages.

4.1.1 Mass balance

The sugar taken from the different places around the sugar processing plant was placed in sealable plastic bags, which were then placed in another sealable bag to keep the relative humidity of the sample close to what it was when it was taken. The relative humidity of the samples was then measured and the samples placed in a vacuum oven at 105°C for three hours to ensure dryness, and then placed over P_2O_5 until ambient temperature was reached. The dry weight was then measured using a Sartorius BP1201S, four decimal place scale.

Using the crystalline and amorphous sorption isotherms at the measured relative humidity the degree of amorphisim was calculated using equation 2.6.

Sample	Measured Relative Humidity	Moisture loss g	Percent amorphisim
Mid Drier	0.585	0.03792	0.0109
Post Drier	0.583	0.0391	0.0195
Post Silo	0.592	0.0387	0.0107
Post Bagger	0.589	0.03741	0.0051

Table 4.1 Gravimetric mass balance degree of amorphisim

There was a very small measured degree of amorphisim detected using the four decimal place scales, however the accuracy of the measurement was effected by the limitation in sample size due to the sensitivity of the scales. Using the limit of this sensitivity, and the sample size at the relative humidity used (~59%), the expected moisture uptake for a sample with a particular amorphous content was used to calculate the limit to which the gravimetric technique could be reliably measured down to. This was calculated at close to 1%, indicating that the results obtained only showed that there was no significant amorphous content at the one percent level.

Given that the amount of potential moisture release from one percent of amorphous sucrose in a sample is still large compared to the total moisture in the crystalline sample, it is necessary to get a more accurate representation of the exact quantity of the amorphous sucrose of the samples.

4.2 Thermal Activity Monitor

4.2.1 Introduction

The TAM instrument is capable of detecting very small heat flows (± 50 nW) produced or absorbed by a chemical or physical reaction. The TAM consists of an extremely well controlled water bath (± 0.0001°C), with four independent calorimeters available for use at any one time.

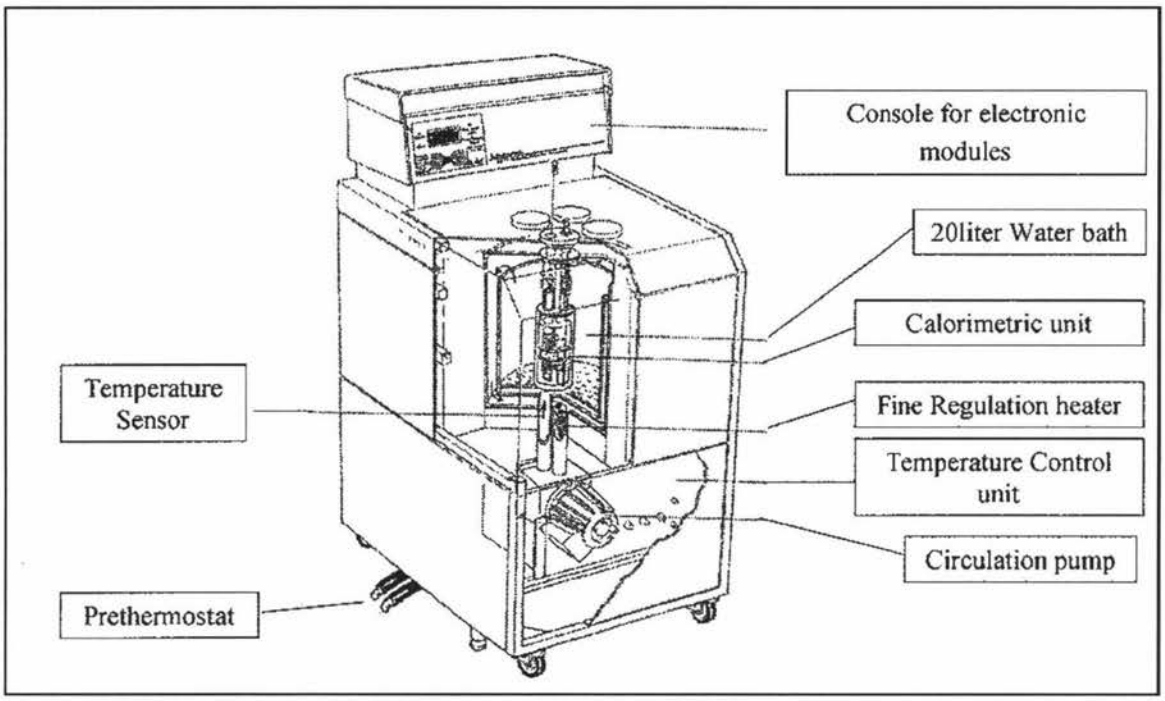

Figure 4.1 TAM Micro-calorimeter

4.2.2 Principal of operation

The TAM is a heat conduction calorimeter. Heat conduction calorimeters measure the heat flow between the reaction vessel and the surrounding environment (which is at a constant temperature) and is measured via a thermopile.

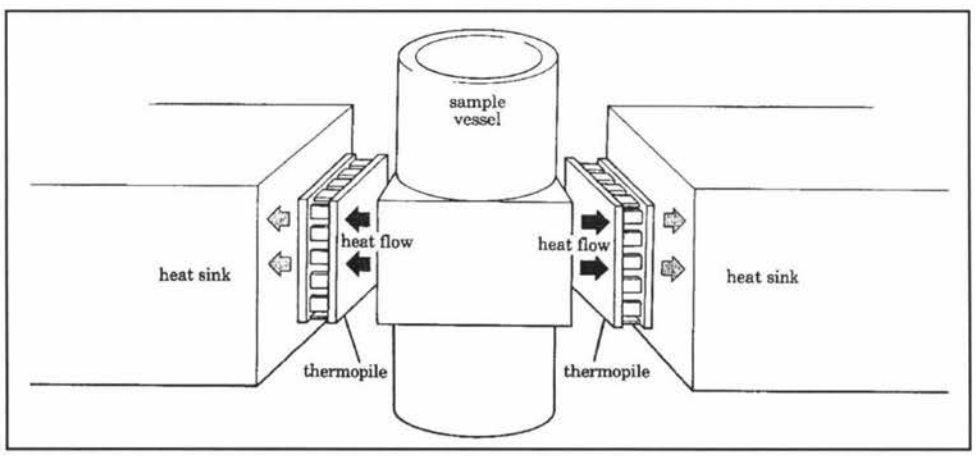

Figure 4.2 Heat conduction principal

Each micro-calorimeter unit contains two ampoule holders surrounded by a pair of thermopile heat sensors in contact with a metal heat sink. One holder contains a sample

and the other a reference, to allow heat capacity effects of the sample holders to be compensated for. When a reaction occurs in the vessel, heat is either generated or absorbed, creating a temperature difference across the thermopiles. This temperature difference is registered by the TAM as a voltage difference, which is then related to the heat flow from the sample.

No significant thermal gradient exists inside the reaction vessel and heat flow follows the Tian equation. Measurements are carried out using the twin heat conduction principal (sample and reference).

The Tian equation is derived from the following balance

Rate of heat production	=	Heat-flow to surrounding	+	Rate of temporary heat accumulation

The equation combines a heat balance around the system with the voltage that will be induced over the Peltier elements.

$$\left(\frac{dQ}{dt}\right)_M = \frac{k}{g}V + \frac{C_p}{g}\frac{dV}{dt} \qquad \text{equation 4.1}$$

There are three methods that can be used to measure the heat of reaction, closed ampoule, controlled relative humidity perfusion, and microsolution. The closed ampoule method was used for the experimental as it provided the most controlled environment for the nature of the work that was being investigated.

4.2.3 Closed ampoule method

4.2.3.1 Introduction

This method is based on the principal that all processes occur and are measured in a closed system. A sample is placed in a glass ampoule and a small open tube containing a saturated salt solution is inserted into the ampoule to achieve a desired relative humidity. The ampoule is then sealed with a teflon covered rubber disk, and the salt solution absorbs/desorbs water until equilibrium is reached. At equilibrium a number of reaction can occur including crystallisation, dissolution, or degradation.

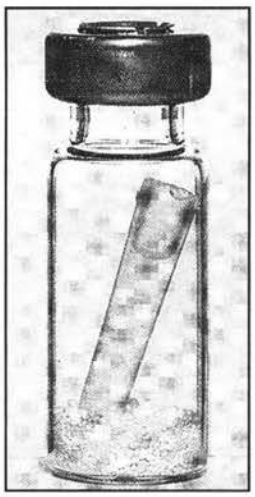

Figure 4.3 Glass ampoule and sample

After thermal equilibrium is reached the sample is placed into the thermopiles and the heat of the subsequent reaction measured.

In order for amorphous sugar to be detected by the TAM, it needs to recrystallise, releasing the heat of crystallisation. For this to occur the RH of the sample must be such that the glass transition temperature of the amorphous part of the sample is lower than the temperature that the TAM is at. To ensure that the reaction proceeded as quickly as possible and that a glass transition and crystallisation occurred in a reasonable time frame, a relative humidity of 87% was used.

4.2.3.2 Experimental method

The experimental work was carried out using the closed ampoule technique on a Thermometric 2277-001 Thermal Activity Monitor at the New Zealand Lactose Company, using a technique developed to measure the amorphous content of lactose.

In order to identify whether amorphous sugar was present in any significant quantities during different stages of the sugar production process, it was necessary to measure the thermal activity of a set of standard samples. The standards were prepared by adding varying weight percentages of spray dried amorphous to completely crystalline sugar. The completely crystalline sugar was prepared by taking sugar from out of the bottom of the second drier, exposing it to a high RH to recrystallise any amorphous content and then oven drying it for three hours at 105°C.
Sugar from this part of the process was used as the basis for the standard samples as it has not been through the screw conveyers, meaning that it should have the most uniform particle distribution and have no dust to alter the surface properties of the sugar. The sugar should also have no added amorphous content, as it has not been through the screw

conveyors (which can grind up and coat the crystal surface with a partially amorphous dust)

The TAM was set up to measure a power range of 0 – 1000μW. The Digitam software used to operate the TAM was started and the experimental method (ampoule) selected. The TAM was started and allowed to run a baseline.

During this time the sample to be measured was prepared.

To get an accurate as possible standard curve, samples of 0.1, 0.25, 0.5, 0.75, 1 and 2 weight percent amorphous content were prepared. This standard curve would then be used to determine the degree of amorphisim of sugar samples from different places in the production process.

For the standard samples approximately 2.0g of sugar was placed into a 20ml glass ampoule and the corresponding weight percentage of amorphous sugar added. A Durham tube was three quarter filled with a saturated potassium chloride solution (87% RH) and placed into the ampoule with the sugar sample. The ampoule was then sealed and wiped to remove any traces of oil or moisture from the surface.

Sugar for the experimental samples were taken from four different locations during the production process. These were at the end of the first and second driers, the bottom of the storage silo, and after the bagging station. The sugar sample was taken and placed in a sealed bag with as much of the air as possible removed. The bag was then placed in another sealed bag, so to keep the sugar as close to the state it was in when sampled. The experimental samples were prepared in the same manor as the standards, without the addition of the amorphous material. To prevent re-crystallisation occurring prior to being measured, all samples were prepared directly before measurement was to take place.

Once the sample was prepared the TAM was changed from baseline mode into equilibration mode, and the standard and reference lowered into the equilibration position within the TAM. After this time the TAM was set to experimental mode and the sample and the reference lowered slowly into the TAM and the power generated by the re-crystallisation of the amorphous material in the standard measured.

4.2.3.3 Results and discussion

The curve for the sucrose with no amorphous content (ie sugar used as base for amorphous standards) area was found and used as a baseline for the sugar samples. This baseline peak is shown in figure 4.4 (page 4 – 7).

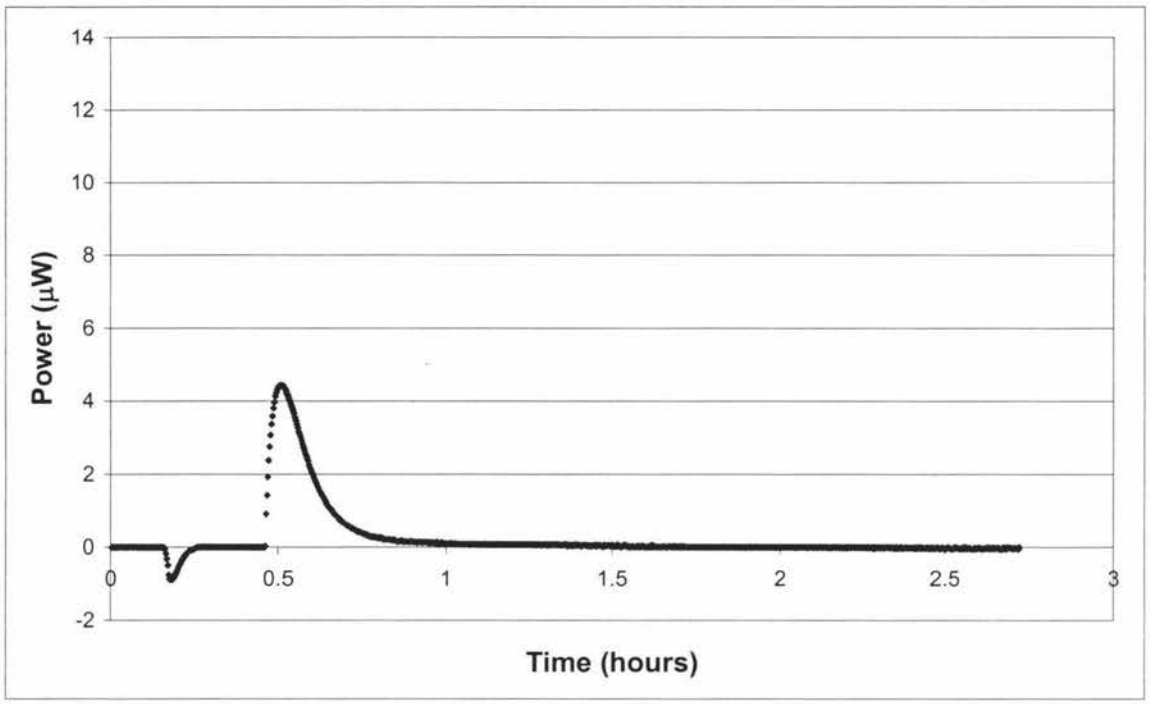

Figure 4.4 Baseline curve for sugar with no amorphous content

The initial peak is formed by the lowering of the sample and reference into the equilibration position. The second baseline peak is caused by the lowering of the sample and the reference into the measurement position, which occurs after only several minutes.

Figure 4.5 (page 4 – 8), shows a typical TAM graph for the standard samples measured, noting that the scale of figure 4.5 is 100 times that of figure 4.4.

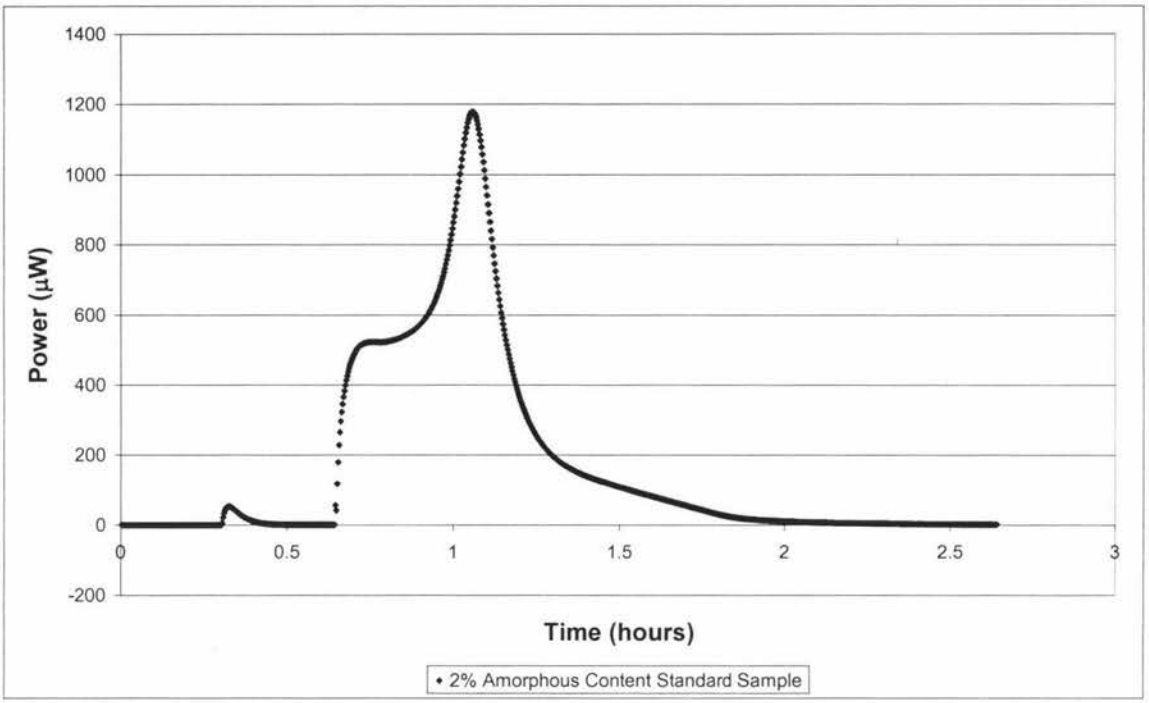

Figure 4.5 Typical TAM graph for amorphous sucrose standard

The graph shows the different process occurring during the measurement process. The first section is linear and represents the baseline measurement. This gives an indication of the amount of disturbance the thermopiles are receiving from the environment within the TAM. The second section of the graph (represented by the small peak) shows the disturbance that is caused when the sample is lowered into the equilibration position. This can be endothermic or exothermic depending on ampoule temperature (equilibration to the same temperature as the TAM – 25°C), and other factors such as absorption of moisture onto the inner surface of the ampoule and evaporation of the salt solution. The third feature on the graph is caused by the absorption of moisture onto the sugar in the sample, several minutes after the sample is placed into the measurement position. This absorption peak begins to plateau then decline (at t = 0.8 hours), but is then increased by the re-crystallisation of the amorphous component of the sample to a maximum of just under 1200µW after an hour.

The TAM software package DIGITAM was then used to analyse the peak data, and provide a maximum peak value, as well as an integral area for the absorption/re-crystallisation peaks for all of the standards. This data is shown in table 4.2.

Sample	Degree Amorphisim (%)	Integrated peak area (μW)	Peak Intensity (μW)
Standard 1	2.0	1582.44	1179.14
Standard 2	1.0	1025	635.239
Standard 3	0.75	571.22	517.108
Standard 4	0.5	353.143	358.934
Standard 5	0.25	142.76	192.453
Standard 6	0.1	8.558	4.663
Standard 7	0	0	0

Table 4.2 Data for amorphous sucrose standards

The integrated peak areas for the samples of an amorphous content of less than one percent were then plotted to obtain the greatest accuracy for the 0 – 1 % amorphous content region.

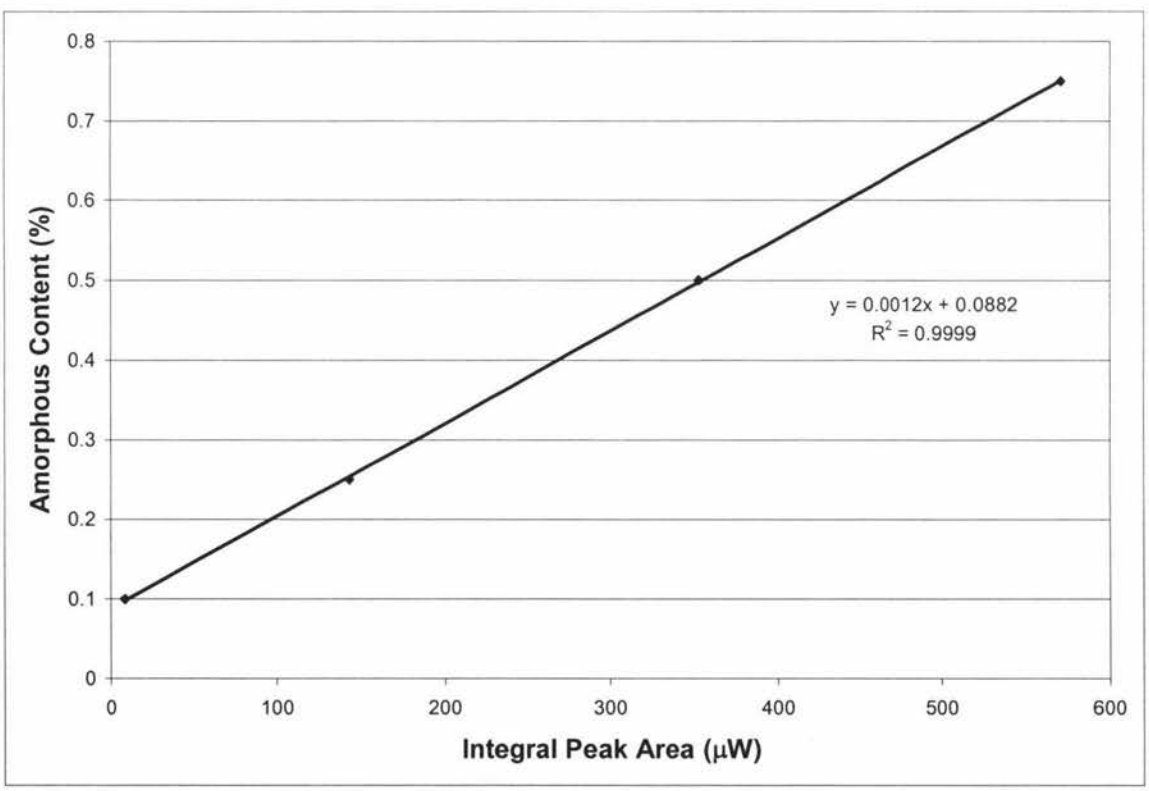

Figure 4.6 Integral peak area curve for amorphous TAM standards

The R^2 of 0.9999 indicates that the fit-line is a very good approximation of the standard curve data to be used in predicting the amorphous content of the sucrose samples. By rearranging the fit-line the equation for the calculation of amorphous content can be found.

$$\text{Amorphous Content} = \text{Integral Peak Area} \times 0.0012 + 0.0882 \qquad \text{Equation 4.2}$$

Again the Digitam software was used to find the maximum peak and integral peak areas from all of the samples. The fit-line obtained from the standard curve data was then used to calculate the degree of amorphisim for the samples.

Sample	Peak Intensity (μW)	Integrated peak area (μW)	Amorphisim (%)
Mid Drier	20.876	6.292	0.1637
Post Drier	29.064	0.8031	0.0978
Post Silo	11.689	0.5612	0.0949
Post Bagger	1.903	0.496	0.0942

Table 4.3 Data for sucrose samples

The data shows that for the post drier, post silo and post bagger, the calculated degree of amorphisim is below the detectable limit for the experimental technique, therefore it is safe to assume that there is no significant amorphous content at the 0.1 percent level.

The data for the mid-drier sample shows the existence of a measurable amorphous content (greater than 0.1 %), which can be seen in figure 4.7 (page 4 – 11), the profile for the mid drier sample. As with the amorphous standard curves, a characteristic secondary peak, indicating amorphous recrystallisation can be seen from the top drier sample, but not from the bottom drier sample.

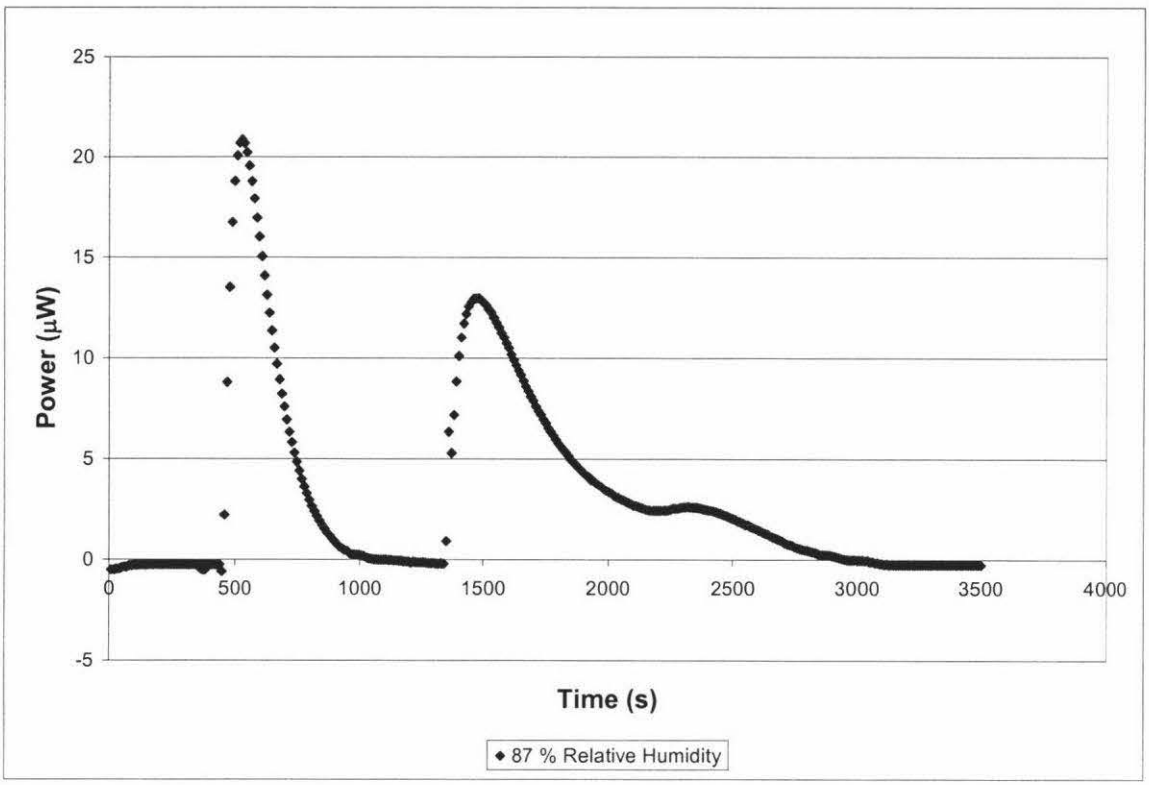

Figure 4.7 TAM curve for mid drier sample showing amorphous content

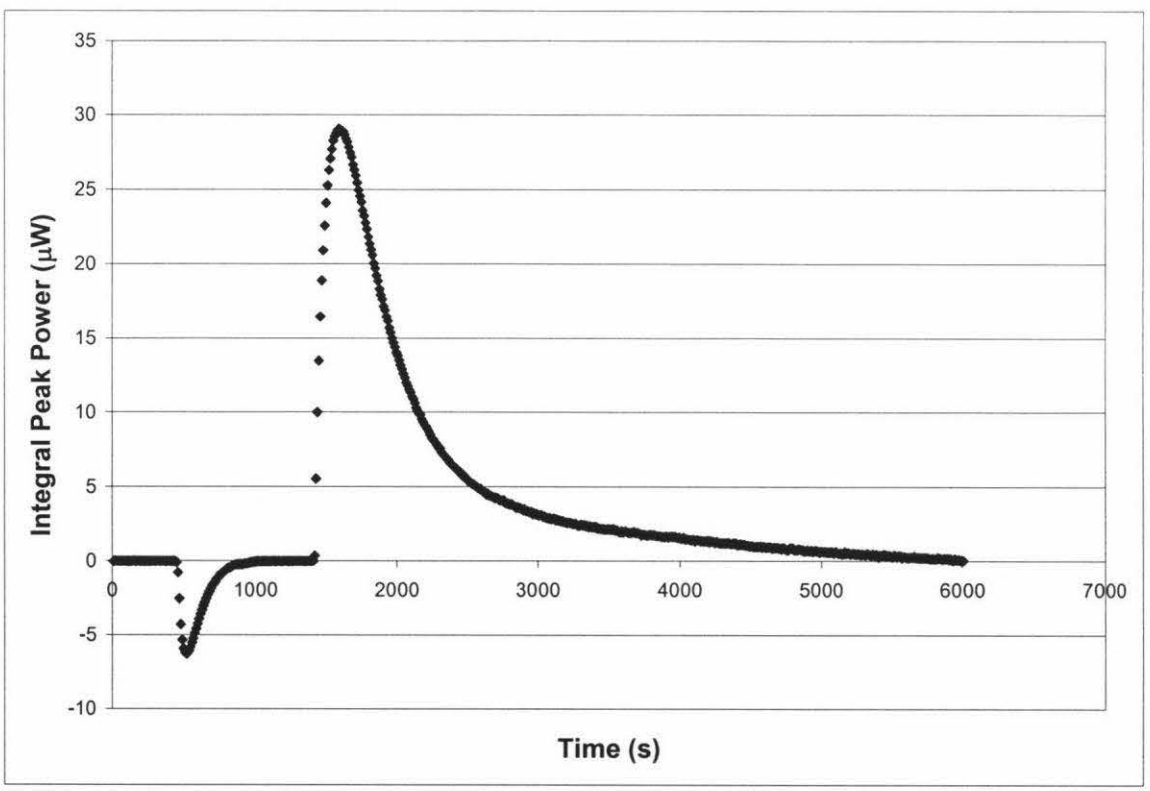

Figure 4.8 TAM curve for post drier sample indicating no amorphous content

The sucrose coming out of the bottom of the top drier did appear to contain a measurable amorphous component that is removed by the end of the second drier. This raises questions about the structure of the amorphous content that exists.

There are two possible forms that the amorphous material could take, the first proposed by Meadows (1994). As discussed in chapter two, this considers the amorphous material as a supersaturated film of sucrose becomes trapped between a surface crust and the surface of the crystal. This film then dissolves the crust and recrystallises on the surface of the crystal below. Given that the diffusion process calculated by Meadows would take more than three hours for a given surface layer thickness and that the residence time in the drier is six minutes, this scenario would appear to be unlikely. It cannot however be totally discounted, as it could be possible to show that the thickness of the surface layer is very small, decreasing the calculated time.

It is also possible that the amorphous content is a viscous, glassy substance on the surface of the crystal, hypothesised by Billings and Paterson (2000). This scenario is possible as the time for recrystallisation is dependent on the porosity of the amorphous material, as well as the humidity of the surrounding environment.

Closure

This chapter has shown that at the 0.1% level of significance we can conclude that there is no amorphous sucrose contained by sugar as it leaves the bagging station.

It would be possible to obtain a more accurate standard curve from the TAM instrument by using it in the 0 – 3000μW range. This would mean that samples could be bigger, allowing less room for experimental inaccuracies in measuring. This would then allow the measurement of an even smaller standard curve sample, increasing the sensitivity of the amorphous content measurement.

CHAPTER 5

Thermal Conductivity of Sucrose

Introduction

Due to the importance of porosity on thermal conductivity, experimental work was carried out to determine the thermal conductivity representative of the sugar being produced. As the bulk density of the sugar will change during transport it was decided to measure the thermal conductivity at the density extremes, the unpacked and packed or "tapped" density. From these values, a sensible value for the thermal conductivity of sugar being transported and stored can be found and used in the moisture transport model.

5.1 Bulk density and porosity measurement

The bulk density was measured by filling a container with a known volume and then measuring the mass of that volume. Two density measurements were made, standard and tapped. The tapped density is measured by tapping the container against the side of the bench during filling to ensure that the particles are packed as tightly together as possible, in order to achieve the greatest mass possible.

The tapped density was measured as 902.37 kg/m^3 and the standard density measured as 797.50 kg/m^3. The average density measured from out of the bottom of the storage silo is 840.04 kg/m^3, indicating that transporting the sugar acts in a similar fashion to tapping the sugar. As transportation from the silo is only a small part of the transportation process and has a noticeable effect on the density of the bulk, the tapped sugar will be used as the basis for the remainder of the experimental work.

The porosity of the samples was then calculated for the standard and tapped samples using equation 5.1 below.

$$\rho_{\text{bulk}} = (1-\varepsilon)\rho_{\text{particle}} \qquad \text{equation 5.1}$$

The porosity of the standard sugar sample was calculated to be 0.4978 and the tapped sample to be 0.4318. Samples from out of the bottom of the silo have a porosity of 0.47.

5.2 Infinite cylinder experimental

Using the infinite cylinder model (equation 2.3), the fraction of accomplished change (1-Y), at differing values of Fourier number ($\alpha.t/r^2$) was calculated by Bronlund (1997).

1-Y	$\alpha.t/r^2$
0.15205	0.1
0.498494	0.2
0.717524	0.3
0.841531	0.4
0.911129	0.5

Table 5.1 Accomplished Temperature Change in an Infinitely Long Cylinder

An infinite cylinder was approximated by using a copper tube 300mm long by 80mm wide. The temperature at the centre of the cylinder was measured at different depths by placing a piece of string with two thermocouples attached at one and two-thirds the way down the length of the cylinder for verifying the one dimensional heat transfer assumption. This was then attached to a polystyrene plug which was placed in the bottom of the tube, and then filled with standard grade white sugar while the string was held taunt. For the tapped density experiment the cylinder was tapped during filling in order to achieve maximum density. With the cylinder full, the top polystyrene plug was put in place and the cylinder sealed at the top and bottom with silicon-coated fibre gaskets, which were then clamped down to ensure the cylinder was watertight. Thermocouples were also taped to the outside of the cylinder using aluminium tape, so the temperature at the outside could be measured and compared with the center temperature, again to validate the one dimensional heat transfer assumption.

The high temperature environment was provided by sparging water at 40 °C from a Grant Y14 water bath into a bucket that was fitted with an overflow return pipe. Once the sugar in the tube had equilibrated to room temperature (~20°C) the cylinder was immersed in the water filled bucket, and the heating profile of the temperature step change recorded using a 1000 series Grant Squirrel Logger.

5.2.1 Results

The data from the Squirrel logger was downloaded using "Squirrelwise" software on a PC and then exported to Excel in a text format.

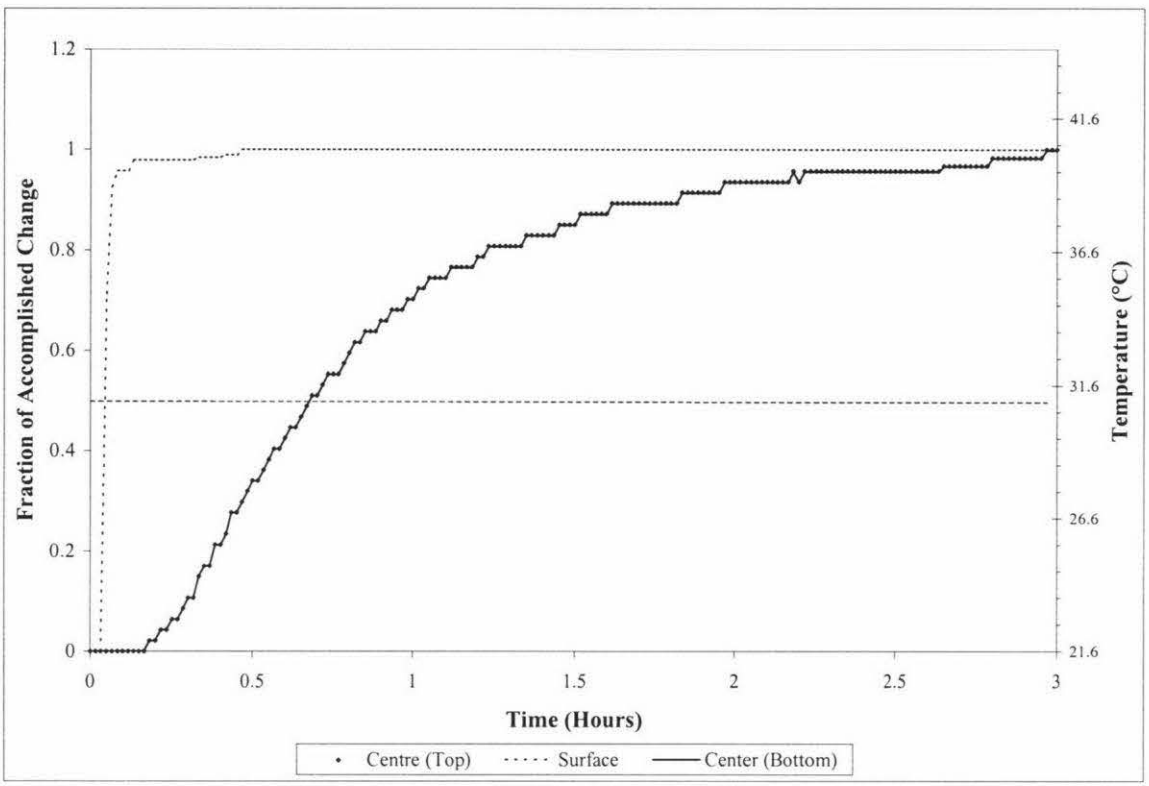

Figure 5.1 Heating Profile for Infinite Cylinder Experiment

As it can been seen from the graph the two thermocouples placed in the center of the cylinder at one and two thirds the way down the cylinder are the same. This indicates that there is minimal heat transfer occurring up and down the length of the cylinder when compared to the heat being transferred from the outside to the inside of the cylinder.

The heating profiles were then plotted on a semi log graph shown in figure 5.2 (page 5 – 4). This makes the data linear, allowing a fit-line to be applied to the most linear portion of the graph. This fit-line was then used to calculate the time required for the different changes in cooling illustrated in table 5.1. Using the relationship model value calculated for α, the thermal conductivity could be calculated from equation 5.2 (Bronlund, 1997).

$$\alpha = \frac{\lambda}{\rho C_p} \qquad \text{equation 5.2}$$

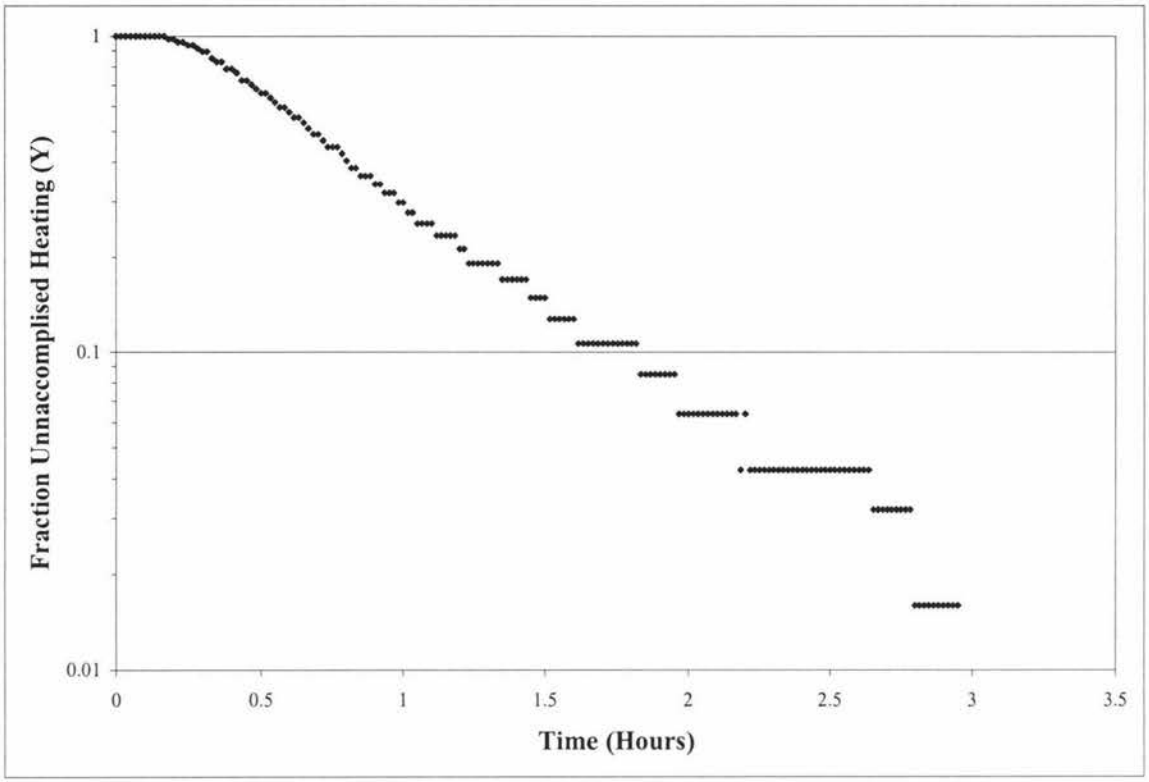

Figure 5.2 Semi-log plot of sucrose infinite cylinder heating profile

To test the fit of the model to the experimental data, a graph of the fraction of accomplished change versus time was generated from the model and plotted as a comparison to the experimental data obtained. This can be seen if figure 5.3 (page 5 – 5).

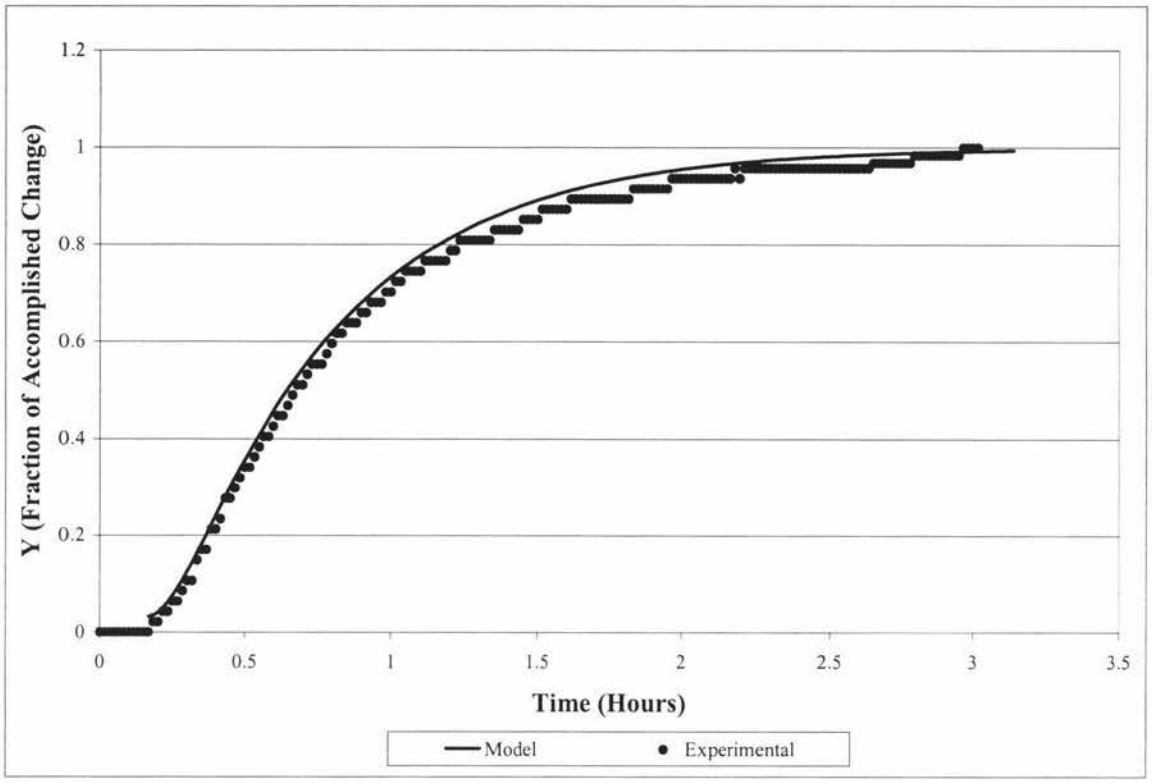

Figure 5.3 Model and experimental data for thermal conductivity experiment.

From the graph it can be seen that the model has predicted the experimental very well, verifying the use of the model to predict the thermal conductivity.

The thermal conductivity data calculated are compared to the values reported by M^{c} Carthy and Fabre (1989), in table 5.2.

Sample	ε	λ	Uncertainty
		(W/mK)	(W/mK)
Standard Tapped	0.4318	0.150	0.0012
Standard Untapped	0.4978	0.136	0.0017
Medium – McCarthy + Fabre	-	0.159	-
Standard – McCarthy + Fabre	-	0.144	-
Extra Fine – McCarthy Fabre	-	0.141	-

Table 5.2 Comparison of thermal conductivity data

The differences in thermal conductivity values for the tapped and untapped samples is caused by the difference in porosity. The tapped sample has a lower porosity, therefore the amount of air resisting the transfer of heat is lower, and therefore the thermal conductivity is higher.

The result obtained for standard sugar by M^{c} Carthy and Fabre (1989), is between the values for the tapped and untapped samples, indicating that the sample had a porosity of between 0.49 and 0.43. As the exact bulk density of the sugar being transported is unknown, it is assumed that it will be closer to that of the tapped sample than the untapped.

Closure

The thermal conductivity of the sugar being used for the validation of the moisture transport model was found using the infinite cylinder method to be 0.136 W/mK for sugar at a bulk porosity of 0.49. The thermal conductivity of tapped bulk sugar with a porosity of 0.43 was measured to be 0.150 W/mK. Due to the movement involved in the transportation of the bulk sugar, it is believed that the tapped porosity will give the best representation of the bulk density of the sugar after it is packed. Therefore the values obtained for the porosity and thermal conductivity for the tapped samples will be used for further calculations.

CHAPTER 6

Caking Strength Measurement

Introduction

In order to model the strength of caked sugar, it was necessary to induce caking under controlled environments and then measure the subsequent caking strength. To get an initial idea of what conditions would be required in order to cake sugar, it was necessary to model the process that is seen to be responsible for the formation of liquid bridges at the points of contact between sugar crystals. The model of this process, capillary condensation, could then be used to identify where caking would be expected to occur and provide an explanation for the experimental data obtained.

6.1 Capillary Condensation

At temperatures below the critical point for an adsorbate, adsorption is generally a multi-layer process. The pores that are present in packed sugar not only effect or limit the number of layers that are adsorbed onto the surface of the crystals, but also introduce the capillary condensation phenomena.

Capillary condensation can be described as a process by which surface tension effects cause the direct condensation of moisture in the pores or "capillaries", formed by the contact points of sugar crystals in a packed bed. In these capillaries the pressure is lower than the surrounding atmosphere, which results in the saturated vapour pressure above the liquid surface being less than the vapour pressure of the bulk air (at the same temperature). If the pressure is lowered enough to cause the vapour pressure to be greater than the saturated partial pressure above the capillary surface, then condensation will occur, even at humidities below 100% saturation in the bulk air.

The vapor pressure required for condensation to occur is related to the size of the capillary, and is measured as the capillary radius (r_k). This, as well as the effects of wetting angle (θ) and surface tension are related by the Kelvin equation (Adamson, 1963).

$$A_w = \frac{P_v}{P_w} = e^{\frac{-2\sigma.\cos\theta.V_0}{r_k.R.(T+273.15)}} \qquad \text{equation 6.1}$$

The Kelvin equation was used to predict the Kelvin radius, where capillary condensation would occur at a given water activity. This allows capillary radius to be estimated at the onset of caking.

It was assumed that the fluid material on the crystal surface was a saturated sucrose solution, so the saturated solution value for surface tension of 84.05 N/m was used (Mathlouthi and Reiser 1995). It was also assumed that the wetting angle (the angle formed between the droplet and the surface it is on), was perfect (zero radians). The value used for molecular volume is calculated from density using the molecular weight of sugar. The value was calculated as $3.28\ 10^{-4}$ m^3 /mol. A graph of the change in capillary radius with water activity is shown in figure 6.1 below.

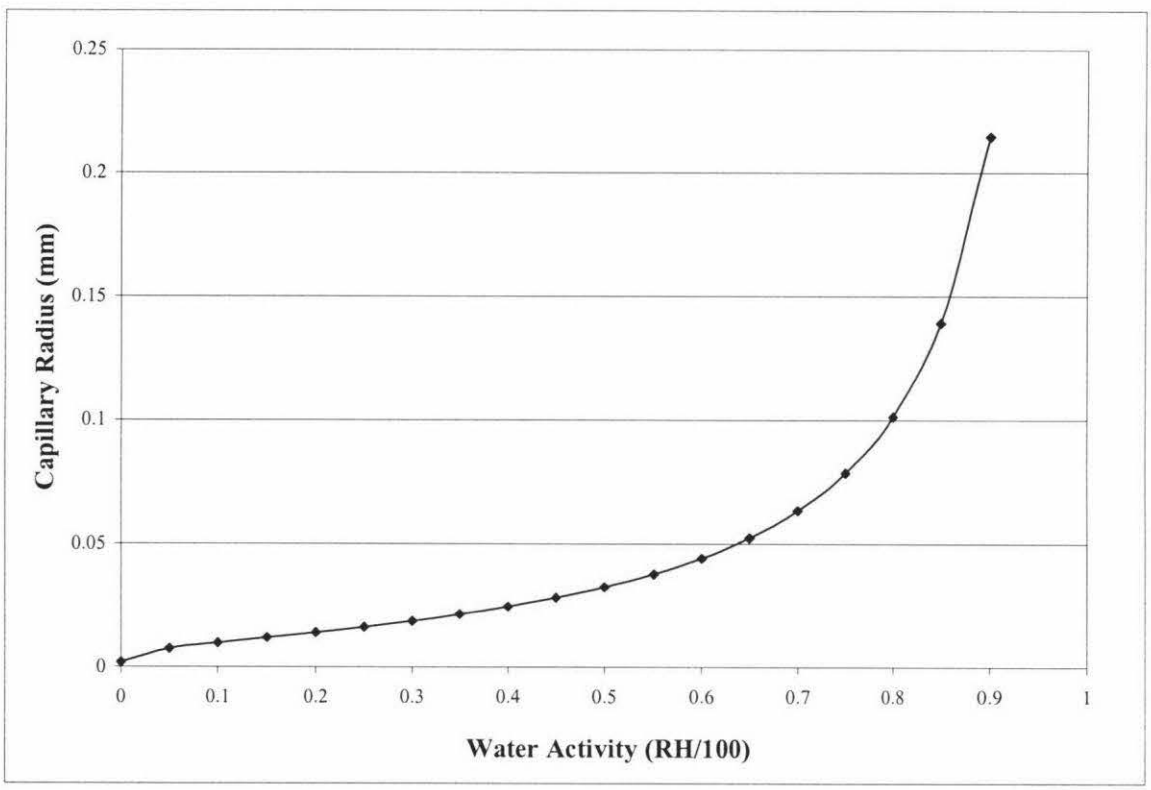

Figure 6.1 Change in Capillary Radius with Water Activity for Sucrose

For a $1m^3$ packed bed at the tapped porosity of 0.43, the amount of space that would be occupied by air would be 0.43 m^3. This is about 80% of the volume occupied as sugar crystals ($0.57m^3$), meaning that the largest possible space between the sugar crystals will be 80% of the size of an "average" sugar crystal. Meadows (1994), assumed an average crystal to have a volume of $0.16mm^3$, giving an average space of $0.128mm^3$.

It can be seen from the shape of the graph that the size of the capillary radius takes off exponentially from a water activity between 0.75 and 0.8, hence one can assume that

significant liquid bridging between the particles will occur from this point onwards. The exponential change in capillary radius will then effect caking, which will also increase exponentially from a water activity of 0.8 onwards.

By measuring the caking strength at different humidities, it will then be possible to create a mechanistic measure of the expected caking of a sugar sample by looking at the Kelvin radius of the bed.

6.2 Caking strength experimental

The results from the Kelvin equation indicated that significant capillary condensation between particles, and hence liquid bridge formation, would not occur below a relative humidity of 75-80%. In order to test this it was necessary to investigate the full range of relative humidities, but with particular focus on the region >75%. The saturated salts solutions used to obtain the required relative humidities were:

Saturated Salt Solution	Relative Humidity
Potassium hydroxide	~ 9 %
Magnesium chloride	~ 33 %
Sodium bromide	~ 59 %
Sodium chloride	~ 75 %
Ammonium chloride	~ 79 %
Ammonium sulfate	~ 81 %
Potassium bromide	~ 84 %
Potassium chloride	~ 87 %
Potassium nitrate	~ 94 %

The penetrometer and blow tester were used for the measurement of caking strength because of their relative ease of use and accuracy. These methods also have the advantage that replicate measurements can be made on a sample, unlike methods such as friability or angle of repose, where the sample is poured out of the container or onto a surface. From the isotherms, and results from the Kelvin equation, it was foreseen that at the higher water activities the sugar might cake to the point where flow would not occur, negating the possibility of getting accurate results from other methods.

6.2.1 Free diffusion Model

The modified free diffusion model of Paterson *et al.* (2000) described in chapter three was used to predict the time it would take for a packed bed sample to come into equilibration with the different salt solutions being used.

The time required for the bed to come to equilibration is shown in table 6.1 below.

Relative humidity %	Moisture content g/100g	Bed Depth mm	Equilibration time (d)
9	0.0104	12.0	12.35
33	0.0183	12.0	3.35
59	0.0340	12.0	1.86
75	0.0663	12.0	1.46
79	0.0865	12.0	1.39
81	0.1019	12.0	1.35
84	0.1392	12.0	1.30
87	0.2188	12.0	1.26
94	4.4396	12.0	1.16

Table 6.1 Predicted equilibration times for experimental packed sugar bed

Times from these predictions were used as guidelines when the samples were left to equilibrate prior to experimentation. To test these predictions the liquid and solid bridge strengths were measured after one, two, and three days.

6.2.2 Liquid bridge strength experimental

To measure the liquid bridge strength, sugar samples were placed in standard laboratory petri dishes, approximately 12mm deep. The samples were then placed in airtight containers containing the saturated salt solutions above, and left to equilibrate for the times determined by the model above. The samples were then removed and the liquid bridge strength measured.

6.2.2.1 Penetrometer

Penetrometer measurements were made by setting the counter weight balance so that an empty container sat weightless above the sample to be measured. Weight was then added to the container by slowly adding water to the container until the "breakthrough" point was observed (the breakthrough point being the point where the penetrometer made a large shift in penetration depth, with the pins completely buried in the sample). The

weight of the water required for breakthrough was then measured and plotted against the water activity that the sample was equilibrated to for the differing equilibration times.

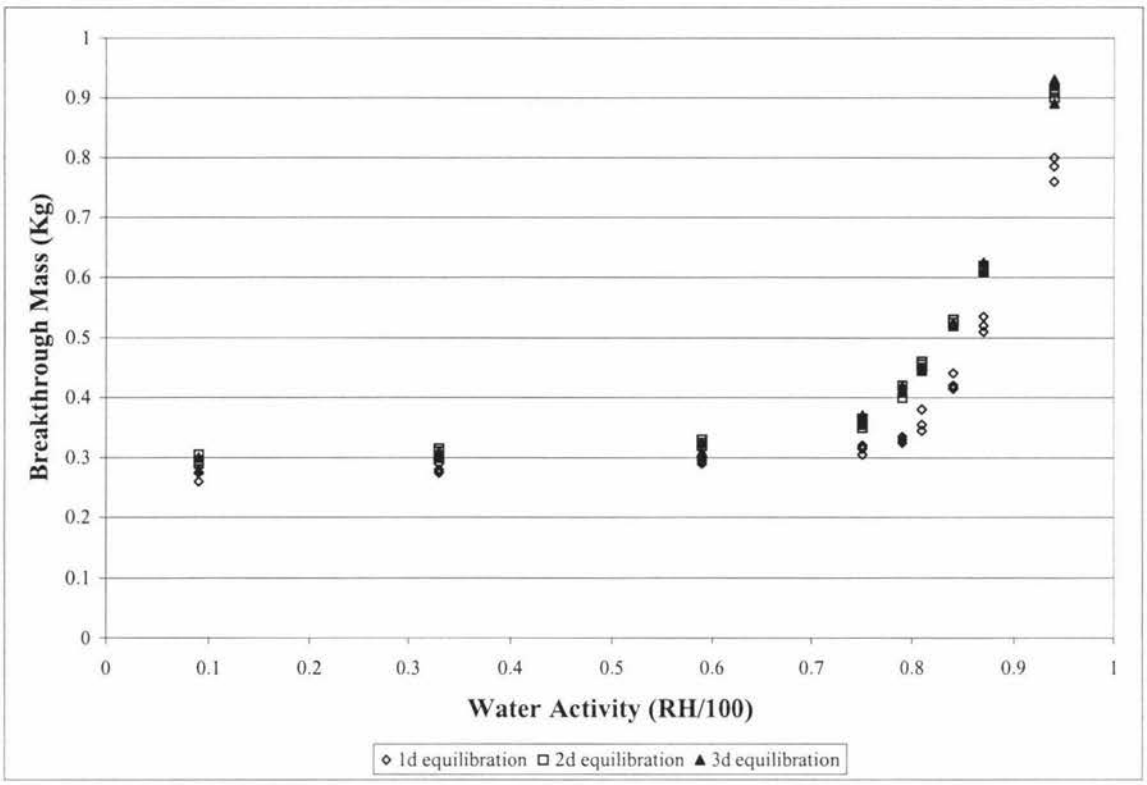

Figure 6.2 Penetrometer data for Liquid Bridge Strength Test

It can be seen from the graph that the two and three – day liquid bridge strengths are very similar. The liquid bridge strength for the sample equilibrated for one day is considerably less than that for the two and three day samples, which indicates that the predicted equilibration times are only approximately correct. Pinpointing the equilibration time is not necessary, as for the model, it is the maximum strength of the liquid bridge that is important, not the time.

The graph also indicates that the onset of significant liquid bridge formation occurs between relative humidities of 75 and 80 %, which gives a value for the breakthrough mass of 0.4 kg. The values for the relative humidity agree with the data that was obtained from the Kelvin model for capillary condensation, explaining the occurrence of liquid bridges between the crystals at the observed relative humidities.

Using the two day equilibration time data a graph of the observed liquid bridge strength was then plotted against the Kelvin radius.

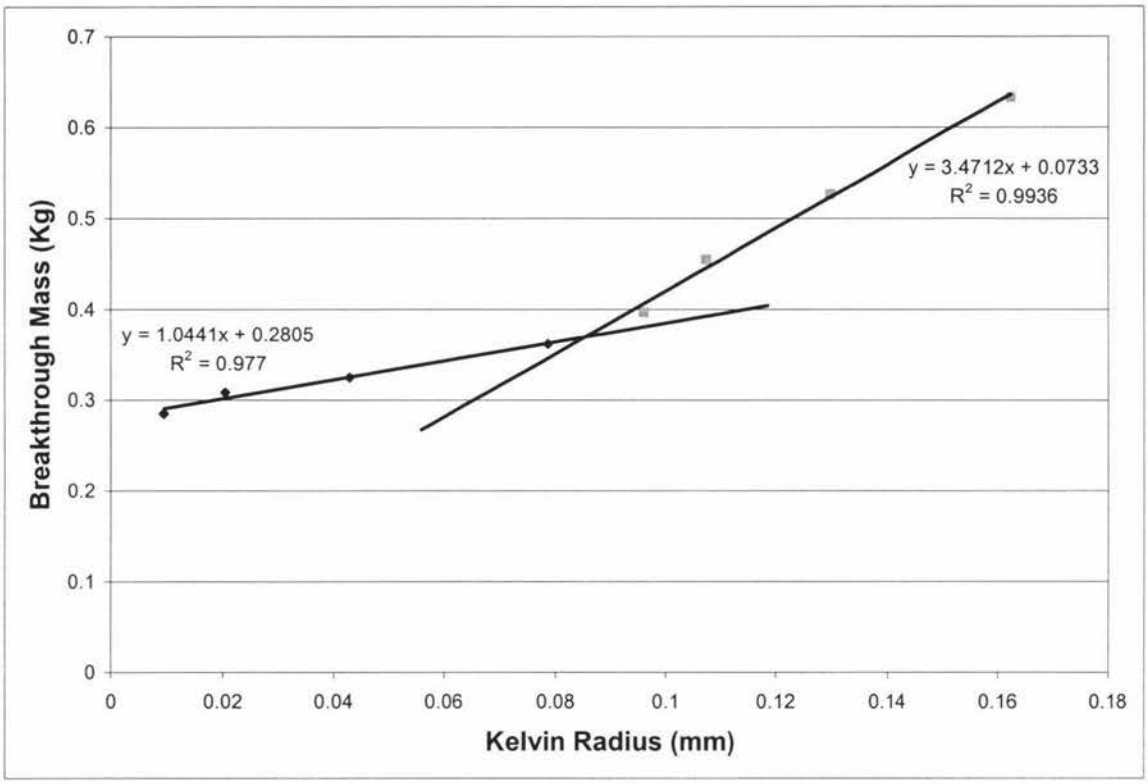

Figure 6.3 Breakthrough mass versus Kelvin radius for penetrometer

As it can be seen in figure 6.4 (page 6 – 7), by interpreting the graph as being two linear relationships, a very good fit is obtained. By solving the equations simultaneously, it was possible to calculate the Kelvin radius at the intersection of the two graphs, 0.0854 mm. By rearranging the Kelvin equation (equation 6.1), the Kelvin radius can be calculated from the water activity.

$$r_k = \frac{\left(\frac{-2\sigma.\cos\theta.V_0}{\ln(A_W)}\right)}{R.(T+273.15)}$$ equation 6.2

A radius of 0.0854mm corresponds to a water activity of 0.767, which is in the range where the capillary radius increases exponentially (from figure 6.1, page 6 – 2), and also the point where the liquid bridge strength began to increase significantly.

This would appear to confirm 0.8 as the critical water activity for the onset of significant liquid bridge formation, as this is the point where a significant number of capillaries are filled with liquid, providing the increased strength observed.

6.2.2.1 Blow tester

Measurements for the blow test data were done by resting the portable blow tester on the surface of the sample and holding in place with a clamp stand. A needle valve was then used to control the airflow from a bottle of compressed air into the blow tester, with the flow-rate increased until the point where the airflow was sufficient to begin dislodging sugar particles from the surface of the sample. This flow-rate was then plotted against the water activity that the samples were equilibrated at, for the different equilibration times.

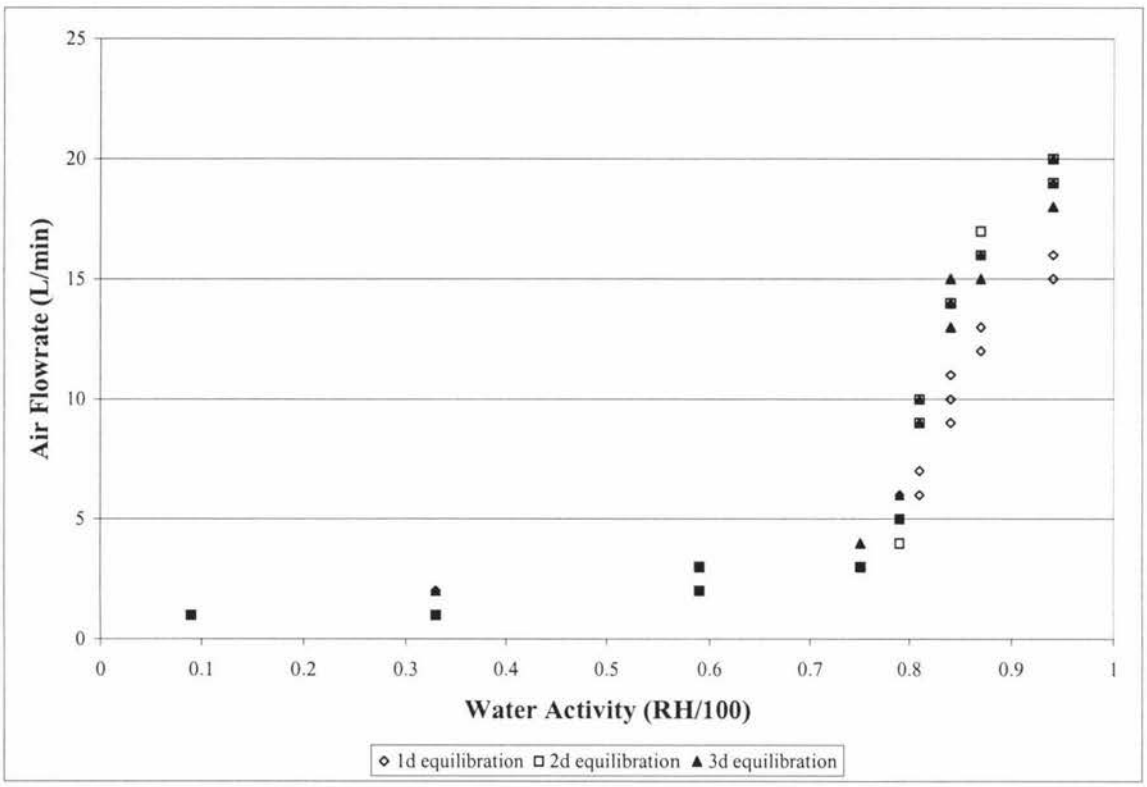

Figure 6.4 Blow test data for Liquid Bridge Strength Test

The blow test data also shows that the difference in strength between the two and three day equilibration time is negligible when compared to the differences between the one and two day equilibration time data. There was expected to be no difference in strength for the 9% RH sample as the equilibration time calculated by the packed bed absorption model, was around 12 days. The 33% sample was expected to show a small difference as it had an equilibration time of 3.3 days, which can be seen above. The rest of the samples should have shown little difference as the predicted equilibration times were calculated at less than two days, which is reflected in the data above.

The graph shows that the strength of the liquid bridges starts to become exponential, hence significant, at an air flow-rate of five litres per minute.

Above values of 94% relative humidity it is hard to measure liquid bridge strength experimentally, as liquification at the surface of the sample begins before the sample has had a chance to equilibrate. Due to this, 94% relative humidity will be assumed to be the maximum relative humidity that sugar will ever be exposed to for any considerable length of time.

As with the penetrometer data, the liquid bridge strength was plotted against the Kelvin radius in order to observe the capillary radius at which significant liquid bridges, of significant strength, began to form.

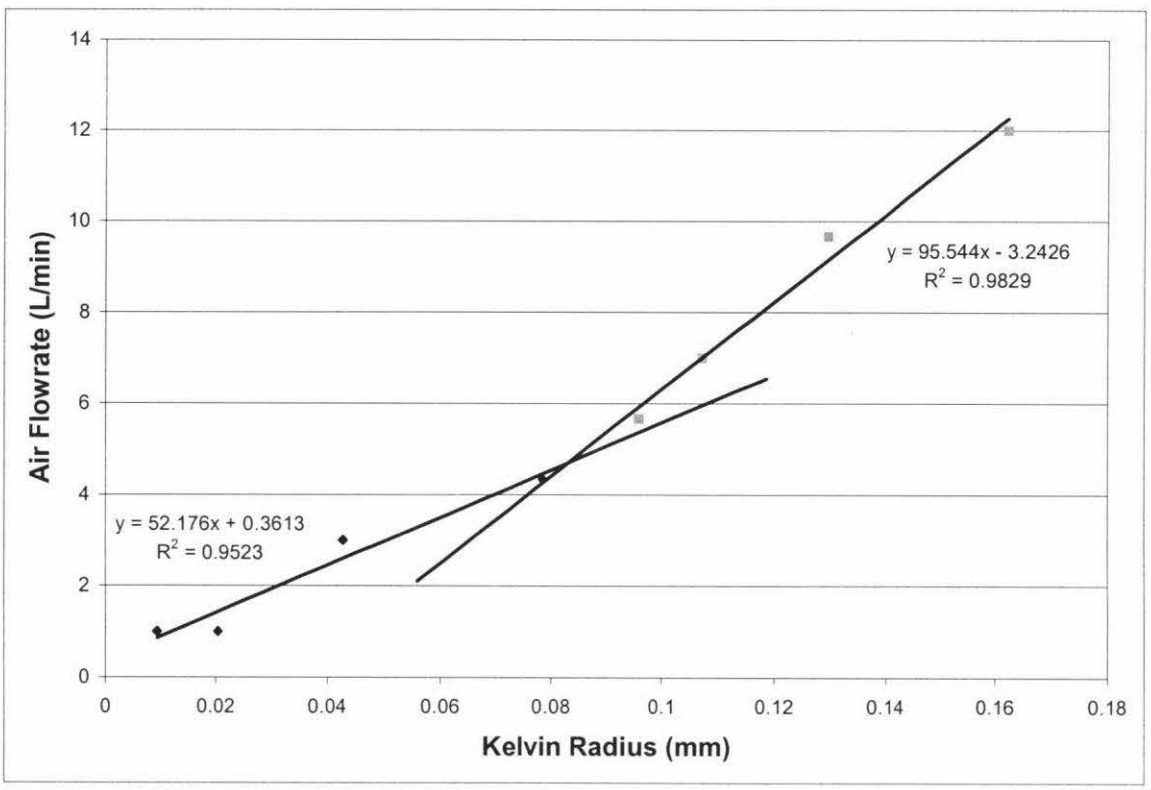

Figure 6.5 Air flow-rate required versus Kelvin radius for blow tester

As with the penetrometer there can be two strong linear relationships plotted, with the size of the capillaries at the intersection being calculated as 0.0831mm. This corresponds to a water activity of 0.7618, which again is in the range where the capillary condensation size begins to increase exponentially. This intersection shows a change of mechanism/sites, probably indicating the point where significant liquid bridges begin to form between particles.

Because of the nature of the forces involved in transportation, we can assume that a little bed strength gained from liquid bridging will be tolerable. For future reference, the critical value for undesirable strength contributed from liquid bridging will be at a water activity of 0.8, which corresponds to a Kelvin radius of 0.1031mm.

6.2.3 Solid bridge strength experimental

Solid bridge formation was defined as the strength that the liquid bridges gained after being allowed to dry and crystallise out. After the liquid bridge equilibration times of one to three days, the samples were left exposed to the ambient conditions that would typically be encountered by sugar after the transportation process (one day).

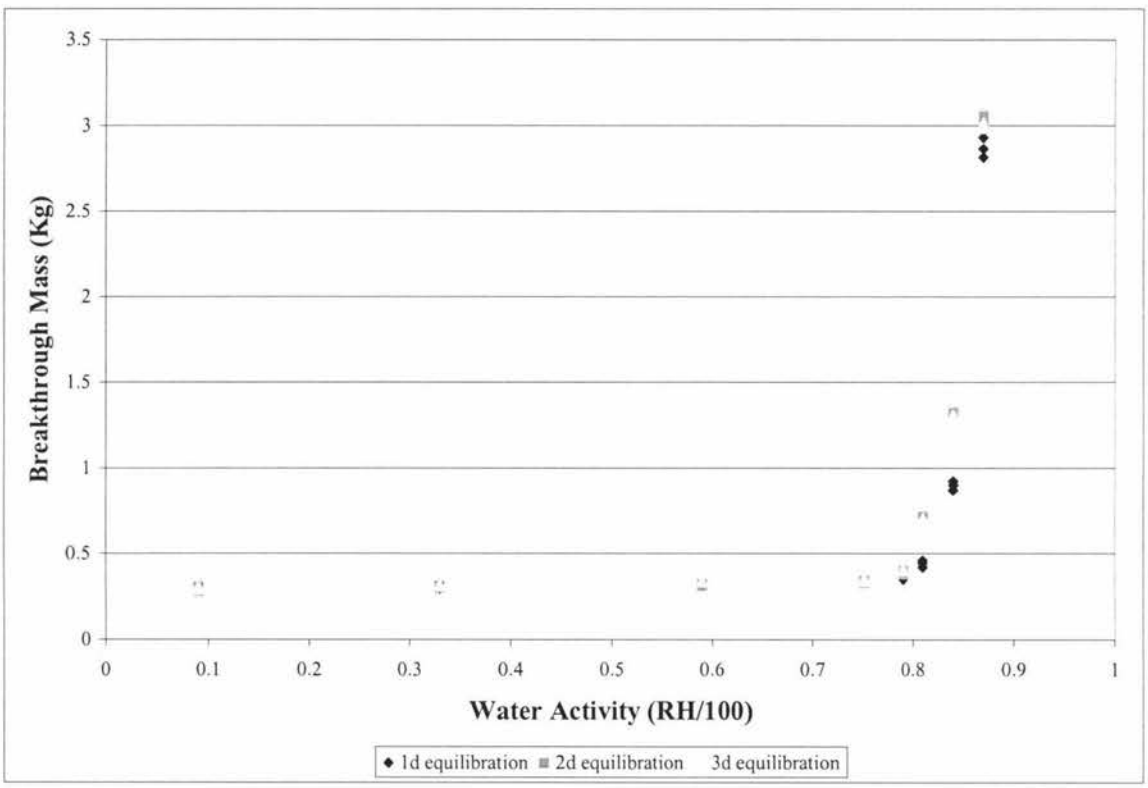

Figure 6.6 Penetrometer solid bridge strength data

The shape of the graph is similar to that of the isotherm for the moisture content of sugar. This would be expected, as the size and concentration of the liquid bridge formed would increase, as the amount of water available for the bridges to form increased.

The graph shows that below a water activity of 0.75 there is no significant solid bridge formation between particles and that the sugar should remain free flowing. At a water activity of greater than 0.8 the strength of the solid bridges increases noticeably, indicating the onset of capillary condensation between crystals. This agrees with the Kelvin equation predictions, which indicated that significant capillary condensation would occur between the crystals at a water activity of between 0.75 and 0.8. This gives a solid bridge strength at the onset of solid bridge formation of 0.708 kg.

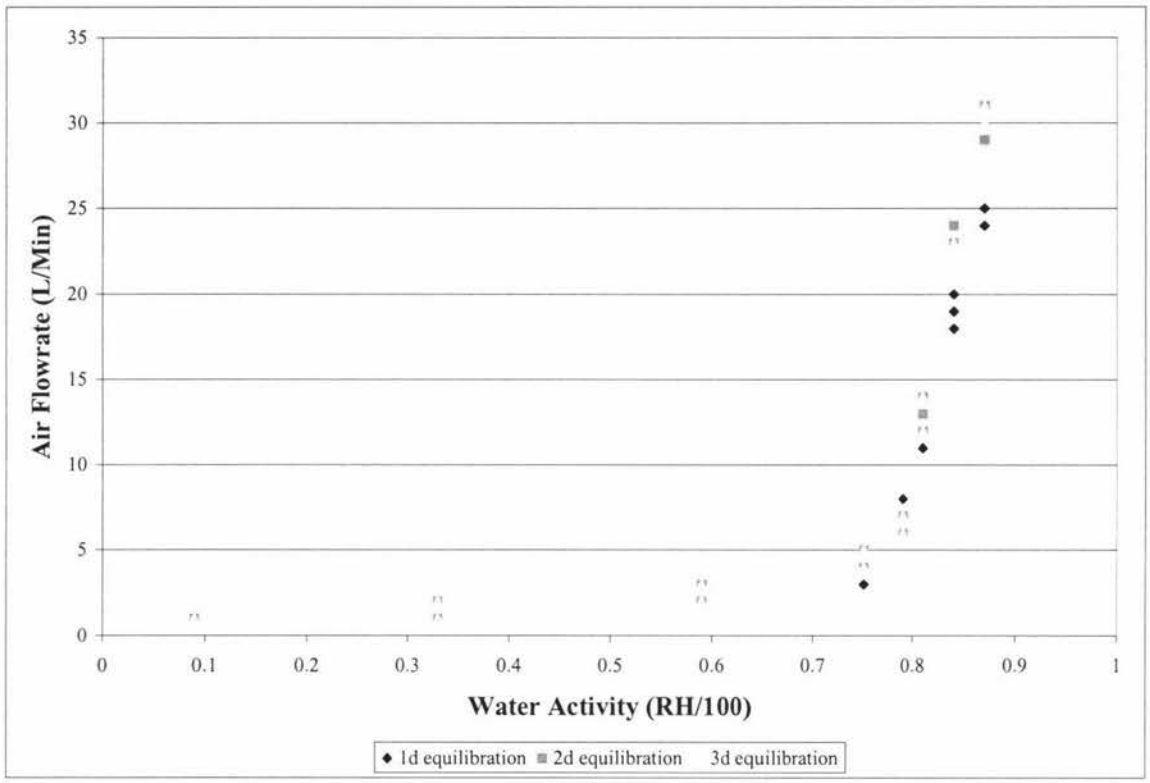

Figure 6.7 Solid bridge blow test strength data

The blow test data is similar to the penetrometer data. The graph shows the increase of strength with water activity at a level above 0.8, with the flow-rate of air required at the onset of solid bridge formation being eight litres per minute.

As with the liquid bridge experimental, plots of solid bridge strength versus the Kelvin radius were then made for both the penetrometer and the blow tester.

Figure 6.8 (page 6 – 11), shows the graph for the penetrometer solid bridge strength versus Kelvin radius. The relationship is similar to that of the liquid bridge with there being two strong linear relationships present. Using equation 6.2 the Kelvin radius at the intersection of the two fit-lines was calculated as 0.0904mm, which corresponds to a water activity of 0.7787, again in the region of the graph in figure 6.1 where the increase becomes exponential.

Figure 6.9 (page 6 – 11), shows the similar result for the graph of the blow test data. The Kelvin radius at the intersection was calculated as 0.0880mm, with the corresponding water activity being 0.7734, which also lies in the region of figure 6.1 where the graph is exponential.

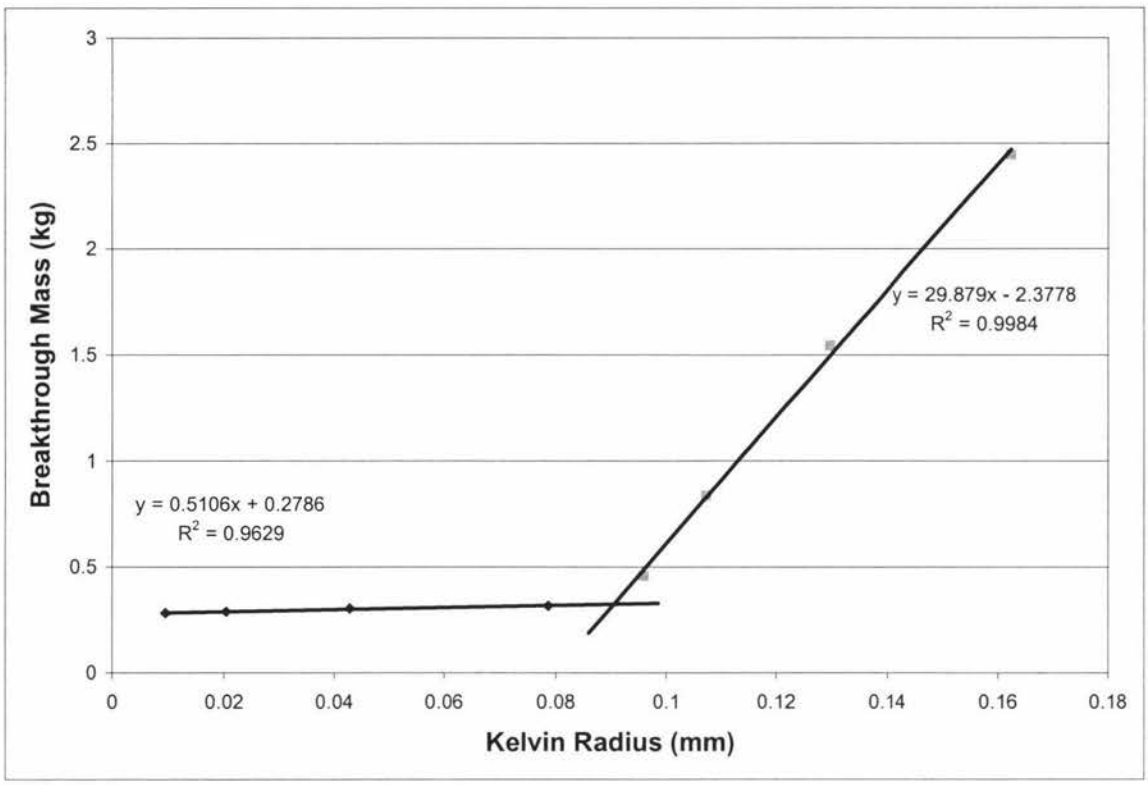

Figure 6.8 Breakthrough mass versus Kelvin radius for penetrometer

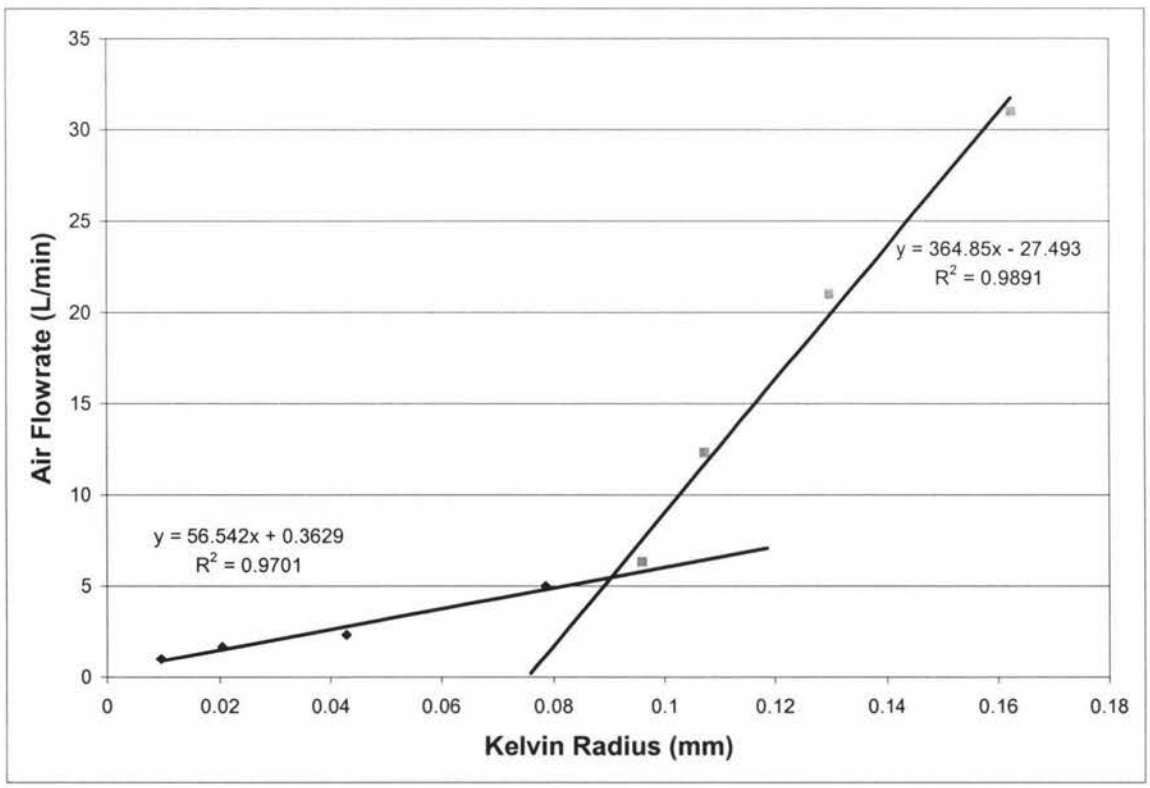

Figure 6.9 Air flowrate required versus Kelvin radius for blow tester

6.3 Summary of results

By using linear relationships between the force required for the two techniques to disrupt the bridges formed by liquid and solid bridging, we can build up a mechanistic model to describe the caking in sugar that is exposed to an environment with a high relative humidity

Table 6.2 shows a summary of the results for the liquid and solid bridge data for the penetrometer and the blow tester.

Experiment	Observed strength at onset of caking	Maximum observed strength
LB penetrometer	0.45 kg	0.908 kg
SB penetrometer	0.708 kg	> 9.0 kg
LB blow tester	8 L/min	21 L/min
SB blow tester	8 L/min	> 50 L/min

Table 6.2 Summary of results for liquid and solid bridge experimental

The results in table 6.2 also show that the difference in force required to break up a solid and a liquid bridge is large. This reinforces the importance of having a way of being able to measure the potential liquid bridge strength of sugar that has come from the dryers, or possibly the silo, so that steps can be taken to avoid the formation of liquid bridges.

The results of the data calculated for the Kelvin radius graphs, is summarised in table 6.3.

Experiment	Strength at onset of caking (y)	Kelvin Radius at fit-line intersection (Mm)	Water Activity at fit-line intersection
LB penetrometer	0.45 kg	0.0854	0.767
SB penetrometer	0.708 kg	0.0831	0.7618
LB blow tester	5 L/min	0.0904	0.7787
SB blow tester	13 L/min	0.0880	0.7734

Table 6.3 Summary of results for Kelvin radius data

It can be seen from table 6.2 that it reasonable to assume that the onset of bridge formation is between 0.76 and 0.78. It is reasonable to assume that at this point the strength that is provided by the bridging will not be able to tolerate the forces encountered during the transportation process. A reasonable estimation of the point where

sucrose will form bridges that will result in the caking of the sucrose is at a water activity of 0.8, which corresponds to a Kelvin radius for the bed of 0.0101mm.

Closure

From the experimental we can see that if solid bridges are allowed to form, then the sugar will be of no use to a customer as it will not be able to be removed from the walls of the container. The data from this chapter will enable us to determine under what conditions liquid bridges are likely to form and will be a useful tool in combating the caking process.
These conditions were to be found at any humidity above 80%, with the subsequent solid bridges forming if the samples were exposed for any length of time to a reduced humidity after the liquid bridges began to form. Having an understanding of what conditions sugar will form liquid bridges will make it possible to take actions to try and prevent or minimise this happening.

CHAPTER 7

Preliminary model application and experimental design

Introduction

In order to design an experiment that would validate the data from the model, the model itself was used to give a guideline to the type of outcome that could be expected from the experimental conditions being used. A set of experimental conditions was devised based on observed values of temperature, porosity and amorphous content, with other factors being varied to test the validity of the model. Once the experimental data has been obtained it will then be possible to try and find the best fit for the model by adjusting certain parameters or try and identify factors that would be responsible for any lack of fit.

7.1 Model Input Parameters

There are five parameters that were initially seen to have an impact on the results from the model. These include the thickness of the slab, the initial water activity of the sugar sample, the porosity of the sample bed, the heat transfer coefficient of the material between the sugar and the heating/cooling plates, and the temperature difference between the plates.

The thickness of the slab was removed from the list of factors, as the validity of the model over changing thickness was validated by Bronlund (1997) and it was not seen as necessary to be repeated. The largest slab thickness was used (100mm), with the model to be run using 10 nodes (making the node depth 10 mm). These values were chosen in a manner to ensure that it would be possible to obtain good values from the blow tester when testing the liquid bridge strength.

It was assumed that the porosity of the sugar and the heat transfer coefficient of the container material were constants, with the porosity being taken as 0.45. This was chosen as it is between the range of 0.43 and 0.49 that was found experimentally in chapter three, although ideally, a tapped density would be best to be achieved. Due to the size of the experimental apparatus, the tapping process was not as easy as the infinite cylinder, so a value slightly greater than the tapped density value was used.

From the conceptual model devised by Bronlund (1997) it could be seen that the two remaining factors, the temperature difference and the initial water activity, would have the largest impact on the movement of moisture. The higher the initial water activity, the more moisture there is available to migrate, theoretically increasing the probability for caking. The larger the temperature difference the higher the driving force and therefore the more severe the migration of moisture.

With the necessary parameters for the model decided, it was used at different temperature differences to find out the maximum water activity that the sample would reach (water activity of the node that was closest to the cold plate). This was then repeated for water activity ranges from 0.2 – 0.7 (typical observed extremes for New Zealand sugar moisture limits) and a graph of this data formed.

7.2 Parameters

The model prompts for key initial parameters to be entered. These ranged from the time step for the model to use to the initial crystallinity of the amorphous component of the sample.

7.2.1 Time

There are three time parameters in the model, time step, printout time, and total simulation time. The time step was set at one second, as larger time steps can cause large variation in model calculations and can slow down or crash the system. It was then a question of how small to set the time step, as the smaller the time step the smaller the magnitude of the calculation and hence the better the accuracy. The time step was investigated by running a model simulation using a standard set of conditions at time intervals of 1.0 and 0.5 seconds, and comparing the values obtained at similar points during the simulation.

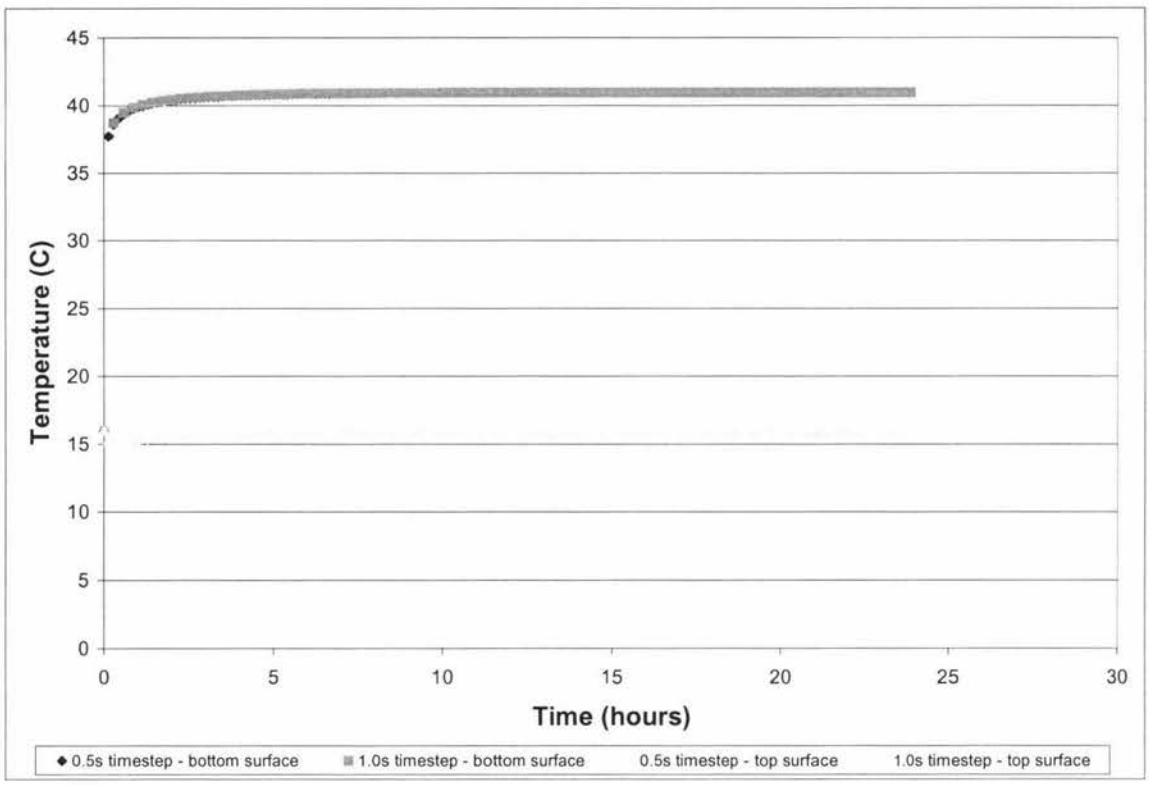

Figure 7.1 Comparison of model temperature values at different time steps

As it can be seen from figure 7.1 the difference in value between the values calculated using the different time steps is very minimal, hence one second was deemed as acceptable to use in the model simulation runs.

The printout interval selects the time at which the experimental data is written on the screen and to the file. This is typically set at 500 seconds. The total simulation time represents the length of the experiment. The model was initially run to find a reasonable timeframe for the experiment to reach steady state, which was just on a day. As a result of this, a total simulation time of 86400 seconds was used (the number of seconds in one day).

7.2.2 Apparatus conditions

There are three apparatus conditions, the number of nodes, the thickness of the slab and whether or not the nodes are initialised separately. For the 100 mm slab there were 10 nodes and the separate initialisation of each was not chosen as it was assumed that they should all be at the same condition at the start of the experiment. The dependence of the number of nodes was tested in the same way that the time step was tested, by running a simulation with 10 nodes, and then the same conditions with 20 nodes, and the values at the same depths compared. This is shown in figure 7.2 (page 7 – 4).

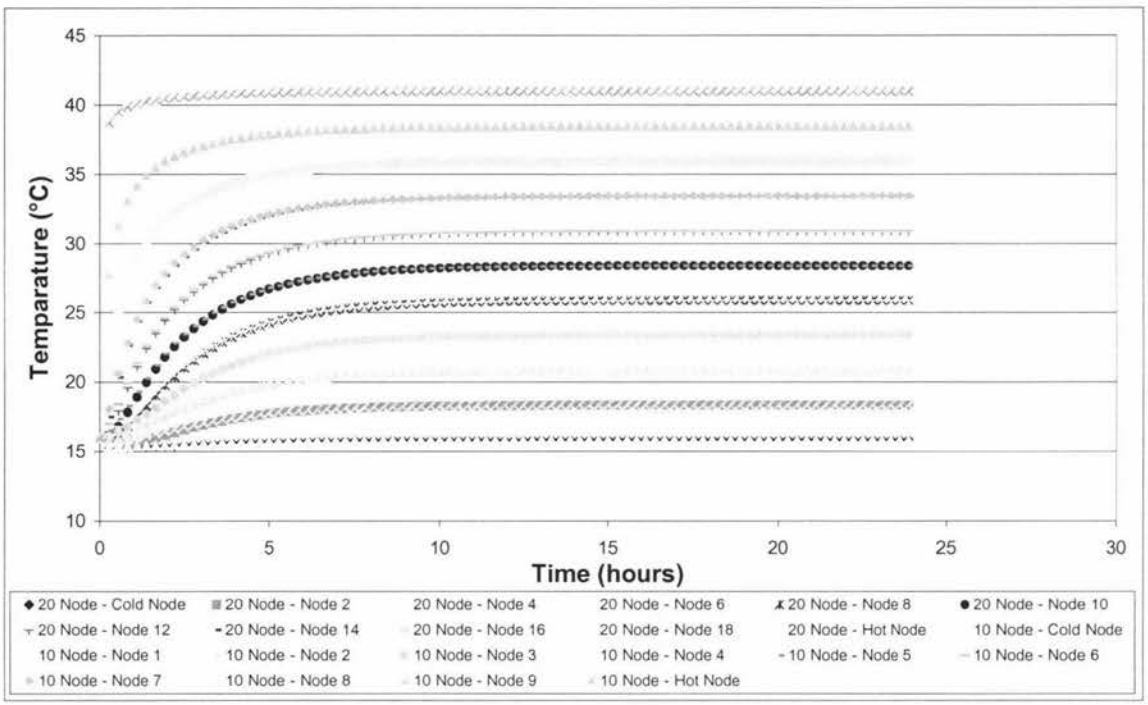

Figure 7.2 Comparison of node temperatures for simulations with varying number of nodes

The graph shows that the temperature values for the 10 node simulation overlap those for the 20 node simulation, indicating that the number of nodes that are used have little effect on the model value at that node depth. Because of the nature of the strength experimental, measurements will be made every 10mm, therefore the number of nodes used when running the model will be 10 for the 100mm slab, to match the model with the experimental node depth.

7.2.3 Initial sugar condition

There are five parameters for describing the state of the sugar, initial sugar temperature and water activity, the percentage that is amorphous and the initial crystallinity of that amorphous fraction, and the porosity of the bed.
The initial sugar temperature was measured as that of sugar left to cool to ambient temperature of the lab as that was temperature controlled at 17 – 18°C, but typically measured at 17.6°C. The initial water activity was identified as a parameter that would effect the outcome of the experiment so was varied throughout the experiment. The amorphous content was entered as the limit of the TAM work, in a worst case scenario sense, with a value of 0.1% being used and also assuming that the 0.1% amorphous component was pure with no initial crystallinity.

The initial porosity used for the initial model runs was 0.45 as discussed above (which was proven to be a good initial guess, with the actual porosity being measured after each experiment and found to be ranged between 0.45 and 0.46)

7.2.4 Temperature and heat transfer parameters

The first temperature parameters allow you to select a constant temperature for the bottom and top plates. If there is a normal shifting of the supply temperature this can be recorded and used as the experimental temperatures as opposed to assuming that the temperature supply will be constant.

The final parameter is the heat transfer coefficient of the plate containing the cooling/heating fluids. An initial heat transfer coefficient of 200 W/mK was used for the stainless steel plates. This is a very high value indicating a very good heat transfer coefficient, which is realistically not the case. By using an initial value for the heat transfer coefficient, the effects of the heat transfer coefficient on the model would be able to be observed more readily than if a more realistic (50 – 100 W/mK), value was used. This would then allow for more efficient fine-tuning of the model to the experimental data, especially for the temperature difference experiments.

7.2.5 Model output

The model has four output files, each containing the value for each of the outputs at every node used by the model (depending on the number of nodes defined in the initial setup). The four output files are temperature, relative humidity, amorphous content, and lumping strength.

Using these outputs and the corresponding parameter settings, the model was run for differing combinations of initial water activity and temperature difference in order to build up a picture of the maximum water activity that would result. It became apparent that different values of cold plate temperature at the same temperature difference would yield different results. This meant that temperature difference alone could not be used as a factor in plotting the graph required to get a picture of the experimental parameters required.

7.3 Experimental design

There were four main experiments that were identified.

The first involved selecting a temperature difference typical of those encountered during transportation when caking has been observed, and select two initial water activities, one that would cause the sample to lump and one that wouldn't. It would then be required to measure the RH and lumping strength at these different initial water activities, to allow the correlation between relative humidity and the subsequent lumping strength.

The second experiment involved selecting a water activity typical of that of the sugar being transported and measuring the RH and the lumping strength at temperatures that would cause one of the samples to lump and the other not.

7.3.1 Initial water activity

A temperature difference of 25°C was chosen for the differing initial water activity experiments. This difference was chosen in a practical manner, as sugar comes out of the bagger at 35°C, and 10°C was measured as the average ambient temperature for the storage area over the start of winter.

By using the model, it appeared that at a temperature difference of 25°C an initial water activity greater than 0.5 would cause the maximum water activity to go higher than 0.8, which was decided from the previous chapter to be the threshold of caking. Therefore in order to cause caking, an initial water activity of greater than 0.5 must be used, and to ensure that the sample would not cake it would need an initial water activity of less than 0.5.

Sugar samples were taken from the bagging station and placed in an airtight plastic bag that was then placed inside another plastic bag. Containers filled with the desired saturated solution were then placed inside the bags and the sugar left to equilibrate for a minimum of two weeks.

To obtain the caking conditions required it was necessary to have a salt with a very low equilibrium relative humidity, and one with a very high equilibrium relative humidity. For the low salt, chromium oxide was considered as it has an equilibrium relative humidity of 35% (Aw = 0.35). Potassium iodide was considered as the high salt as it has an equilibrium relative humidity of 69% (Aw = 0.69). These two relative humidities were then run using the model to see if the outcome was a product that did not reach a water activity of 0.8 and one that did exceed a water activity of 0.8.

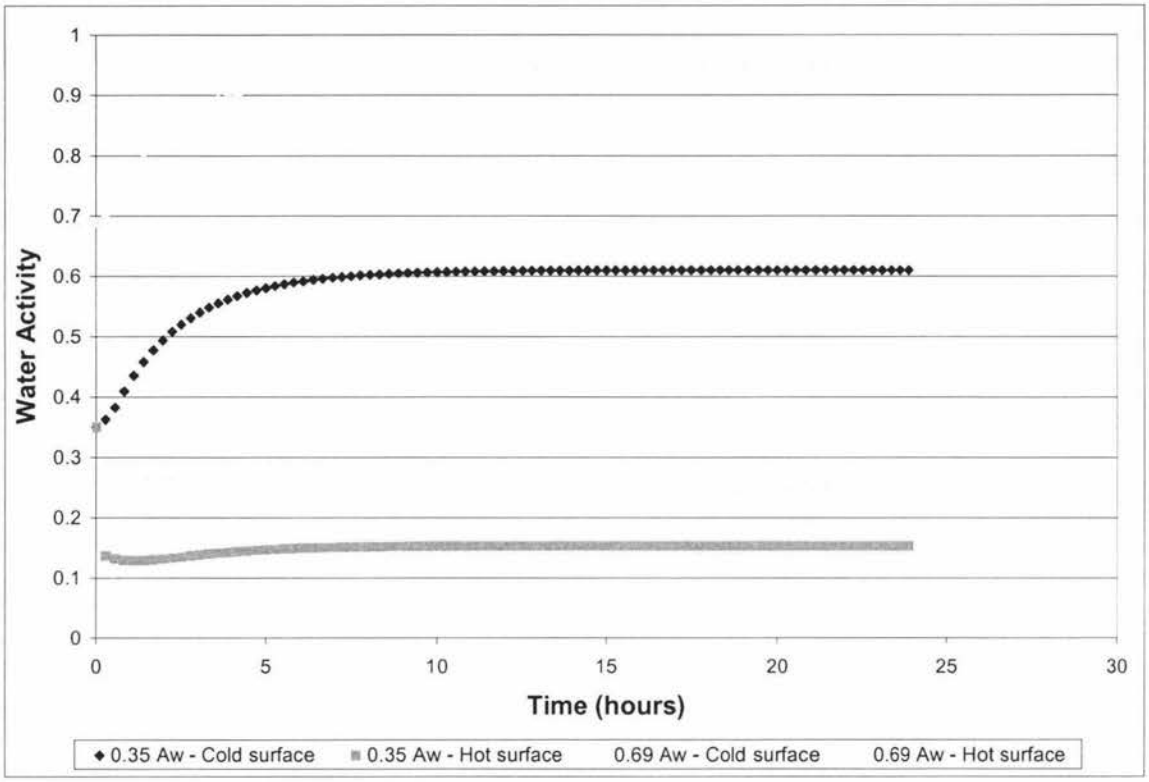

Figure 7.3 Model prediction of water activity distribution between a hot plate at 40 °C and a cold plate at 15 °C

As it can be seen in figure 7.1 (page 7 – 3), the model predictions yield the desired results for the experiment.

7.3.2 Temperature gradient

Typical measured moisture contents of sugar from out of the bagger had quite a large variance, between 0.035 and 0.015%. The typically observed value during experimentation was 0.022%, which translated to a water activity of 0.46. Using the model in the same way as with the relative humidity, the 25° C temperature difference will produce a maximum water activity of 0.72, which is well inside the lumping threshold.

For the run with caking, a temperature difference of 35° was chosen, with a theoretical maximum water activity at the top node of 0.86.

7.4 Experimental apparatus

The experimental rig consisted of three polystyrene rings, all 1200 mm in diameter and 100 mm thick with a 400 mm diameter hole removed from the center ring. These dimensions were used in order to ensure that any heat transfer was occurring in only one dimension, as this is the basis of the model.

Two baffled, stainless steel plates were sunk into the centers of the top and bottom plate in order to provide the temperature difference across the sugar sample. The temperature difference was supplied by using the laboratory cold tap (~15°C) and a Grant Series water bath was used to heat the bottom node water supply to the temperature required for the desired temperature difference.
Sealed holes in the center of the plates covered with Watman filter paper were used to measure the relative humidity at the top and bottom nodes by inserting a Hy-Cal relative humidity probe. As only one probe was available for use, three of the runs measured the top node relative humidity, and the run with the high initial water activity had the bottom node relative humidity measured as a check.

The center ring had holes placed through either side at the interval required to get the desired node depth. Type T thermocouples were then split through the middle and threaded through the holes so that the thermocouple junctions were in the center of the middle cavity. This allowed the measurement of the temperatures at the different node depths.

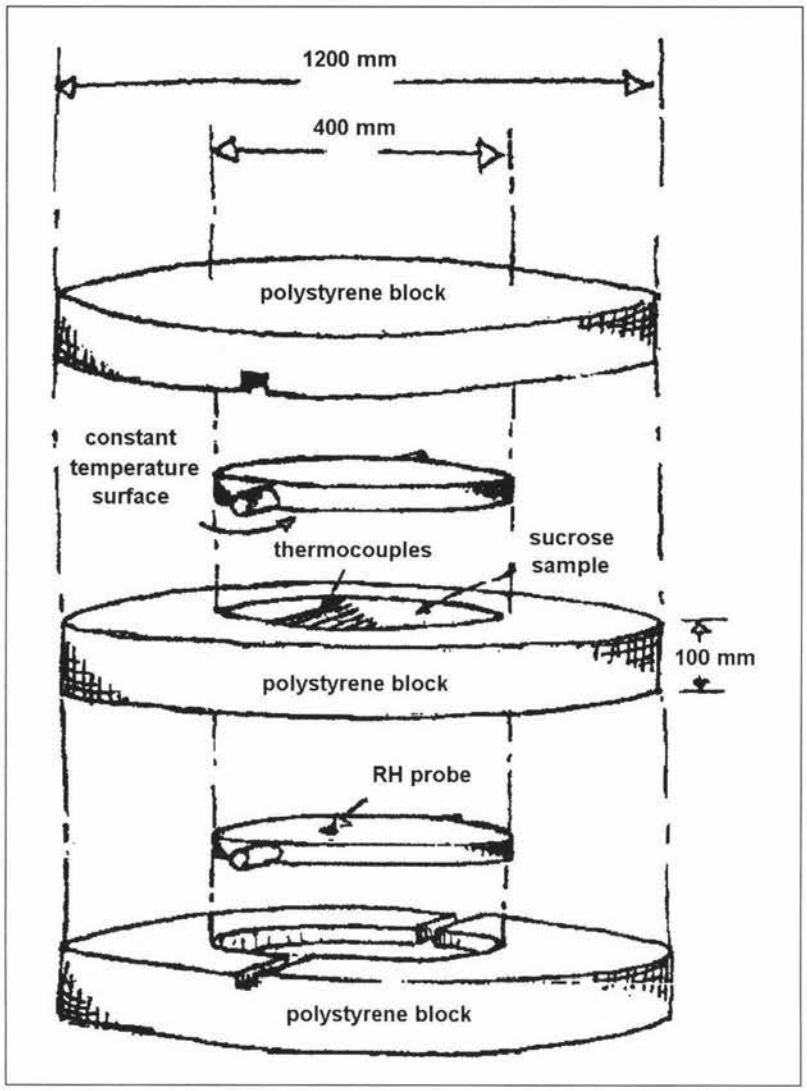

Figure 7.4 Experimental rig design (adapted from Bronlund, 1997)

7.5 RH probe calibration

To be sure of the accuracy of the relative humidity probe, the probe was calibrated by measuring the relative humidity of known constant relative humidity saturated salt solutions. The relative humidity measured by the Grant Squirrel Logger was measured and plotted against the known relative humidity of the salt solutions and a fit-line plotted.

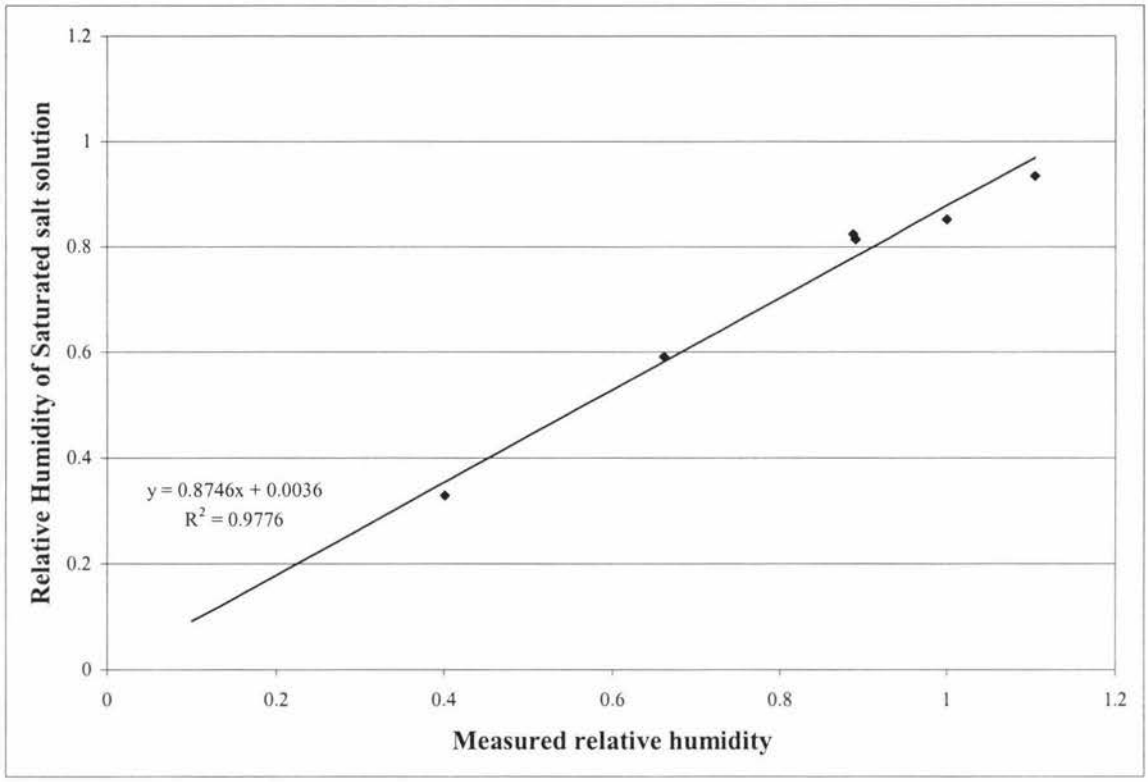

Figure 7.5 Calibration curve for relative humidity probe

The fit-line (equation 7.1), gives close to a 98 % explanation of the observed results, which was deemed as acceptable for the purpose of the experimental work.

$$y = 0.8746x + 0.0036 \qquad \text{equation 7.1}$$

Equation 7.1 will be used to adjust all of the relative humidity results obtained from the squirrel logger, in order to get a closer representation to the actual relative humidity within the experimental rig.

Closure

Using the model to help with some predictions of outcomes from different experimental conditions has helped in designing the experiments so that the outcome is approximately known. This will help with the experiments so that scenarios like the bottom node reaching an excessively high relative humidity (>95%) can be avoided, making the accuracy, repeatability and control of the experiments better.

CHAPTER 8

Experimental Results and Model Comparison

Introduction

Experiments were allowed to run until an equilibrium state was reached, where the data indicated from the squirrel logger would not fluctuate more than 0.6° C in a half-hour period. This was typically around 12 hours. After it was decided that steady state had been reached the hot and cold water supply was turned off and the liquid bridge strength at the top surface of the rig (cold node) measured using the blow tester. One node depth (10mm) was then carefully scraped away (in a position away from where the first measurement was taken so the sugar would have not been disturbed) using a ruler, and the strength re-measured. This was done for all of the nodes except the very bottom (hot) node.

8.1 Temperature Gradient

Two temperature gradients were used for the experiments carried out, 25 and 35°C. The cold temperature was measured as the temperature of the cold flowing tap in the lab and the temperature of the water bath was then set to either 25 or 35°C above that. The sugar starting temperature was at ambient temperature, typically 16°C.

Once the data for the experiment had been collected it was plotted against the model data used to simulate the experiment, with attention being paid to the differences in the graph and the parameters that would be likely to cause these differences. These parameters were then modified within the model between experimentally found extremes or values that made sense.

8.1.1 25°C temperature gradient

Figure 8.1 (page 8 – 2), shows the first plot of the experimental data versus the first run of the model.

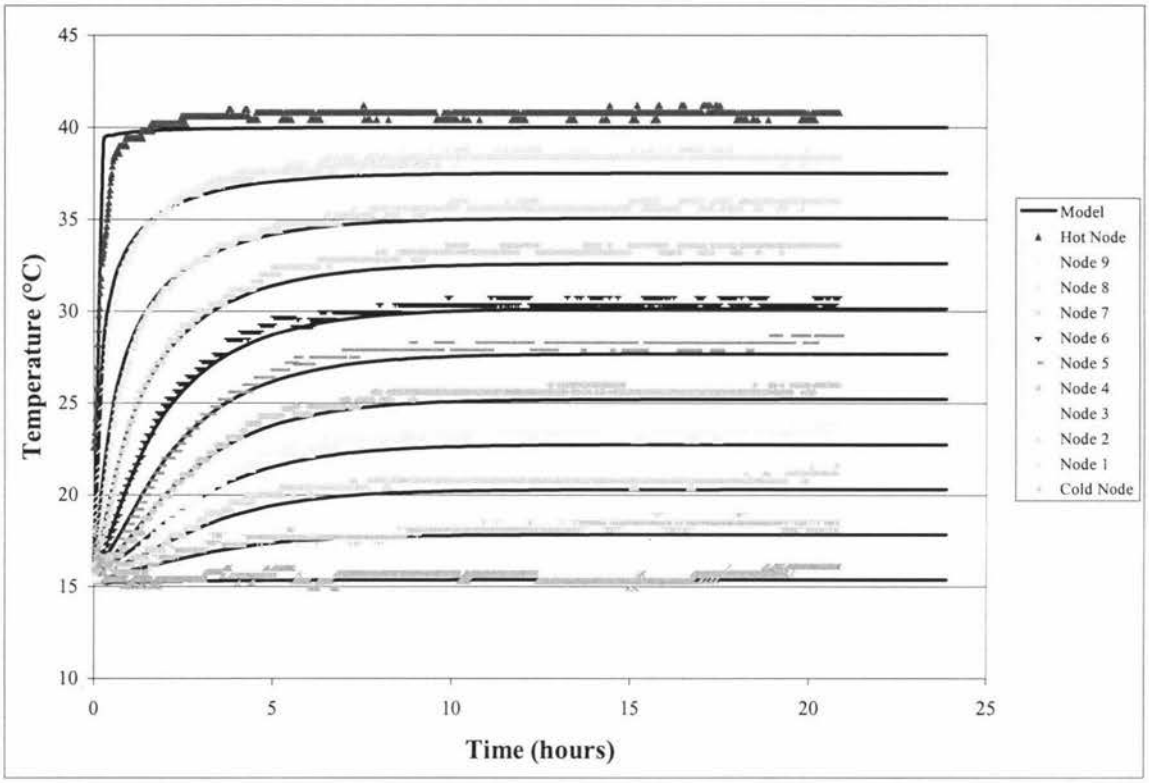

Figure 8.1 Experimental and model data for 25°C temperature gradient.

The plot shows that the general shape of the data between the model and the experimental data is good. There is a lot of scatter in the experimental data, but this is believed to be caused by the fact that the Squirrel logger is not a computer run logging system, meaning that the logger is not properly grounded. This causes implications when considering the nature of the experimental rig, which would effectively act as a large antenna in a factory of moving equipment, inherently being susceptible to signal noise.

The general shape of the experimental and model curves is similar, but the values for the model curve are slightly lower than the experimental curve. This indicates that the heat transfer coefficient that was chosen for the model (200 W/mK), is too high and a more realistic lower value for the stainless steel plates needs to be used (<100 W/mK). It is also a possibility that the porosity may need adjusting, as air is an insulator and the more pore space is allowed for, the slower and more reduced the effects of heat transfer will be.

Figure 8.2 (page 8 – 3), shows the data replotted, with the heat transfer coefficient in the model changed from 200 W/mK to 100 W/mK.

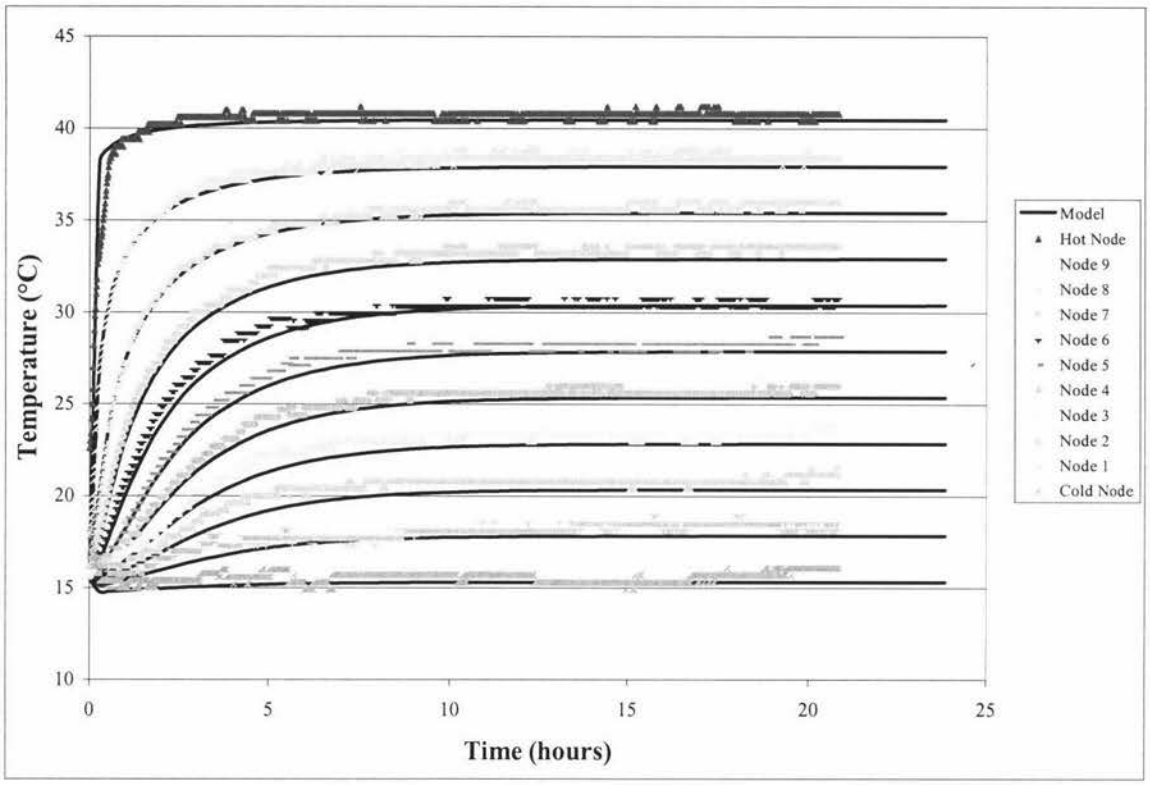

Figure 8.2 Model approximation with reduced heat transfer coefficient

Figure 8.2 shows a definite improvement of the fit of the model data to the experimental values at longer times, but the heat transfer coefficient needs to be reduced further. Once a heat transfer coefficient is found that brings the model and the experimental data to an acceptable point the effect of the porosity on the data fit can then be investigated.

Figure 8.3 (page 8 – 4), shows the fit of the model and the experimental data with the heat transfer coefficient then being reduced to 60 W/mK.

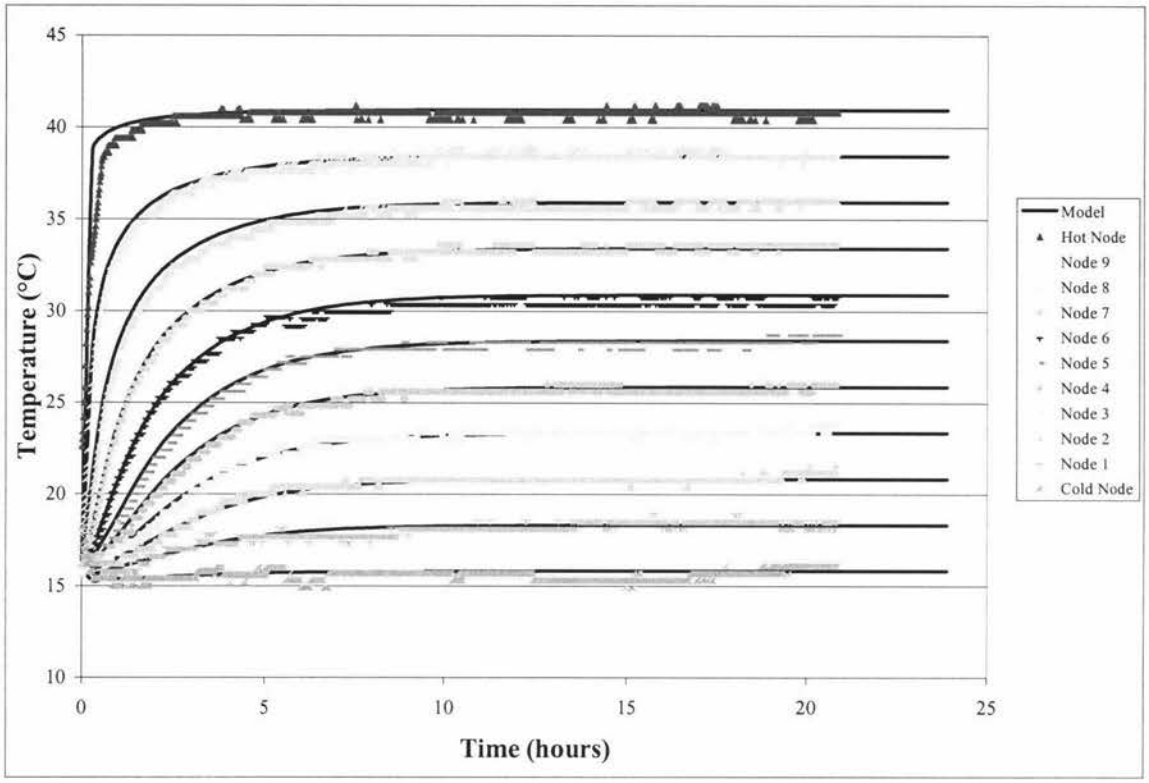

Figure 8.3 Best model approximation of experimental data

The model data shown in figure 8.3 is the closest representation of the experimental data. If the heat transfer coefficient was to be lowered any further, the data would increase further which is undesirable, especially for the hotter nodes.

With a suitable heat transfer coefficient found it is now possible to investigate the effects of the other factor that could be seen as having an effect on the temperatures calculated by the model, the porosity.

The model was run with the porosity set at the largest that it could be (standard bulk density, $\varepsilon = 0.49$), and the smallest (tapped density porosity $\varepsilon = 0.43$) to investigate the effect that the density of the product during storage and transportation could have on the effect on liquid bridging.

Figure 8.4 (page 8 – 5), shows the model predictions for samples with a porosity of 0.43 and 0.49 at 25°C.

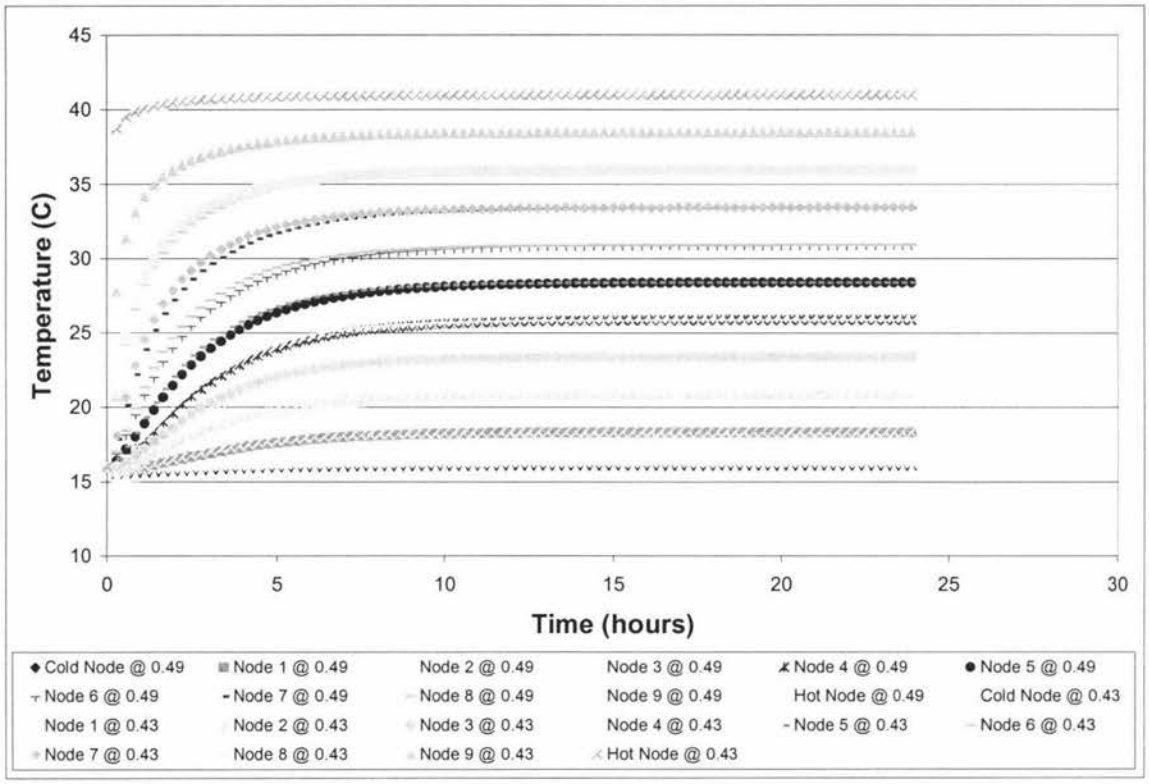

Figure 8.4 Effect of porosity on model temperature using best fitted model parameters

Figure 8.4 shows that whether or not the sample is at is tapped or standard bulk density, there is negligible effect on the model node temperatures, indicating a negligible effect on moisture transportation and therefore lumping. For future use of the model the porosity will be taken as 0.45, as this is the porosity of sugar measured under similar conditions to that used to fill the rig.

8.1.2 35°C temperature gradient

Figure 8.5 (page 8 – 6), shows the experimental versus model data for the 35° C temperature gradient experiment. Because of the fit of the 25°C model data the initial heat transfer coefficient used was 60 W/mK.

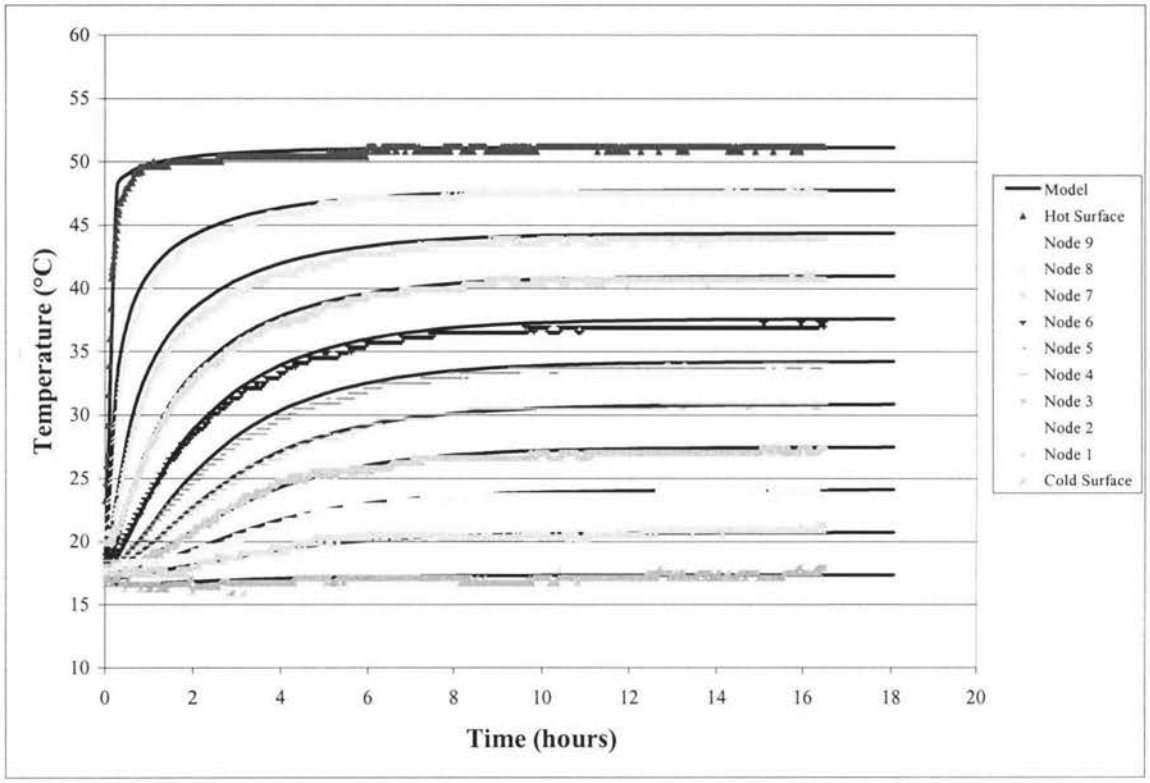

Figure 8.5 Experimental and model data for 35°C temperature gradient

As it can be seen by the graph the experimental data is represented well by the model data with a heat transfer coefficient of 60 W/mK. With the 25°C temperature gradient experiment it would be assumed that the increased temperature gradient would have little or no effect on the magnitude of difference created by a change in the porosity. Again it was decided that 0.45 would be the best value to be used for the porosity of the sample in the experimental rig due its size and weight (the 100mm ring used close to 12 kg of sugar). This made it nearly impossible to have a tapped sample, but some settling of the sample did occur during the packing of the rig.

The graphs for the 35°C temperature gradient again showed a lot of scatter in the data, again being put down to the fact that the setup of the rig would be prone to noise created within the factory.

8.2 Relative humidity

There were three water activities that were used in the investigation of the models fit to experimental data. As discussed in chapter seven there were two samples that were specifically humidified in order to produce desired caking effects (with one humidity causing caking and the other not), and one sample that was used at the observed humidity as it came out of the bagging station.

Due to only having one humidity probe it was not possible to measure the humidity at the top and bottom nodes simultaneously, but measurements were made for each and the corresponding model node compared.

8.2.1 Initial sample water activity = 0.35

Due to the hygroscopic nature of sucrose, it is more difficult to remove moisture from a sample than it is to absorb moisture onto it. Because of this, the sample to have the low initial water activity was left to equilibrate for the longest time, four weeks. The water activity was measured prior to the sample being placed in the rig, then the relative humidity of the sample was measured, and then adjusted using the calibration data (equation 7.1).

The relative humidity of the sample prior to being placed in the rig (once adjusted), was 33%. The first experimental data point was also measured as 33% which is good as it was feared that the sugar would quickly take up moisture upon exposure to the ambient atmosphere, and yield a higher starting point than was desired. The relative humidity profile was then measured with the plates set up for a temperature gradient of 25°C.

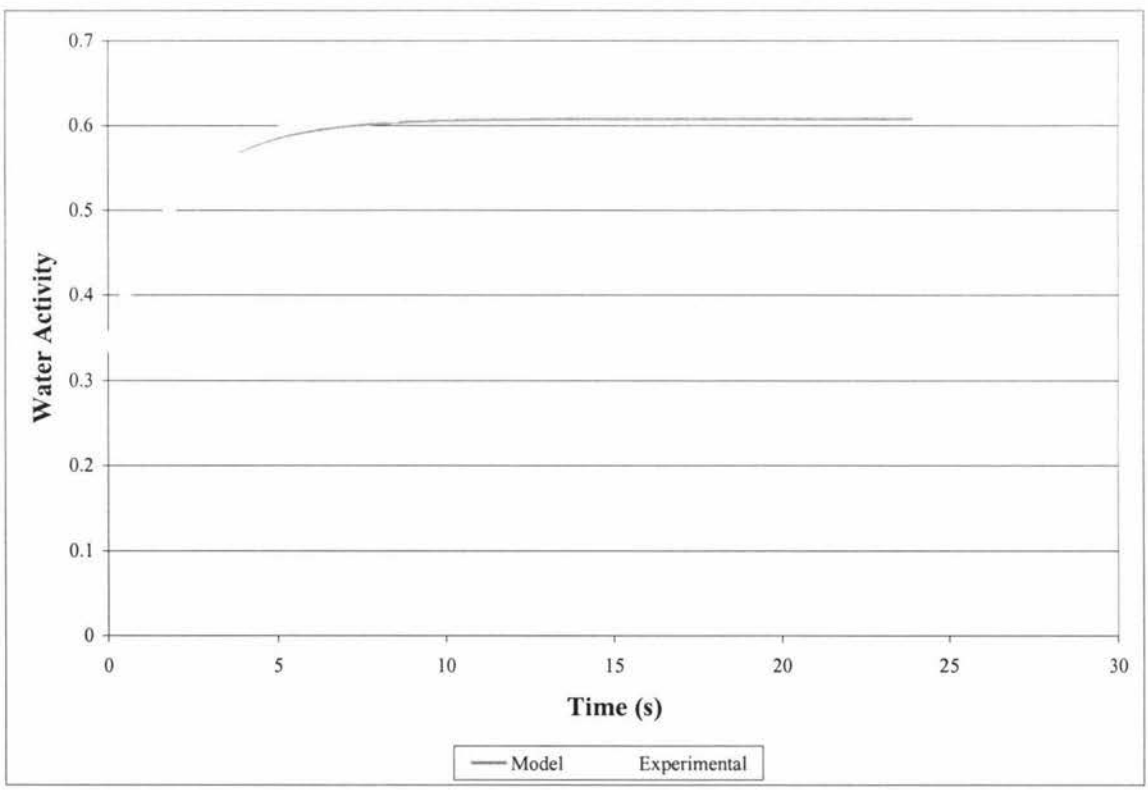

Figure 8.6 Top node water activity profile for a sample with initial Aw = 0.33

Figure 8.6 above, shows that the model fits the experimental data extremely well. The experimental data ends up having a slightly higher steady state water activity. A possible cause for this is that the temperature of the cold plate (using water supplied from a cold tap) and the temperature of the sugar, although left at ambient temperature, may not have been the same at the start of the run.

Unlike the temperature data, the relative humidity data shows no sign of noise, indicating that the RH probe has a better capacity to take measurements in the surrounding environment, also because of the difference in nature between the two pieces of equipment.

Although the fit of the data was good, the effect that the porosity of the sample has on the relative humidity profile generated by the model was investigated, and is shown in figure 8.7 below.

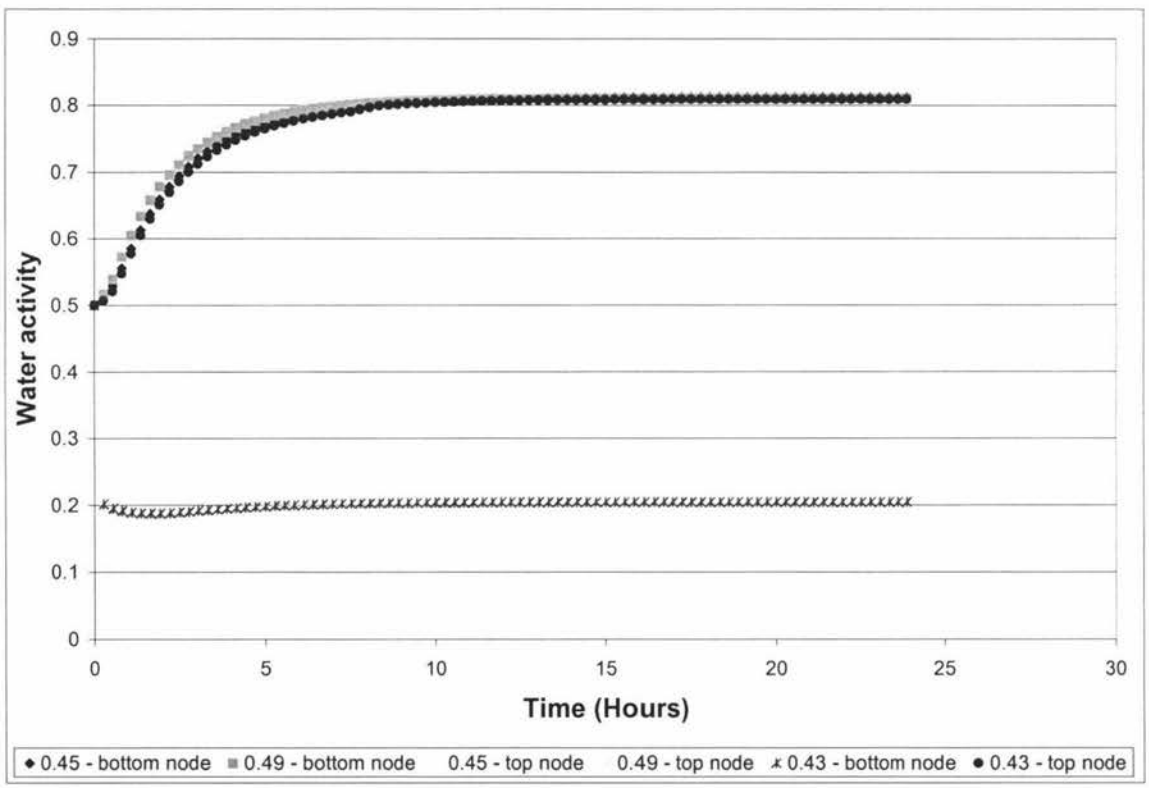

Figure 8.7 Effect of porosity on model relative humidity predictions at 25°C

The graph shows that at the lower water activity values (hot plate), the porosity has very little, if no effect on the model predictions for the water activity. At the higher water activity values (cold plate), there is a significant difference in the values of water activity in the first five hours. In the first five hours the lower the model value for the porosity, the lower the water activity, with all predictions ending up with roughly the same water activity at steady state.

As the experimental data appears to be quite close to the model prediction in the first five hours, and seeing that porosity has very little effect on the steady state of water activity, it was decided that altering the porosity from its initial value of 0.45 would not achieve a better fit for the experimental data.

8.2.2 Initial sample water activity = 0.46

The samples with the water activity initially at 0.46 are the samples that were taken from sugar that had come straight off the bagging line. The samples were kept in the bag while the initial reading was taken, then the sucrose was taken straight from the bag and placed into the experimental rig, and the change in relative humidity measured with time. As sugar at this relative humidity was readily available it was possible to do two experiments over a 100mm slab thickness, one at 25°C and another at 35°C temperature gradients. This would give insight into the effect of increased temperature gradient on the relative humidity profile of the slab.

Figure 8.8 below, shows the relative humidity profiles of two samples measured at temperature gradients of 25 and 35°C, with initial cold plate temperatures of 15.2 and 15.4°C and hot plate temperatures of 40.2 and 50.4°C.

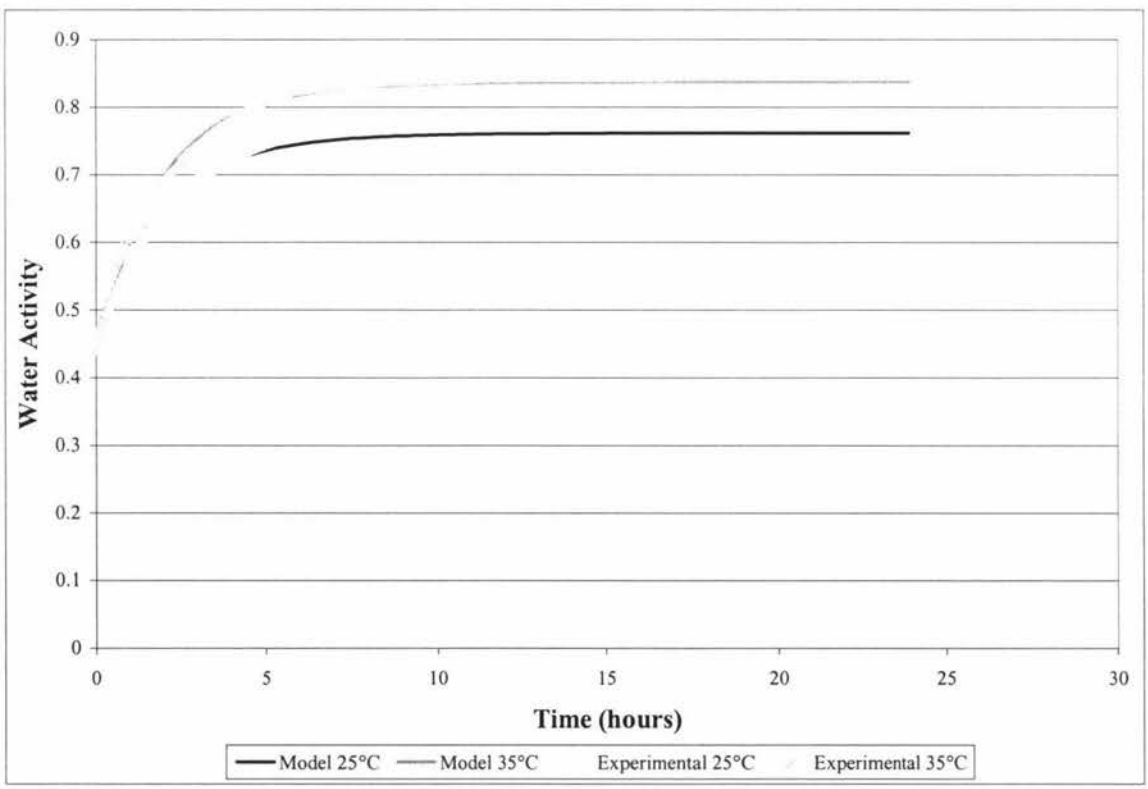

Figure 8.8 Cold node water activity profile for a sample with initial Aw = 0.46

The graph shows that both of the modelled series of data represent the experimental data very well. Again, the experimental measurements of the water activity are slightly higher than the model predictions, but as it can be seen the temperature gradient has an effect on the observed steady state relative humidity of the sample. A 10°C difference in temperature gradient creates a water activity difference of 0.072, so a slight difference in temperature between the sucrose sample and the cold node temperature could explain the observed differences. The initial rates of the two experiments are different and the model has successfully predicted this.

8.2.3 Initial sample water activity = 0.69

The high initial water activity sample was left for three weeks in order to take up the moisture required to achieve a water activity of 0.69. The water activity measured before the sample was placed in the experimental rig was 0.66, which was slightly lower than was intended. The first measured reading however was close to 0.68.

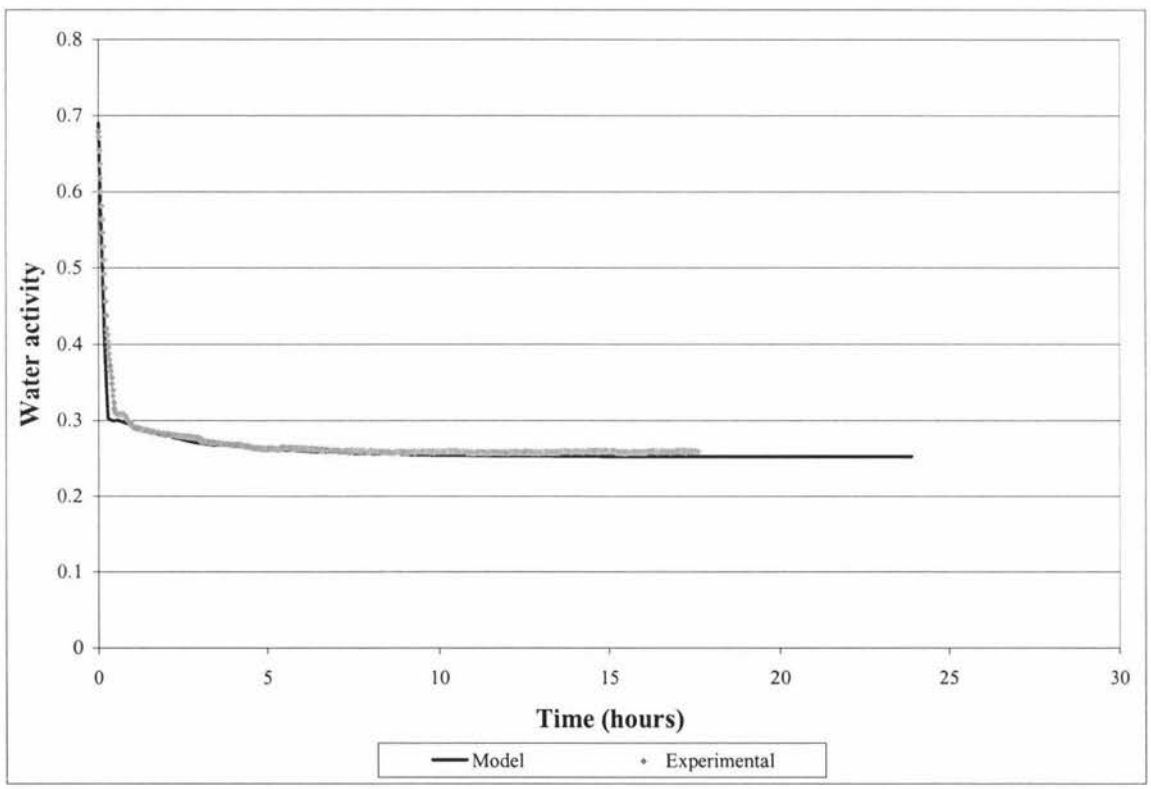

Figure 8.9 Bottom node water activity profile for a sample with initial Aw = 0.69

Figure 8.9 shows that unlike the previous experiments, the initial model data fit is not as good, yet the steady state value for the water activity is closer. The only experimental difference between the measurements taken for the top node and the bottom node is that a

piece of filter paper was used on the bottom node, in order to prevent sucrose from filling the cavity used to house the sucrose. This will have created an added resistance to mass transfer of moisture to/from the relative humidity probe, causing a delay in the probes response, and explaining why the initial data is not as well fitted.

8.3 Strength

The experimental strength data was found by using the technique reported by Bronlund (1997). A portable blow tester used by Paterson *et al* (2001), was also used to determine the flowrate at which the lumped sugar was disrupted, then a 10mm layer was scraped away and the tests repeated, until the bottom most node was reached. This was repeated for the four initial water activities investigated above, with the difference in temperature gradient investigated also.

8.3.1 Initial sample water activity = 0.33

Figure 8.10 shows the model approximation for the experimental strength data at a temperature gradient of 25°C.

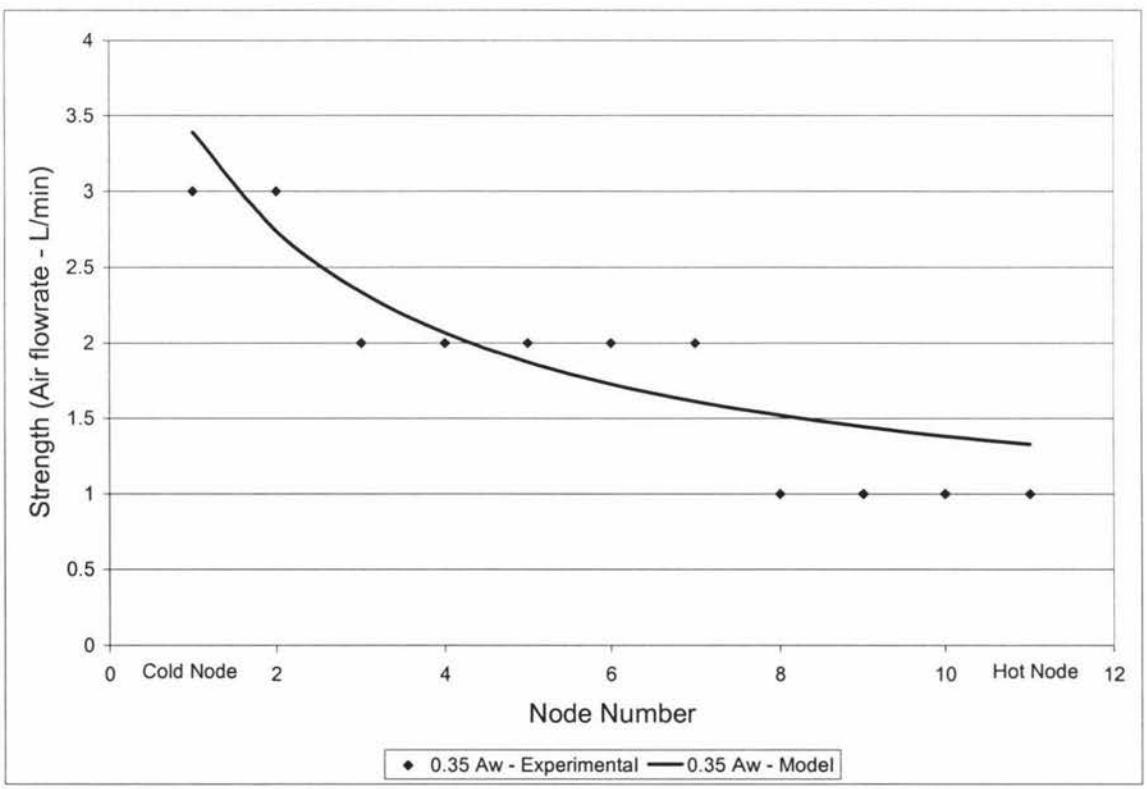

Figure 8.10 Lumping strength profile for a sample with initial Aw = 0.33

The model data does follow the trends that are outlined by the experimental data. Because of the scale of the flow-meter being used to measure the flow-rate of the gas through the blow tester, it was impossible to make measurements that were more accurate than one litre per minute. This has meant that at lower strength values, the blow tester has not produced results that are accurate enough to ascertain how accurate the model is. Because of this, the experiments where the initial water activity is higher, which should produce samples with a higher lumping strength, will have to be used to determine the fit of the model caking strength data to the experimental.

8.3.2 Initial sample water activity = 0.46

Figure 8.11 shows the model and experimental data for the sucrose samples initially at a water activity of 0.46, with temperature gradients across the top and bottom plates of 25 and 35°C.

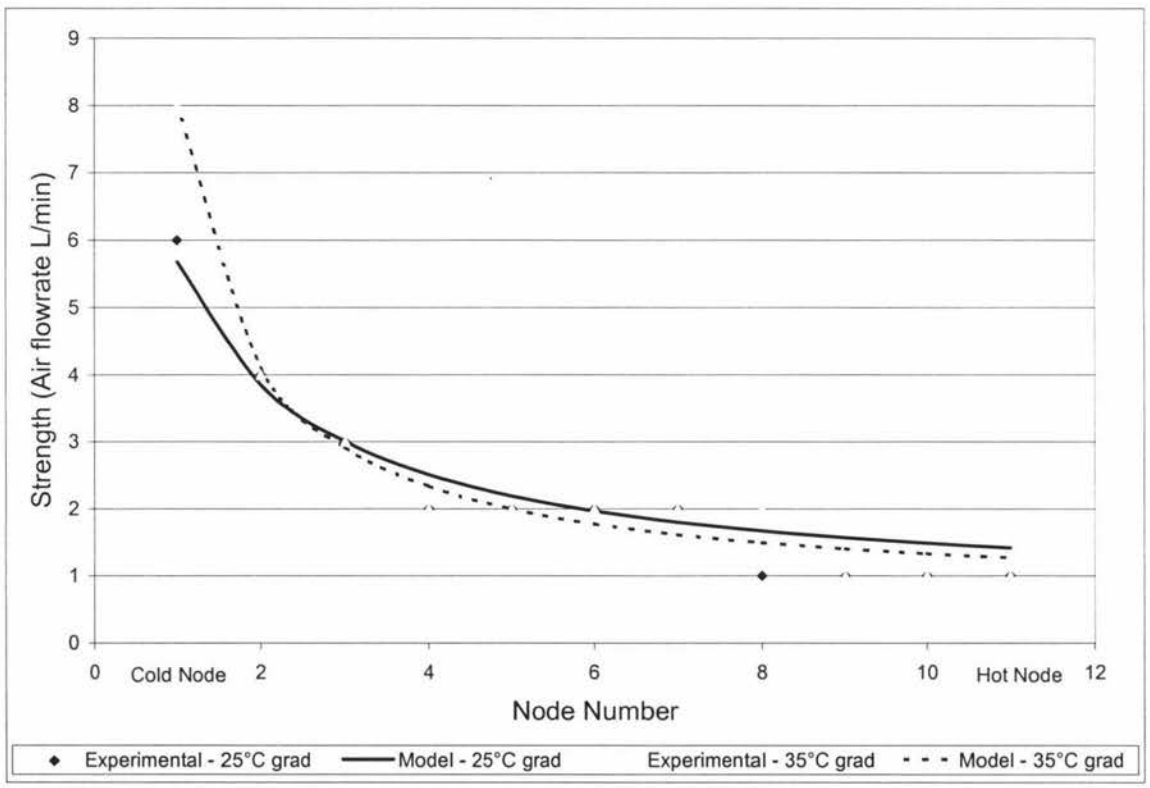

Figure 8.11 Lumping strength profile for a sample with initial Aw = 0.46

The results for this experiment are similar to those for the initial water activity of 0.33 experiment, with good correlation between the model predictions and the experimental values, despite the inaccuracy of the experimental method. It would have been ideal to use a more accurate flow-meter to record the results for the nodes with a lower relative

humidity, and then perhaps changed the flow-meter once the measurements recorded came closer to the maximum value readable for the flow-meter.

8.3.3 Initial sample water activity = 0.69

Due to the inaccuracy at the lower lumping strength levels in the previous two experiments, a flow-meter with 0.2 liter per minute increments was used in order to try and confirm the accuracy of the blow tester. The effect of the porosity on the model strength prediction was also plotted, as the strength function is based on relationships between the water activity and the corresponding Kelvin radius.

Figure 8.12 shows the model and experimental data for the sucrose sample initially at a water activity of 0.69, with a temperature gradient across the top and bottom plates of 25°C.

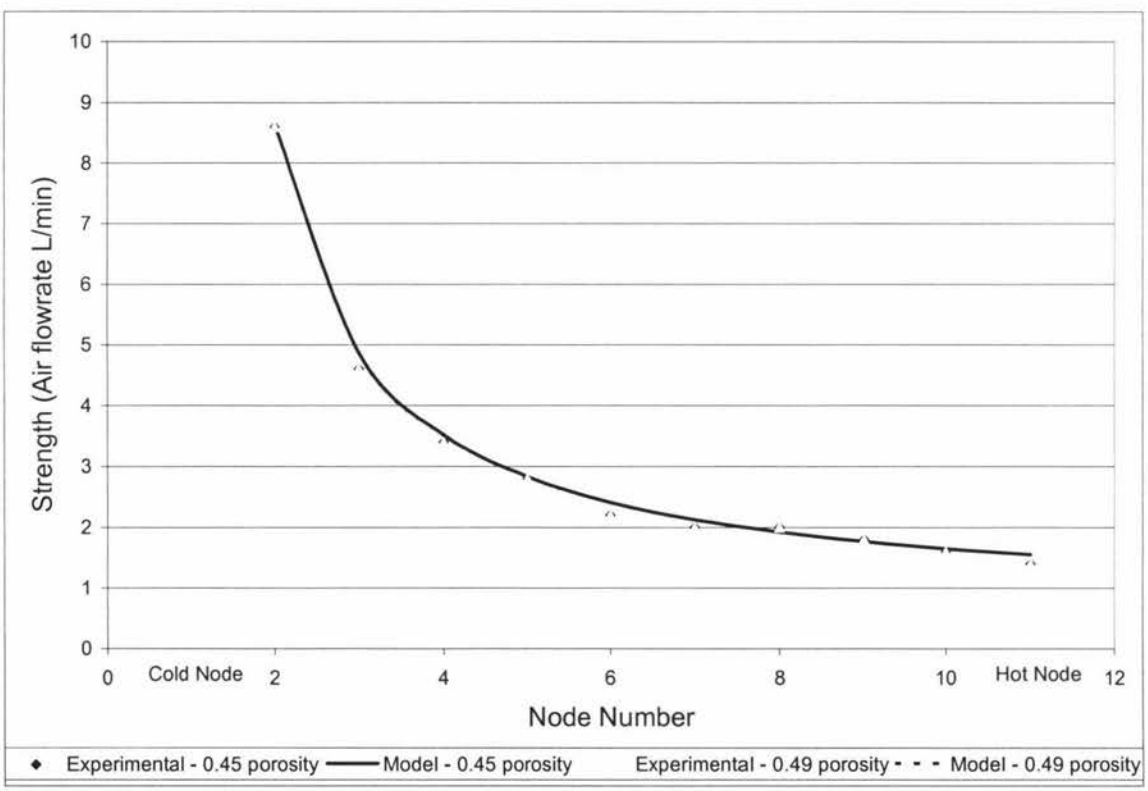

Figure 8.12 Lumping strength profile for a sample with initial Aw = 0.69

Both the model and the experimental data indicate that there is little difference between in lumping strength at the two different porosity's, with the model data overlying itself exactly.

Using the flowmeter with the finer increments, it has been shown that the experimental and model data do have a good fit.

The maximum value predicted by the model at the cold node was not plotted, as it was impossible to measure the value due to its extreme magnitude. As stated in chapter six, the maximum measurable value for the blow tester was 50 litres per minute, where the value predicted by the model at the cold node was 78 and 79 litres per minute for the initial values of porosity, those being 0.45 and 0.49 respectively. The slight difference in result for the model data at the two different porosity's is expected, because of the strength function being based on water activity and Kelvin radius. A change in the porosity of the sample bed would change the capillary condensation conditions, which changes the Kelvin radius and therefore the lumping strength.

Closure

This chapter has shown that the mathematical model successfully predicts the temperature, relative humidity, and caking strength gradients measured experimentally. Hence the model has been validated and can be used to predict what will happen under different environmental conditions.

CHAPTER 9

Model Application – Results and Discussion

Introduction

With the model validated, it was possible to use the model to predict situations that would arise under various conditions of initial water activity at differing hot and cold plate temperatures, and different starting conditions for the sugar, as results for the same temperature gradient at different cold surface temperatures are different.

These results can be applied to different situations that can occur during the sucrose production process and suggest improvements to the process in order to try and minimise, if not eliminate, the caking problems encountered.

9.1 Model results

The model was run for different values of hot and cold plate temperatures rather than picking a base temperature such as an average ambient temperature for a particular season, and then having the hot temperature based on a particular temperature gradient. This approach was taken, as during the initial model use for the aid in experimental design, it was realised that the temperature gradient approach would not produce a useful process control tool. This is because if a situation arose where the temperature gradient was not close to that which had been used, interpolation would be needed in order to get a useful indication of the condition that would transpire.

By using an individual hot/cold plate temperature approach, it would be possible to design a graph that would give a maximum line, and any combination of conditions that yielded a point below that line would be safe from the effects of temperature gradient induced caking.

This was done by running the model at different hot and cold plate temperatures for differing values of initial water activity. A worst case scenario is produced when the model is run with the initial temperature of the sucrose, and hot plate at the same temperature. Under cooling conditions, a maximum is produced, with this value being dependent on initial conditions used. Figure 9.1 (page 9 – 2), shows this scenario, with the sucrose having an initial water activity of 0.325, hot and cold temperatures of 30 and 0°C respectively and with the sucrose assumed to be at 30°C, at time zero.

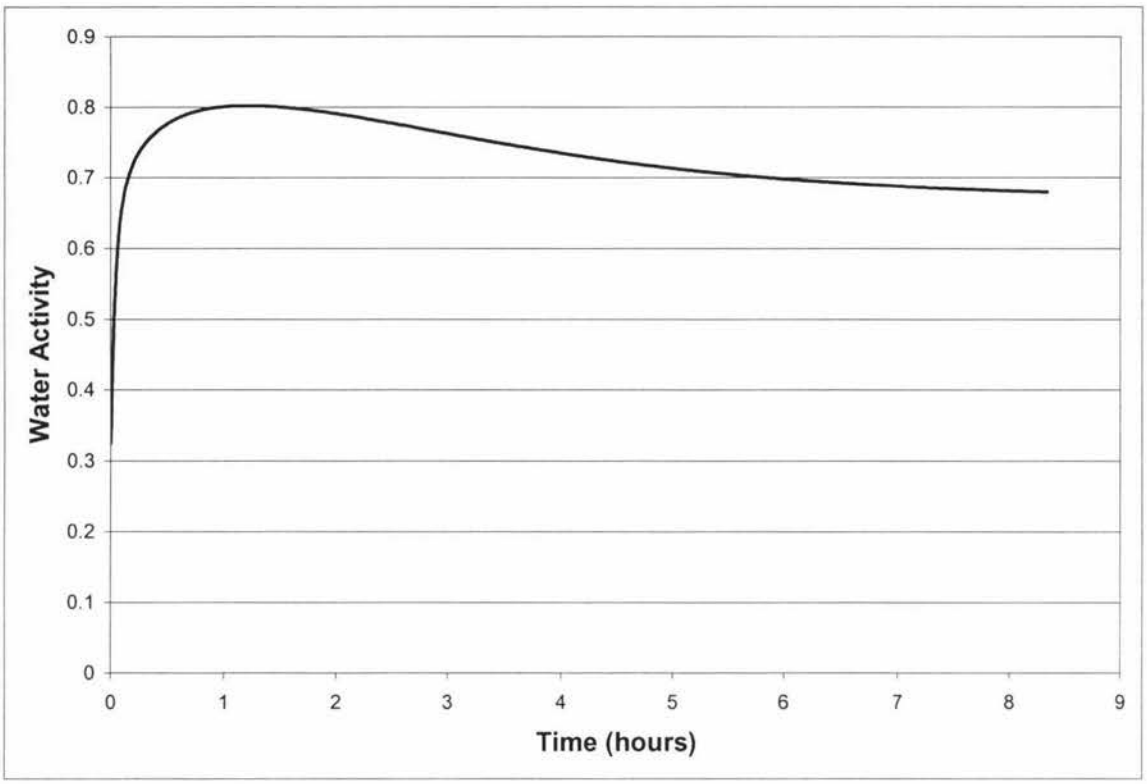

Figure 9.1 Model cold node water activity profile showing a maximum at 0.8

The model was then run under for different sets of initial hot and cold temperatures, modifying the initial water activity until the maximum water activity reached was as close to 0.8 as possible. This data was then plotted on a graph, shown in figure 9.2 (page 9 – 3).

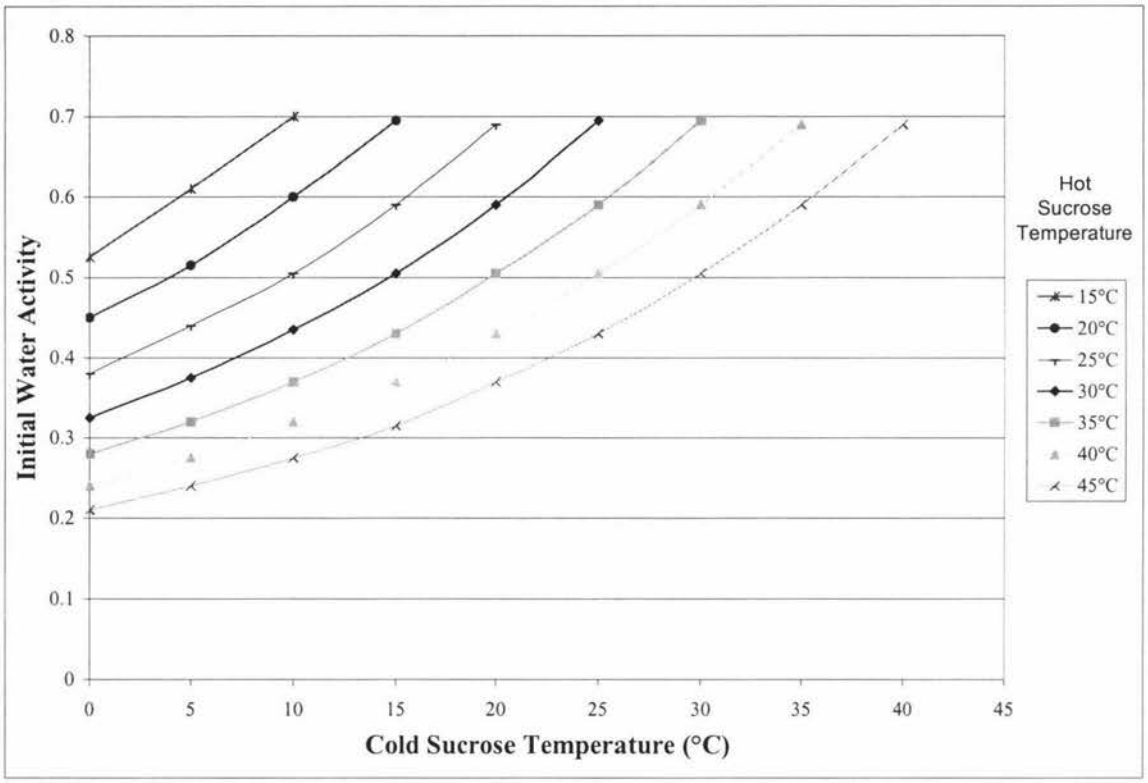

Figure 9.2 Initial water activity resulting in maximum water activity of 0.8 for different induced temperature conditions

Each of the lines in the graph represents the limit for each set of conditions. If the present conditions produce a point on the graph that is above the line, then the product can be expected to cake.

The severity of the caking will depend on the distance from the line, but as the line represents a maximum water activity of 0.8 there is the possibility the transportation may disrupt the liquid bridging enough so that caking is not evident. However, if the product is stored without transportation for a period of more than a day, it is also possible that irreversible caking may occur.

9.2 Discussion

The graph shown in figure 9.2 above is a very powerful tool for process control and improvement. Knowing the conditions that will lead to the caking is beneficial to the company in many ways.

A key use for the information that is provided in figure 9.2 is to be able to predict the impact of temperature cycles on sucrose that has been produced.

There are three possible temperature cycle scenarios:

1. If the sucrose leaving the packaging area is at a temperature higher than the ambient temperature of the air where it will be stored or transported, a temperature gradient will exist. As a result a humidity gradient will also occur, and moisture will be transported to the outer surface of the container, increasing the relative humidity and hence the chance of lumping at the outer surface.

2. During the day the surface of the container will heat up creating a temperature gradient between the sucrose at the container surface, and the sucrose at the center of the container. This will force moisture to the centre of the container, increasing the relative humidity.

3. During the night the surface of the container will cool down, creating a temperature gradient between the sucrose at the container surface and the middle, forcing moisture to the outside of the container.

In all three of these situations, if the initial water activity of the sample is known, figure 9.2 can be used to predict the chance that the sucrose will reach a maximum water activity of 0.8 and therefore risk the chance of lumping.

This can also be used from the other perspective by using the known temperature conditions of the sucrose as is packaged, and the conditions that it will be stored under, to set limits for the water activity of the sucrose when it is packaged.

This would help in optimising production, as it would allow different runs to be allocated to different customers, based on initial and environmental conditions. If a slightly warmer, wetter batch of sucrose was produced, instead of sending it to the next customer on the list, it would be possible to allocate that batch to a local customer where the temperature gradients are less extreme. This minimises the chances of the product caking and also minimises the wasting, or need for recycling of product. This reduces production lead times, as less product is having to be recycled because of quality, caking of product occurs less, and therefore increasing customer satisfaction.

Using seasonal temperature patterns it will also be possible to optimise the temperatures and/or the residence times in the driers, depending on the ambient conditions and the state of the sugar leaving the centrifuges. By coupling this with a mass and energy balance of the driers, it will be possible to optimise the running of the driers on a seasonal, monthly even hourly basis, minimising the cost of the drying process.

This leads into further opportunities to improve the drying process by considering options such as a recycle, to increase the time before the sugar enters the silo, and reducing the temperature of the sugar as it leaves the silo to be packed.

Closure

This chapter has shown that the data based on the verified model can be used to build up a picture that will help in understanding how sucrose produced will react to different temperature conditions for any given initial water activity. This can then be applied to the storage and transportation conditions that a customer's sucrose will be exposed to, helping to minimise the chances of sending a product that will cake to that customer.

The importance of knowing the initial water activity of the sucrose has also been highlighted, as the water activity of the sucrose is the only process parameter that can be controlled.

CHAPTER 10

Conclusions and Suggestions for Future Work

10.1 Conclusions

This work has identified the major contributing mechanism for the lumping and caking of bulk sucrose and the conditions under which this occurs.

The content of amorphous sucrose that exists during different stages of the production process was assessed using a thermal analysis monitor, a special type of calorimeter. Significant (greater than 0.1%) traces of amorphous sucrose were found to exist at the end of the first rotary drier (~80°C). By the time the sucrose from which the sample had been taken, reached the end of the second drier (five minutes residence time at 45°C), the amorphous material had dissolved or recrystallised.
Samples from the bottom of the silo and after the packaging process were shown to have no significant traces of amorphous sucrose, indicating the mechanism responsible for the caking of bulk sucrose is the humidity/temperature gradient mechanism.

Investigations into capillary condensation were made to determine the point where significant capillary condensation between sucrose particles in a packed bed occurs. This point was found to be at a water activity of 0.76, with the occurrence of capillary condensation causing the formation of liquid bridges between the sucrose particles in the bed, lumping the sucrose. With continued capillary condensation, the liquid bridges were then seen to fill the pores between the particles, leading to increased lumping strength before total liquification of the bed at water activities greater than 0.94. A relationship between the water activity and the size of the capillary radius was formed and then the strength of the lumped bed was correlated to this radius as well.

The lumped bed was then exposed to an environment that had a lower water activity. It was found that with time the liquid bridges between the particles began to crystallise and form solid bridges, far superior in strength to the liquid bridges.

A model which describes the one-dimensional transportation of moisture as a result of a temperature gradient was then adapted from work done with lactose and the model validated. The model was then used in conjunction with the critical water activity to construct a graph based on the initial water activity of the sucrose and the hot and cold temperatures creating the temperature gradient. This provided a graph that can be used to determine the conditions under which a sample at a certain pack temperature and initial

water activity can be stored at, or what initial water activity is required to ensure that the present temperature conditions do not cause the product to cake. This is a very powerful tool, especially when compared against the plant experience of lumping conditions.

As a result of this work it is seen as quite important that the measurement of the quality of the sucrose be moved away from moisture content and toward water activity, mainly because of the ease and accuracy of measurement.

10.2 Suggested Future Research

This work has highlighted several areas, which could be investigated in order to improve the quality of the sucrose that is currently being produced

- Effect of using auger screw conveyors for transportation within production
    - Contribution to amorphous content through grinding in conveyors
    - Effect of particle size on critical water activity for lumping
    - Investigate the effect of dust on the surface
        - increased ability to take up moisture due to increased surface area
- More accurate TAM determination of amorphous contents out of primary and secondary driers
- If decreasing the temperature of the sparged air into the silo will decrease sugar temperature in a way that allows exposure to colder storage/transportation conditions (decrease temperature gradient)
- Use of model graph in optimising drier
    - Temperatures
    - Residence times
    - Feasibility of third drier/cooler to increase overall drying and hence decrease packing temperature

REFERENCES

Adamson, A. W. (1963). Physical Chemistry of Surfaces, John Wiley and Sons, New York.

Bagster, D. F. (1970). "Cause, prevention and measurement of the caking of refined sugar - a review (part 1)." International Sugar Journal, 72(861), 263-267.

Billings, S.W. and Paterson, A.H.J. (2000). "Sorption rates onto amorphous sucrose", Proceedings of the 7th Annual New Zealand Engineering and Technology Postgraduate Conference, 49 – 54.

Bronlund, J. (1997). "Modelling the Caking of Bulk Lactose." PhD Thesis, Massey University, Palmerston North, New Zealand.

Bruijn, J. M. and Marijnissen, A. W. (1996). "Moisture Content of Sugar Crystals and Influence of Storage Conditions." Proceedings of the Conference on Sugar Processing Research, 183-196.

Chinachoti, P. and Steinberg, M. (1986a). "Moisture hysteresis is due to amorphous sugar." Journal of Food Science, 51(2), 453-455.

Chinachoti, P. and Steinberg, M. P. (1986b). "Crystallinity of sucrose by x-ray diffraction as influenced by absorption versus desorption, waxy maize starch content, and water activity." J. Food Sci., 51(2), 456-9, 463.

Cussler E. (1976), "Multicomponent Diffusion", Elsevier Scientific Publication Company, New York.

Foster, K. (2000). Doctorate Thesis in Progress, Massey University, Palmerston North, New Zealand.

Gal (1975). "Recent advances in techniques for the determination of sorption isotherms." In "Water relations in foods", (Duckworth R.B. EDS), Academic Press, London.

Gao, D. and Rytting, J. (1997). "Use of solution calorimetry to determine the extent of crystallinity of drugs and excipients." International Journal of Pharmaceuticals, 151(2), 183-192.

Gekas, V. (1992). Transport Phenomena of Foods and Biological Materials, CRC Press, Boca, Raton.

Grayson, M. (1979). Kirk-Othmer Encyclopaedia of Chemical Technology, John Wiley and Sons, New York, 116-123.

Helderman, W. (1927). Z. Physical Chemistry, 130, 396.

ICUMSA 20th Session, Colorado Springs, S. 11, Density, 265-270.

Iglesias, H. A. and Chirife, J. (1982). Handbook of Food Isotherms : Water Sorption Parameters for Food and Food Components, Academic Press Inc., New York, U.S.A.

Johari, G. P., Hallbrucker, A., and Mayer.E. (1987). "The Glass Transition of Hyoerquenched Water." Nature, 330, 552-553.

Ludlow, D. K. and Aukland, N. R. (1990). "Caking and flowability problems of sugar in a cold environment." Powder Handling and Processing, 2(1), 21-24.

Lyle, O. (1957). Technology for Sugar Refinery Workers, Chapman and Hall Publishers, London,U.K.

MacCarthy, D. A. and Fabre, N. (1989). "In "Food Properties and Computer Aided Engineering of Food Processing Systems" (Singh,P. and Medina,A.). Kluwer Academic Publishers.", 105-111.

Mak, F. K. and Kelly, F. H. C. (1976). "Some physical and chemical properties of sucrose surfaces." Z. Zuckerind., 26(11), 713-18.

Mathlouthi, M. and Reiser, P. (1995). Sucrose. Properties and applications, Blackie Academic and Professional, Glasgow, U.K.

Mayer, E. (1988). "Hyperquenching of water and their dilute aqueous solutions into their glassy states: any approach to cryo-fixiation." Cryoletters, 9, 66-77.

Meadows, D. M. (1994). "Towards a clearer understanding of refined sugar conditioning - a process model." Publ. Tech. Pap. Proc. Annu. Meet. Sugar Ind. Technol., 53, 387-404.

Murakami, E. and Okos, M. Measurement and Prediction of the Thermal Properties of Food. In *Food Properties and computer-aided engineering of food processing systems*. (Singh R.P. and Medina A.G. Eds), Kluwer Academic Publishers. 3 - 48.

Palmer, K. J., Dye, W. B., and Black, D. (1956). "X-Ray diffractometer and Microscopic Investigation of Crystallisation of Amorphous Sucrose." Agricultural and Food Chemistry, 4(1), 77-81.

Pancoast, H. M. and Junk, W. R. (1980). Handbook of Sugars, AVI Publishing Company, Westport, Connecticut, U.S.A.

Pennington, N. L. and Baker, C. W. (1990). Sugar, a Users Guide to Sucrose, Van Nostrand Reinhold, New York, U.S.A.

Patterson, A. H. J., Bronlund J., Brooks, G. (2001). "The Blow Test for measuring the stickiness of powders." Submitted to the New Zealand Dairy Journal, 2001

Roge, B. and Mathlouthi, M. (2000). "Caking of sucrose crystals: effect of water content and crystal size." Zuckerindustrie (Berlin), 125(5), 336-340.

Roos, Y. and Karel, M. (1991). "Amorphous state and delayed ice formation in sucrose solutions." International Journal of Food Science and Technology, 26, 553-565.

Roth, Dieter. (1976). "Amorphous icing sugar produced during crushing and recrystallisation as the cause of agglomeration and procedure for its avoidance". Doctorate Thesis, University of Karlsruhe. (Translated from German by P.M.E. Merten).

Shahhosseini, S. "on line moisture measurement of sugar using microwave techniques." Unknown.

Thompson, P. (1998). "Drying, cooling and bulk storage of sugar." International Sugar Journal, 100(1193), 223-230.

Troller, J. (1983). "Methods to Measure Water Activity." Journal of Food Protection, 46(2), 129-134.

Appendix A1

Nomenclature

a,b,c	GAB isotherm coefficients	
A	Cross sectional area	m^3
Aw	Water Activity	
C_p	Specific heat capacity	kJ/kgK
da	Degree amorphisim	%
D	Moisture diffusivity	kg/m^3
h_g	Enthalpy in gas phase	J/kg
h_{lv}	Latent heat of vaporisation of water	J/kg
h_s	Enthalpy of solid phase	J/kg
h_v	Enthalpy of water vapor	J/kg
H	Absolute humidity	kg H_2O/kg dry air
J	Bessels function	
$J_{v/s}$	Moisture flux by adsorption onto solid	kg/s
k′	Free diffusion model reaction rate constant	
k	Glass transition material constant	
l	Bed depth	m
m	Counter	
M	Moisture content of solid phase	kg H_2O/kg dry solid
n	Number of moles	mol
n′	Material sorption isotherm slope	
p	Water vapour pressure	Pa
P_v	Vapour Partial Pressure	
P_w	Water Partial Pressure	
Q	Heat flow	μW
r	Radius	m
R	Universal gas Constant	J K/mol
r_k	Kelvin Radius	m
S	Sucrose solubility	%
T	Temperature	°C
T_g	Glass transition temperature	°C
t	time	s
V	Volume	m^3
V_0	Molecular Volume	m^3 /mol
w_1	Glass transition component 1 mass fraction	kg
w_2	Glass transition component 2 mass fraction	kg
X	Mass fraction	
Y	Fraction of unaccomplished change	

Greek Nomenclature

α	Thermal diffusivity	m^2/s
β	Beta coefficient	
ε	Porosity	
λ_g	Thermal conductivity gas phase	W/m°C
λ_s	Thermal conductivity solid phase	W/m°C
η	Viscosity	Pa.s
η_g	Viscosity at glass transition temperature	Pa.s
ρ_a	Density of air	kg dry air/m^3
ρ_s	Density of solid	kg/m^3
ρ_{20}	Density at 20°C	kg/m^3
σ	Surface tension	N/m
θ	Wetting angle	radians

Appendix A2

Program Source Code

Program description

The model is a modified version of the model written for the caking of lactose powders by John Bronlund.

The programming technique used is object orientated programming, with several functions being called by a main function, Sucrosecake.cpp. This function is responsible for the initislisation of the variables, the printing of the data and contains the code that controls the model solutions.

The Node unit consists of air and sucrose objects. There are classes to describe the left, right and internal nodes of the model as well as a function to calculate the heat and moisture transportation between the nodes.

The Sucrose unit declares a class that describes the physical properties of the sucrose such as moisture relations.

The AirProps unit describes a class that describes the air, with the air state being defined setting the temperature, pressure and humidity, with all other properties of air being calculated from these three.

A2 1.1 AirProps Unit

Airprops.h

```
//a class to define the fundamental properties of air
#ifndef AirProps_H_
#define AirProps_H_

class AirProps {

public:
```

```
double  Temperature;                // °C
double  Humidity;                   // kg/kg dry air

const   double  Pressure;           // = 101300 Pa

const   double DryAirSpecHeat;      // = 1006 J/kg°C
const   double WaterVapSpecHeat;    // = 1875 J/kg°C
const    double GasConstant;        // = 8.413 Nm/mol°C
const    double LatentHeat;         // = 2.5e6 J/kg

// Class AirProps constructor
AirProps(char[],double,char[],double);

void SetAirProps(char ina[], double aa, char inb[], double bb);

//  Sets the Temperature and Humidity
double AirTemperature(char INa[],double a,char INb[]="None",double b=42);

double AirHumidity(char INa[],double a,char INb[]="None",double b=42);

// Dry air density kg/m3
double AirDensity();
double AirDensity(char INA[],double A,char INB[]="None",double B=42);

// Vapour Pressure (Pa) from Humidity
double VapPressure();
double VapPressure(char INA[],double A,char INB[]="None",double B=42);

// Saturated Vapour Pressure (Pa) from AirTemp
double SatVapPressure();
double SatVapPressure(char INA[],double A,char INB[]="None",double B=42);

// RH from Humidity and AirTemp
double RH();
double RH(char INA_RH[],double A_RH,char INB_RH[]="None",double B_RH=42);

// Air Enthalpy J/kg dry air
double AirEnthalpy();
double AirEnthalpy(char INA[],double A,char INB[]="None",double B=42);

};

#endif          //AirProps_H_
```

Airprops.cpp

```
//Class to define the properties of air
#include <string.h>
#include <math.h>
#include "c:\caking\ver 1.0\airprops.h"


//AirProps Constructor
AirProps::AirProps(char INA[], double A, char INB[], double B) :
        Pressure(1013e2),                   // Pa
        DryAirSpecHeat(1006),               // J/kg°C
        WaterVapSpecHeat(1875),             // J/kg°C
        GasConstant(8.413),                 // Nm/mol°C
        LatentHeat(2.5e6)                   // J/kg
        {
                SetAirProps(INA,A,INB,B);
        };

void AirProps::SetAirProps(char ina[], double aa, char inb[], double bb)
{
        Temperature = AirTemperature(ina,aa,inb,bb);
        Humidity = AirHumidity(ina,aa,inb,bb);
};

//Air Humidity Functions
double AirProps::AirHumidity(char INa[], double a, char INb[] ,double b)
{
        double dummyH;

        //rearrange arguments so "Humidity" is last if it is present.
        if (stricmp(INa,"Temperature") == 0)
        {
                char * INc = INb;
                double c;
                c = b;
                INb = INa;
                b = a;
                INa = INc;
                a = c;
        }

        //set INb to "Temperature" if second argument is not given
        if (stricmp(INb,"None") == 0)
        {
                INb = "Temperature";
```

```
        b = Temperature;
    }

    //check if INb = "Humidity" and changes it so INa = "Humidity
    if (stricmp(INb,"Humidity") == 0)
    {
        INa = INb;
        a = b;
    }

    //Calculations

    //Humidity
    if (stricmp(INa,"Humidity") == 0)
    {
        dummyH = a;
    }

    //RH and Temperature
    if ((stricmp(INa,"RH") == 0) && (stricmp(INb,"Temperature") == 0))
    {
        dummyH = 18.0*a*exp(23.4795-3990.56/(b+233.833))
                    /(29.0*(Pressure-a*exp(23.4795-3990.56/(b+233.833))));
    }

    //AirDensity and Temperature
    if ((stricmp(INa,"AirDensity") == 0) && (stricmp(INb,"Temperature") == 0))
    {
        dummyH = 18.0*(273.15/(22.4*(273.15+b)*a)-1/29.0);
    }

    //Air Enthalpy and Temperature
    if ((stricmp(INa,"AirEnthalpy") == 0) && (stricmp(INb,"Temperature") == 0))
    {
        dummyH = (a-DryAirSpecHeat*b)/(WaterVapSpecHeat*b+LatentHeat);
    }

    return dummyH;
};

//Temperature Functions
double AirProps::AirTemperature(char INa[],double a,char INb[] , double b)
{
    double dummyTemp;

    //rearrange arguments so "Humidity" is last if it is present.
```

```
if (stricmp(INa,"Humidity") ==0)
{
        char * INc = INb;
        double c;
        c = b;
        INb = INa;
        b = a;
        INa = INc;
        a = c;
}

//set INb to "Humidity" if second argument is not given
if (stricmp(INb, "None") == 0)
{
        INb = "Humidity";
        b = Humidity;
}

//checks if INb = "Temperature" and changes it so INa = "Temperature"
if (stricmp(INb,"Temperature") == 0)
{
        INa = INb;
        a = b;
}

//Calculation code

//Temperature
if (stricmp(INa,"Temperature") == 0)
{
        dummyTemp = a;
}

//RH and Humidity inputed from user
else if ((stricmp(INa,"RH") == 0) && (stricmp(INb,"Humidity") == 0))
{
        dummyTemp = 3990.56/(23.4795-log(29*b*Pressure
                                        /(18+29*b)/a))-233.833;
}

//AirEnthalpy and Humidity from user
else if ((stricmp(INa,"AirEnthalpy") == 0) && (stricmp(INb,"Humidity") == 0))
{
        dummyTemp = (a-b*LatentHeat)
                                /(DryAirSpecHeat+b*WaterVapSpecHeat);
}
```

```
        //AirDensity and Humidity from user
        else if ((stricmp(INa,"AirDensity") == 0) && (stricmp(INb,"Humidity") == 0))
        {
                dummyTemp = (273.15/(a*22.4*(1/29.0+b/18.0)))-273.15;
        }

        return dummyTemp;
};


//AirDensity Functions
double AirProps::AirDensity()
{
        return 1/(22.4*(273.15+Temperature)*(1/29.0+Humidity/18.0)/273.15);
};

double AirProps::AirDensity(char INA[],double A,char INB[],double B)
{
        double Humidity_int = AirHumidity(INA,A,INB,B);
        double Temperature_int = AirTemperature(INA,A,INB,B);
        return 1/(22.4*(273.15+Temperature_int)*(1/29.0+Humidity_int/18.0)/273.15);
};


//Vapour Pressure Functions
double AirProps::VapPressure()
{
        return 29*Humidity*Pressure/(18+29*Humidity);
};


double AirProps::VapPressure(char INA[],double A,char INB[],double B)
{
        double Humidity_int = AirHumidity(INA,A,INB,B);
        return 29*Humidity_int*Pressure/(18+29*Humidity_int);
};


//Saturated Vapour Pressure Functions
double AirProps::SatVapPressure()
{
        return exp(23.4795-3990.56/(Temperature+233.833));
};
```

```
double AirProps::SatVapPressure(char INA[],double A,char INB[],double B)
{
        double Temperature_int = AirTemperature(INA,A,INB,B);
        return exp(23.4795-3990.56/(Temperature_int+233.833));
};


//Relative Humidity Functions
double AirProps::RH()
{
        return VapPressure()/SatVapPressure();
};

double AirProps::RH(char INA_RH[],double A_RH,char INB_RH[],double B_RH)
{
        return VapPressure(INA_RH,A_RH,INB_RH,B_RH)
                                /SatVapPressure(INA_RH,A_RH,INB_RH,B_RH);
};


//Air Enthalpy Functions
double AirProps::AirEnthalpy()
{
        return DryAirSpecHeat*Temperature+Humidity

        *(WaterVapSpecHeat*Temperature+LatentHeat);
};


double AirProps::AirEnthalpy(char INA[],double A,char INB[],double B)
{
        double Temperature_int = AirTemperature(INA,A,INB,B);
        double Humidity_int = AirHumidity(INA,A,INB,B);

        return DryAirSpecHeat*Temperature_int+Humidity_int
                        *(WaterVapSpecHeat*Temperature_int+LatentHeat);
};
```

A2 1.2 Node unit

Node.h

```
#ifndef Node_H_
#define Node_H_

#include <iostream.h>
#include <stdlib.h>
#include "c:\caking\ver 1.0\Sucrose.h"
#include "c:\caking\ver 1.0\AirProps.h"

enum Boolean {Yes, No};

class Ambient {
public:
char label[10];
Boolean ConstantTemperature;
double Temperature;
double TempArray[1000];
double TimeInterval;
double htc;
friend iostream;
friend fstream;

Ambient(char* nm);
void SetAmbient(double temp,double h);
void GetAndSetValues();
void UpdateAmbient(double t);
};

class Node {

public:

Sucrose L;
static double Time;
static double dt;
static double dx;
double Heat;
double Water;
double Vol;
double Tempnew,EffMCnew;
Node();
void SetNode(char inA[],double ina,char inB[],double inb,char inC[],double inc,
```

```
        char inD[] = "None",double ind = 42,char inE[] = "None",double ine = 42);

void GetAndSetValues();
void UpdateAir();
};

class InternalNode : public Node {
public:
void Transport(Node L_Node, Node R_Node);
};

class LeftNode : public Node {
public:
void Transport(Ambient L_Node,Node R_Node);
};

class RightNode : public Node {
public:
void Transport(Node L_Node,Ambient R_Node);
};

#endif          //Node_H_
```

Node.cpp

```
#include <string.h>
#include <math.h>
#include <iostream.h>
#include <fstream.h>
#include "c:\caking\ver 1.0\Sucrose.h"
#include "c:\caking\ver 1.0\AirProps.h"
#include "c:\caking\ver 1.0\Snode.h"


double Node::dt=0;
double Node::dx=0;
double Node::Time=0;

double aow = 0.0;

Ambient::Ambient(char* nm) {
        strcpy(label,nm);
        SetAmbient(20,60);
        TimeInterval=300;
```

```
};

void Ambient::SetAmbient(double temp,double h) {
        int I=0;
        while(I<300)
        {
                TempArray[I]=temp;
                I++;
        }
        htc = h;
};

void Ambient::GetAndSetValues() {
        double IntA,IntB;
        char answer;
        cout << "Use constant temperature for " << label << " (y/n)?" << '\t';
        cin >> answer;
        if (answer == 'n') {
                char filename[13];
                cout << "Enter temperature history filename ";
                cin >> filename;
                ifstream infile(filename);
                int I=0;
                while(!infile.eof()) {
                        infile >> TempArray[I];
                        I++;
                }
                infile.close();
                cout << "Enter time interval for file" << filename;
                cin >> TimeInterval;
                cout << "Enter heat transfer coefficient        ";
                cin >> htc;
        }
        else {
                cout << label << " Boundary Temperature (°C)   " << '\t';
                cin >> IntA;
                cout << label << " Boundary HTC              " << '\t';
                cin >> IntB;
                SetAmbient(IntA,IntB);
                }
};

void Ambient::UpdateAmbient(double t) {
         double fract=0, ipart=0;

         fract = modf( (t/TimeInterval), &ipart);
```

```
    int I = (int)ipart;
        Temperature = TempArray[I]+(TempArray[I+1]-
TempArray[I])*fract/TimeInterval;
};

Node::Node() {
        Vol = 1e-5;
        Water = 0;
        Heat = 0;
};

void Node::GetAndSetValues() {
        double IntA,IntB;
        cout << "Initial Sucrose Temperature (°C)" << '\t';
        cin >> IntA;
        cout << "Initial Sucrose Water Activity  " << '\t';
        cin >> IntB;
        L.SetAirProps("Temperature",IntA,"RH",IntB);
        cout << "Initial Percent Amorphous              " << '\t';
        cin >> IntA;
        cout << "Initial Crystallinity of Amorphous" << '\t';
        cin >>IntB;

        if (IntB ==0) {L.SetAmorphous("PercentAmorph",IntA);}

        else {L.SetAmorphous("PercentAmorph",IntA,"Crystallinity",IntB);};

        cout << "Porosity                                                " << '\t';
        cin >> IntB;

        if (IntB == 0) {L.SetPorosity();}

        else {L.SetPorosity(IntB);};
};

void Node::UpdateAir()
{
      L.SetAirProps("Temperature",Tempnew,"RH",L.RH("EffectiveMC",EffMCnew));
};

void InternalNode::Transport(Node L_Node, Node R_Node)
{
double Tempmin = (L.Temperature+L_Node.L.Temperature)/2;
double Tempmax = (L.Temperature+R_Node.L.Temperature)/2;

Heat = Heat+dt*Vol/pow(dx,2)*L.TConduct*(L_Node.L.Temperature
```

```
                        -2*L.Temperature+R_Node.L.Temperature)
                        +L.Diffusivity("Temperature",Tempmin)*(L.WaterVapSpecHeat
                        *Tempmin+L.LatentHeat)*(L_Node.L.Humidity
                        *L_Node.L.AirDensity()-L.Humidity*L.AirDensity())
                        -L.Diffusivity("Temperature",Tempmax)
                        *(L.WaterVapSpecHeat*Tempmax
                        +L.LatentHeat)*(L.Humidity*L.AirDensity()
                        -R_Node.L.Humidity*R_Node.L.AirDensity());

double PAmorphOld = L.PercentAmorph;
L.NewAmorphState(dt);

Water = Water+dt*Vol/pow(dx,2)*(L.Diffusivity("Temperature",Tempmin)
                        *(L_Node.L.Humidity*L_Node.L.AirDensity()-L.Humidity
                        *L.AirDensity())-L.Diffusivity("Temperature",Tempmax)
                        *(L.Humidity*L.AirDensity()-R_Node.L.Humidity
                        *R_Node.L.AirDensity()));

Water = Water - Vol*(1-L.Porosity)*L.ParticleDensity*aow
                                *(PAmorphOld-L.PercentAmorph);

double diffMC = L.MoistureContent();
double diffT = L.Temperature;
double EffMC = L.MoistureContent();
double Temp = L.Temperature;

while ((fabs(diffMC)>1e-50) && (fabs(diffT)>1e-2))
 {
        Tempnew = (Heat-Vol*L.Porosity*L.AirDensity("Temperature",Temp)
                *L.LatentHeat *L.AirHumidity("RH",L.RH("EffectiveMC",EffMC),
                "Temperature",Temp))/(Vol*L.Porosity*L.AirDensity("Temperature"
                ,Temp)*(L.DryAirSpecHeat+L.AirHumidity("RH",L.RH
                ("EffectiveMC",EffMC),"Temperature",Temp)*L.WaterVapSpecHeat)
                +(1-L.Porosity)*Vol*L.ParticleDensity*(L.SucroseSpecHeat+EffMC
                *L.WaterSpecHeat));

        EffMCnew = (Water-L.Porosity*Vol*L.AirHumidity("RH",L.RH("EffectiveMC"
                ,EffMC),"Temperature",Temp)*L.AirDensity("Temperature",Temp))
                /((1-L.Porosity)*Vol*L.ParticleDensity);

        diffT = Temp-Tempnew;
        diffMC = EffMC-EffMCnew;
        Temp = Tempnew;
        EffMC = EffMCnew;
}
};
```

```
void LeftNode::Transport(Ambient L_Node, Node R_Node)
{
        double Tempmax = (L.Temperature+R_Node.L.Temperature)/2;

        Heat = Heat+2*dt*Vol/dx*(L_Node.htc*(L_Node.Temperature
                        -L.Temperature)-L.TConduct/dx*(L.Temperature
                        -R_Node.L.Temperature)
                        -L.Diffusivity("Temperature",Tempmax)/dx
                        *(L.WaterVapSpecHeat*Tempmax
                        +L.LatentHeat)*(L.Humidity*L.AirDensity()
                        -R_Node.L.Humidity*R_Node.L.AirDensity()));

  double PAmorphOld = L.PercentAmorph;
        L.NewAmorphState(dt);

  Water = Water+2*dt*Vol/pow(dx,2)*(-L.Diffusivity("Temperature",Tempmax)
                        *(L.Humidity*L.AirDensity()
                        -R_Node.L.Humidity*R_Node.L.AirDensity()));

  Water = Water - Vol*(1-L.Porosity)*L.ParticleDensity*aow
                        *(PAmorphOld-L.PercentAmorph);

 double diffMC = L.MoistureContent();
 double diffT = L.Temperature;
 double EffMC = L.MoistureContent();
 double Temp = L.Temperature;
 while ((fabs(diffMC)>1e-50) && (fabs(diffT)>1e-2))
 {
        Tempnew = (Heat-Vol*L.Porosity*L.AirDensity("Temperature",Temp)
                *L.LatentHeat*L.AirHumidity("RH",L.RH("EffectiveMC",EffMC),
                "Temperature",Temp))/(Vol*L.Porosity*L.AirDensity("Temperature",
                Temp)*(L.DryAirSpecHeat+L.AirHumidity("RH",L.RH("EffectiveMC",
                EffMC),"Temperature",Temp)*L.WaterVapSpecHeat)+(1-L.Porosity)
                *Vol*L.ParticleDensity*(L.SucroseSpecHeat+EffMC*L.WaterSpecHeat))

        EffMCnew = (Water-L.Porosity*Vol*L.AirHumidity("RH",L.RH("EffectiveMC"
                ,EffMC),"Temperature",Temp)*L.AirDensity("Temperature",Temp))
                /((1-L.Porosity)*Vol*L.ParticleDensity);

        diffT = Temp-Tempnew;
        diffMC = EffMC-EffMCnew;
        Temp = Tempnew;
        EffMC = EffMCnew;
        }
```

```
};

void RightNode::Transport(Node L_Node,Ambient R_Node)
{
double Tempmin = (L.Temperature+L_Node.L.Temperature)/2;

 Heat = Heat+2*dt*Vol/dx*(-R_Node.htc*(L.Temperature-R_Node.Temperature)
        +L.TConduct/dx*(L_Node.L.Temperature-L.Temperature)
        +L.Diffusivity("Temperature",Tempmin)/dx*(L.WaterVapSpecHeat*Tempmin
        +L.LatentHeat)*(L_Node.L.Humidity*L_Node.L.AirDensity()-
        L.Humidity*L.AirDensity()));

 double PAmorphOld = L.PercentAmorph;
        L.NewAmorphState(dt);

Water = Water+2*dt*Vol/pow(dx,2)*(L.Diffusivity("Temperature",Tempmin)
                *(L_Node.L.Humidity*L_Node.L.AirDensity()
                -L.Humidity*L.AirDensity()));

Water = Water - Vol*(1-L.Porosity)*L.ParticleDensity*aow
                        *(PAmorphOld-L.PercentAmorph);

double diffMC = L.MoistureContent();
double diffT = L.Temperature;
double EffMC = L.MoistureContent();
double Temp = L.Temperature;

while ((fabs(diffMC)>1e-50) && (fabs(diffT)>1e-2))
{
Tempnew = (Heat-Vol*L.Porosity*L.AirDensity("Temperature",Temp)*L.LatentHeat
        *L.AirHumidity("RH",L.RH("EffectiveMC",EffMC),"Temperature",Temp))
        /(Vol*L.Porosity*L.AirDensity("Temperature",Temp)*(L.DryAirSpecHeat
        +L.AirHumidity("RH",L.RH("EffectiveMC",EffMC),"Temperature",Temp)
        *L.WaterVapSpecHeat)+(1-L.Porosity)*Vol*L.ParticleDensity
        *(L.SucroseSpecHeat+EffMC*L.WaterSpecHeat));

EffMCnew = (Water-L.Porosity*Vol*L.AirHumidity("RH",L.RH("EffectiveMC"
        ,EffMC),"Temperature",Temp)*L.AirDensity("Temperature",Temp))
        /((1-L.Porosity)*Vol*L.ParticleDensity);

diffT = Temp-Tempnew;
diffMC = EffMC-EffMCnew;
Temp = Tempnew;
EffMC = EffMCnew;
}
};
```

A2 1.3 Sucrose Unit

Sucrose.h

```
#ifndef Sucrose_H_
#define Sucrose_H_

#include "c:\caking\ver 1.0\Airprops.h"


class Sucrose : public AirProps {

        public:

        double Porosity;            // voidage fraction
        double PercentAmorph;       // amount of amorphous material
        double Crystallinity;       // crystallinity of amorphous portion

        double TConduct;                                // effective thermal conductivity

        const double ParticleDensity; // Sucrose particle density kg/m3
        const double SucroseSpecHeat; // Sucrose specific heat capacity J/kg°C
        const double WaterSpecHeat;   // liquid water specific heat capacity J/kg°C


        //constructor
        Sucrose();              // sets porosity, airspace,PercentAmorph and Crystallinity

        void SetAmorphous(char INa[],double a,char INb[]="Crystallinity",
                                        double b = 1e-15);
        void SetPorosity(double epsilon = 0.45);
        void NewAmorphState(double timestep);
        double NewCrystallinity(double timestep);
        double RateConstant();
        double TGlass();
        double MoistureContent(char IN[]="None",double in=42,
                                char INb[]="None",double inb=42);

        // effective moisture content f(RH) kg/kg dry Sucrose

        double MC_Crystalline(char IN[]="None",double in=42);
```

```
        // moisture content of crystalline Sucrose g/100g dry Sucrose

        double MC_Amorphous(char IN[]="None",double in=42);

        // moisture content of amorphous Sucrose g/100g dry Sucrose

        double Diffusivity(char IN[]="None",double in=42);
        double RH();
        double RH(char INa[],double a,char INb[]="None",double b = 42);
        double LumpingStrength();
};


#endif          //Sucrose_H_
```

Sucrose.cpp

```
//code deals with the interaction between the sucrose in equilibrium with air
//defines fundamental properties as from experimental with any others obtained
//through calls from other embedded functions

#include "c:\caking\ver 1.0\Airprops.h"
#include "c:\caking\ver 1.0\Sucrose.h"
#include <string.h>
#include <math.h>

Sucrose::Sucrose() :
        AirProps("Humidity",0.011,"Temperature",20),
        ParticleDensity(1588),
        SucroseSpecHeat(1235),
        WaterSpecHeat(4180)
        {
                SetPorosity();
                TConduct = 0.150384;
                SetAmorphous("PercentAmorph",0.01,"Crystallinity",1e-18);
        };


void Sucrose::SetPorosity(double epsilon)
{
        Porosity = epsilon;
};
```

```
void Sucrose::SetAmorphous(char INa[],double a,char INb[], double b)
{
        if (stricmp(INa,"Crystallinity") == 0)
        {
                char * INc = INa;
                double c = a;
                INa = INb;
                a = b;
                INb = INc;
                b = c;
        }

        if (stricmp(INa,"PercentAmorph") == 0)
                PercentAmorph = a;

        if (stricmp(INb,"Crystallinity") == 0)
                Crystallinity = b;

};

void Sucrose::NewAmorphState(double timestep)
{
  if((1-Crystallinity) > 0)
  {
        PercentAmorph = PercentAmorph/(1-Crystallinity)
                                *(1-NewCrystallinity(timestep));
        Crystallinity = NewCrystallinity(timestep);
        }

  else Crystallinity = 1;
};

double Sucrose::NewCrystallinity(double timestep)
{
        const double Avrami_m = 3;

        double dummy_Cry;

        if ((PercentAmorph > 0) && (RateConstant() > 0) && (Crystallinity < 1))
        {
                dummy_Cry = Crystallinity+timestep*Avrami_m*(1-Crystallinity)
                        *pow((-log(1-Crystallinity)),(Avrami_m-1)/Avrami_m)
                        *pow(RateConstant(),(1/Avrami_m));
        }

        else dummy_Cry = Crystallinity;
```

```
        if (dummy_Cry > 1)
        dummy_Cry = 1;

        return dummy_Cry;
};

double Sucrose::RateConstant()
{
        const double Avrami = 3, C1 = 35.43, C2 = 108.38, C3 = 3e27;
        double K;

        if (Temperature > TGlass())
        {
        K = C3*pow(exp(-C1/(8.314e-3*(C2+Temperature-TGlass()))), Avrami);
        }
        else {K = 0;}

  return K;
};

double Sucrose::TGlass()
{
        const double Tg1 = 101;
        const double Tg2 = -135;
        const double K = 4.2;

        return ((1-MC_Amorphous())*Tg1+K*MC_Amorphous()*Tg2)/
                                ((1-MC_Amorphous())+K*MC_Amorphous());
};


double Sucrose::MoistureContent(char INa[],double ina,char INb[],double inb)
{
        if (stricmp(INa,"None") == 0) {
                INa = "RH";
                ina = RH();
        }

        if (stricmp(INb,"None") == 0)
                inb = PercentAmorph;

        return MC_Crystalline(INa,ina)+MC_Amorphous(INa,ina)*inb;
};

double Sucrose::MC_Crystalline(char IN[],double in)
```

```
{
  const double GAB_A = -0.0125;
  const double GAB_B = -29.0078;
  const double GAB_C = 1.037366;
  double Aw = 0.99;

        if (stricmp(IN,"None") == 0) {
                IN = "RH";
                in = RH();
        }
//ensure that the RH and hence the MC dosn't go out of the valid range (0<Aw<1)
if (RH() >=0.99)

return (GAB_A*GAB_B*GAB_C*Aw/((1-GAB_B*Aw)
                *(1+(GAB_C-1)*GAB_B*Aw)))/1000;

else

return (GAB_A*GAB_B*GAB_C*in/((1-GAB_B*in)
                *(1+(GAB_C-1)*GAB_B*in)))/1000;

};

double Sucrose::MC_Amorphous(char IN[],double in)
{
 const double AM_GAB_A = 9.490471;
 const double AM_GAB_B = 0.969582;
 const double AM_GAB_C = 2.356199;

double Aw = 0.99;

        if (stricmp(IN,"None") == 0) {
                IN = "RH";
                in = RH();
        }

//ensure that the RH and hence the MC dosn't go out of the valid range (0<Aw<1)

if (RH() >= 0.99)
 return (AM_GAB_A*AM_GAB_B*AM_GAB_C*Aw/((1-AM_GAB_B*Aw)
                *(1+(AM_GAB_C-1)*AM_GAB_B*Aw)))/1000;

else

return (AM_GAB_A*AM_GAB_B*AM_GAB_C*in/((1-AM_GAB_B*in)
                *(1+(AM_GAB_C-1)*AM_GAB_B*in)))/1000;
```

```
};

double Sucrose::Diffusivity(char IN[],double in)
{
	if (stricmp(IN,"None") == 0) {
		IN = "Temperature";
		in = Temperature;
	}

	return Porosity*(0.0017255*(in+273.15)-0.2552)/10000;
};

double Sucrose::RH()
{
	return AirProps::RH();
};

double Sucrose::RH(char INa[],double a,char INb[],double b)
{
	if ((stricmp(INa,"EffectiveMC") == 0) || (stricmp(INb,"EffectiveMC")==0))
	{
		if ((stricmp(INb,"EffectiveMC") == 0))
		{
			char * INc = INb;
			double c;
			c = b;
			INb = INa;
			b = a;
			INa = INc;
			a = c;
		}

		if ((stricmp(INb,"None")==0))
		{
			INb = "PercentAmorph";
			b = PercentAmorph;
		}


	if((stricmp(INa,"EffectiveMC")==0)&&(stricmp(INb,"PercentAmorph")==0))
	{
		double Try1=0,Try2=1,MCalc=1,aw;
		while (fabs(MCalc-a)>1e-15)
		{
			aw=(Try1+Try2)/2;
```

```
                    MCalc = MoistureContent("RH",aw,INb,b);
                    if ((MCalc-a)<0) {Try1 = aw;}
                    else {Try2 = aw;}
                }
                return aw;
        }
}
else {return AirProps::RH(INa,a,INb,b);}
};
```

A2 1.4 Sucrosecake Unit

Sucrosecake.cpp

```
#include <iostream.h>
#include <fstream.h>
#include <string.h>
#include <conio.h>
#include <math.h>
#include "c:\caking\ver 1.0\Snode.h"
#include "c:\caking\ver 1.0\Sucrose.h"
#include "c:\caking\ver 1.0\AirProps.h"

enum {size = 15};
char filename[13];

ofstream outfile_RH;
ofstream outfile_Amorph;
ofstream outfile_Temp;
ofstream outfile_Tg;
ofstream outfile_MC;
ofstream outfile_Strength;

InternalNode Inside[size];
LeftNode BottomNode;
RightNode TopNode;
Ambient BottomAmbient("Bottom"),TopAmbient("Top");

int NumberNodes,menu_option;

double Tfinish,Tprint;
enum OutType {Temp,MC,RH,Humidity,Tg,Amorph,Strength};
```

```
int menu();
void PrintOut(OutType);
void keypress();


OutType X1,X2, X3, X4;

void main() {

Start:;

cout.setf(ios::left|ios::fixed);
cout.precision(3);

menu_option = menu();

X1 = Temp;
X2 = RH;
X3 = MC;
X4 = Strength;

clrscr();

cin.width(sizeof(filename));
cout << "Results file name                " << '\t';
cin >> filename;
cout << endl;
char fname[13],gname[13], hname[13];
strncpy(fname,filename,13);
strncpy(gname,filename,13);
strncpy(hname,filename,13);

outfile_RH.open(strcat(filename,".RH"));
if(!outfile_RH) cerr<<"couldn't open RH outfile"<<endl;

outfile_Temp.open(strcat(fname,".tmp"));
if(!outfile_Temp) cerr<<"couldn't open amorphous outfile"<<endl;

outfile_MC.open(strcat(gname,".MC"));
if(!outfile_MC) cerr<<"couldn't open MC outfile"<<endl;

outfile_Strength.open(strcat(hname,".Str"));
if(!outfile_Strength) cerr<<"couldn't open Str outfile"<<endl;

Node::Time = 0;
```

```
//Get the initial experimental parameters and conditions
cout << "Time step                    " << '\t';
cin >> Node::dt;
cout << "Print out interval           " << '\t';
cin >> Tprint;
cout << "Total Simulation time                " << '\t';
cin >> Tfinish;

cout << "Number of nodes              " << '\t';
cin >> NumberNodes;

double Thickness;
cout << "Slab thickness                       " << '\t';
cin >> Thickness;
Node::dx = (Thickness/NumberNodes);

char answer;
cout << "Initialise each node seperately?   " << '\t';
cin >> answer;
if (answer == 'n') {
        double IntA,IntB,IntC,IntD,IntE;
        cout << "Initial Sucrose Temperature (°C)" << '\t';
        cin >> IntA;
        cout << "Initial Sucrose Water Activity  " << '\t';
        cin >> IntB;
        cout << "Initial Percent Amorphous   " << '\t';
        cin >> IntC;

  cout << "Initial Crystallinity of Amorphous" << '\t';
        cin >> IntD;
        cout << "Porosity                             " << '\t';
        cin >> IntE;


//setup the initial conditions
        BottomNode.L.SetAirProps("Temperature",IntA,"RH",IntB);
        if (IntD == 0) {
                BottomNode.L.SetAmorphous("PercentAmorph",IntC);}
        else {

        BottomNode.L.SetAmorphous("PercentAmorph",IntC,"Crystallinity",IntD);};
        if (IntE == 0) {}
        else {BottomNode.L.SetPorosity(IntE);};

        BottomNode.Water = BottomNode.L.Porosity*BottomNode.Vol
                *BottomNode.L.Humidity*BottomNode.L.AirDensity()
```

```
        +(1-BottomNode.L.Porosity)*BottomNode.Vol
        *BottomNode.L.ParticleDensity*BottomNode.L.MoistureContent();

BottomNode.Heat = (BottomNode.L.DryAirSpecHeat
        *BottomNode.L.Temperature
        +BottomNode.L.Humidity*(BottomNode.L.WaterVapSpecHeat
        *BottomNode.L.Temperature+BottomNode.L.LatentHeat))
        *BottomNode.L.Porosity*BottomNode.Vol*BottomNode.L.AirDensity()
        +(BottomNode.L.SucroseSpecHeat
        *BottomNode.L.Temperature+BottomNode.L.WaterSpecHeat
        *BottomNode.L.Temperature*BottomNode.L.MoistureContent())
        *(1-BottomNode.L.Porosity)*BottomNode.Vol
        *BottomNode.L.ParticleDensity;

TopNode.L.SetAirProps("Temperature",IntA,"RH",IntB);
if (IntD == 0) {
        TopNode.L.SetAmorphous("PercentAmorph",IntC);}
else {
        TopNode.L.SetAmorphous("PercentAmorph",IntC,"Crystallinity",IntD);};
if (IntE == 0) {}
else {TopNode.L.SetPorosity(IntE);};

TopNode.Water = TopNode.L.Porosity*TopNode.Vol*TopNode.L.Humidity
        *TopNode.L.AirDensity()+(1-TopNode.L.Porosity)*TopNode.Vol
        *TopNode.L.ParticleDensity*TopNode.L.MoistureContent();

TopNode.Heat = (TopNode.L.DryAirSpecHeat*TopNode.L.Temperature
        +TopNode.L.Humidity*(TopNode.L.WaterVapSpecHeat
        *TopNode.L.Temperature+TopNode.L.LatentHeat))*TopNode.L.Porosity
        *TopNode.Vol*TopNode.L.AirDensity()+(TopNode.L.SucroseSpecHeat
        *TopNode.L.Temperature+TopNode.L.WaterSpecHeat
        *TopNode.L.Temperature*TopNode.L.MoistureContent())
        *(1-TopNode.L.Porosity)*TopNode.Vol*TopNode.L.ParticleDensity;

for (int i = 1;i < NumberNodes;i=i+1) {
        Inside[i].L.SetAirProps("Temperature",IntA,"RH",IntB);
        if (IntD == 0) {
                Inside[i].L.SetAmorphous("PercentAmorph",IntC);}
        else {
                Inside[i].L.SetAmorphous("PercentAmorph",IntC,
                        "Crystallinity",IntD);};
        if (IntE == 0) {}
        else {Inside[i].L.SetPorosity(IntE);};

        Inside[i].Water = Inside[i].L.Porosity*Inside[i].Vol*Inside[i].L.Humidity
                *Inside[i].L.AirDensity()+(1-Inside[i].L.Porosity)*Inside[i].Vol
```

```
                    *Inside[i].L.ParticleDensity*Inside[i].L.MoistureContent();

                Inside[i].Heat = (Inside[i].L.DryAirSpecHeat*Inside[i].L.Temperature
                    +Inside[i].L.Humidity*(Inside[i].L.WaterVapSpecHeat
                    *Inside[i].L.Temperature+Inside[i].L.LatentHeat))
                    *Inside[i].L.Porosity*Inside[i].Vol*Inside[i].L.AirDensity()
                    +(Inside[i].L.SucroseSpecHeat*Inside[i].L.Temperature
                    +Inside[i].L.WaterSpecHeat*Inside[i].L.Temperature
                    *Inside[i].L.MoistureContent())*(1-Inside[i].L.Porosity)
                    *Inside[i].Vol*Inside[i].L.ParticleDensity;
        };
}
else {};

//Set up the initial ambient conditions
BottomAmbient.GetAndSetValues();
TopAmbient.GetAndSetValues();
cout << endl;cout << endl;
PrintOut(X1);
PrintOut(X2);
PrintOut(X3);
PrintOut(X4);


//Start of main program loop calculations
double Telapsed = 0;

while (Node::Time <= Tfinish) {
        Node::Time = Node::Time + Node::dt;
        Telapsed = Telapsed + Node::dt;
        BottomAmbient.UpdateAmbient(Node::Time);
        TopAmbient.UpdateAmbient(Node::Time);

        BottomNode.Transport(BottomAmbient,Inside[1]);
        Inside[1].Transport(BottomNode,Inside[2]);

        for(int i=2;i < (NumberNodes-1);i=i+1) {
                Inside[i].Transport(Inside[i-1],Inside[i+1]);
        };

        Inside[NumberNodes-1].Transport(Inside[NumberNodes-2],TopNode);
        TopNode.Transport(Inside[NumberNodes-1],TopAmbient);
        BottomNode.UpdateAir();

        for (int i=1;i<NumberNodes;i=i+1) {
                Inside[i].UpdateAir();
```

```
        };

        TopNode.UpdateAir();

        if (Telapsed >= Tprint) {
                PrintOut(X1);
                PrintOut(X2);
                PrintOut(X3);
                PrintOut(X4);
                Telapsed = 0;
                };
};

outfile_RH.close();
outfile_Temp.close();
outfile_MC.close();
outfile_Strength.close();

keypress();

cout<<"Do you want to run the simulation again y or n  =>";
char restart;
cin>>restart;

if(restart == 'y')  goto Start;

else exit(0);
};// end of main


int menu()
{
 clrscr();

 cout<<"Enter startup option"<<endl<<endl
    <<"1. Set output to Temperature"<<endl
    <<"2. Set output to RH "<<endl
    <<"3. Quit"<<endl<<endl
    <<"=>";

 int option;

 cin>>option;

 return option;
}
```

```
void PrintOut(OutType x)
{
double rk, lumping_strength;
cout.precision(0);
int i;
switch(x)
{

 case Temp:

        if(menu_option == 1)
        {
        cout << Node::Time << " ";
        cout.precision(3);
        cout<<BottomNode.L.Temperature<<" ";
        }

        outfile_Temp << Node::Time << "  ";
        outfile_Temp << BottomNode.L.Temperature << "  ";

        for (i=1;i<NumberNodes;i=i+1)
        {
         if(menu_option == 1)
                cout << Inside[i].L.Temperature << " ";
                outfile_Temp << Inside[i].L.Temperature << "  ";
          };

          if(menu_option == 1)
                cout << TopNode.L.Temperature << endl;
                outfile_Temp << TopNode.L.Temperature << endl;
                break;

 case Amorph:

        outfile_Amorph << Node::Time << "  ";
        outfile_Amorph << BottomNode.L.PercentAmorph << "  ";

        for (i=1;i<NumberNodes;i=i+1)
        {
                 outfile_Amorph << Inside[i].L.PercentAmorph << "  ";
           };

        outfile_Amorph << TopNode.L.PercentAmorph << endl;
        break;
```

```
case RH:

        if(menu_option == 2)
        {
                cout << Node::Time << " ";
                cout.precision(3);
                cout << BottomNode.L.RH() << " ";
        }

        outfile_RH << Node::Time << "  ";
        outfile_RH << BottomNode.L.RH() << "  ";

        for (i=1;i<NumberNodes;i=i+1)
        {
         if(menu_option == 2)
                cout << Inside[i].L.RH() << " ";
                outfile_RH << Inside[i].L.RH() << "  ";
        };

        if(menu_option == 2)
                cout << TopNode.L.RH() << endl;

        outfile_RH << TopNode.L.RH() << endl;
        break;


case Tg:

        outfile_Tg << Node::Time << "  ";
        outfile_Tg << (BottomNode.L.Temperature-BottomNode.L.TGlass()) << "  ";

        for (i=1;i<NumberNodes;i=i+1)
        {
         outfile_Tg << (Inside[i].L.Temperature-Inside[i].L.TGlass()) << "  ";
        };

        outfile_Tg << (TopNode.L.Temperature-TopNode.L.TGlass()) << endl;
        break;



case Strength:

        outfile_Strength << Node::Time << "  ";
```

```
        //calculate kelvin radius
            rk = 1000*((-0.0551 / log(BottomNode.L.RH()))
                        / ( 8.314*(273.15+BottomNode.L.Temperature)));
        //calculate strength
            lumping_strength = 58.694*rk + 0.6669;

        outfile_Strength << lumping_strength << "  ";

          for (i=1;i<NumberNodes;i=i+1)
                {
                        rk = 1000*((-0.0551 / log(Inside[i].L.RH()))
                                / ( 8.314*(273.15+Inside[i].L.Temperature)));

                        lumping_strength = 58.694*rk + 0.6669;

                        outfile_Strength << lumping_strength << "  ";
                };

        rk = 1000*((-0.0551 / log(TopNode.L.RH()))
                        / ( 8.314*(273.15+TopNode.L.Temperature)));

        lumping_strength = 58.694*rk + 0.6669;

        outfile_Strength << lumping_strength << endl;
        break;

case MC:

        cout.precision(5);
        outfile_MC << Node::Time << "  ";
        outfile_MC << BottomNode.L.MoistureContent() << "  ";

        for (i=1;i<NumberNodes;i=i+1)
        {
                outfile_MC << Inside[i].L.MoistureContent() << "  ";
        };

       outfile_MC << TopNode.L.MoistureContent() << endl;
       break;

 }//closing of the switch

};//closing of the printout function

void keypress()
```

```
{

cout<<endl<<"Press any key to continue";
getch();
clrscr();

}
```